Semi-Discrete Iteration Methods in X-Ray Tomography

Dissertation

zur Erlangung des Grades des
Doktors der Naturwissenschaften
der Fakultät Mathematik und Informatik
der Universität des Saarlandes

von

Jonas Vogelgesang

Saarbrücken
2020

Tag des Kolloquiums:	26. Juni 2020
Dekan:	Prof. Dr. Thomas Schuster
Vorsitzender:	Prof. Dr. Sergej Rjasanow
Berichterstatter:	Prof. Dr. Dr. h.c. mult. Alfred K. Louis
	Prof. Ming Jiang, Ph.D.
Akademische Mitarbeiterin:	Dr. Anne Wald

Contents

Abstract

The goal of computerized tomography is to gain knowledge about the inner structure of an object by non-invasive resp. non-destructive measurements. Therefore, X-rays are sent through the object to be inspected and the decrease in intensity of the rays after leaving the object is measured. Despite a large number of extensively studied methods for the reconstruction of the measured data exists, they can only be used to a limited extent in many practical applications due to non-regular measurement geometries or incomplete data. For the systematic investigation of this problem, iterative methods based on a semi-discrete operator model are proposed. These methods, in particular the semi-discrete Landweber-Kaczmarz method and the semi-discrete Kaczmarz method, are investigated in a general setting for solving systems of linear operator equations. Subsequently, the presented methods are applied to the reconstruction problem in CT and verified by numerical simulations with synthetic and measured data. Particularly Voxel and generalized Kaiser-Bessel window functions (Lewitt-Blobs) are investigated as possible basis functions. Finally, the incorporation of *a priori* information in the operator model is considered and the SART (Simultaneous Algebraic Reconstruction Technique) is discussed as a special case of the semi-discrete iteration methods.

Zusammenfassung

Das Ziel der Computertomographie (CT) ist es, durch nicht-invasives bzw. zerstörungsfreies Messen Erkenntnisse über die innere Struktur eines Objekts zu gewinnen. Dabei werden Röntgenstrahlen durch das zu inspizierende Objekt geschickt und die Intensitätsabnahme der Strahlen nach Verlassen des Objekts gemessen. Trotz einer Vielzahl an umfassend untersuchten Methoden zur Rekonstruktion der gemessenen Daten, können diese in vielen praktischen Anwendungen aufgrund nicht-regulärer Messgeometrien oder unvollständigen Daten nur begrenzt eingesetzt werden. Zur systematischen Untersuchung dieser Problemstellung werden in dieser Arbeit iterative Verfahren auf der Basis eines semi-diskreten Operatormodells vorgestellt. Diese Verfahren, im Speziellen das semi-diskrete Landweber-Kaczmarz Verfahren und das semi-diskrete Kaczmarz Verfahren, werden zunächst in einem allgemeinen Rahmen zur Lösung von Systemen linearer Operatorgleichungen untersucht. Anschließend werden die vorgestellten Verfahren auf das Rekonstruktionsproblem in der CT angewandt und durch numerische Simulationen mit synthetischen und gemessenen Daten verifiziert. Dabei werden speziell Voxel und verallgemeinerte Kaiser-Bessel Fensterfunktionen (Lewitt-Blobs) als mögliche Basisfunktionen untersucht. Abschließend wird die Einbeziehung von *a priori* Informationen in das Operatormodell betrachtet und das SART (Simultaneous Algebraic Reconstruction Technique) als Spezialfall der semi-diskreten Iterationsverfahren diskutiert.

Acknowledgments/Danksagung

An dieser Stelle möchte ich mich bei allen Menschen bedanken, die mich während meines Studiums und speziell während meiner Promotionszeit an der Universität des Saarlandes unterstützt und begleitet haben.

An erster Stelle gilt mein Dank meinem Betreuer Herrn Univ.-Prof. Dr. rer. nat. Dr. h.c. mult. Alfred K. Louis, der mich zu meinem Promotionsvorhaben ermutigt und motiviert hat, und dieses überhaupt erst ermöglicht hat. Während meiner Zeit als Doktorand und wissenschaftlicher Mitarbeiter hat er sich stets dafür eingesetzt, dass ich unter besten Bedingungen forschen kann. Er hat mir ermöglicht an internationalen Konferenzen teilzunehmen und dort über meine Forschung zu berichten. Auch nach meiner Zeit als wissenschaftlicher Mitarbeiter an der Universität des Saarlandes war er stets um mein Promotionsvorhaben bemüht.

I also want to thank Professor Ming Jiang for his advices, his hospitality and the opportunity to visit Peking university. I would also like to thank him for being the co-referee of this thesis.

Außerdem möchte ich mich bei allen ehemaligen Kollegen des Lehrstuhls von Herrn Prof. Louis bedanken, die mich schon als Student während meines Bachelor- und Masterstudiums herzlichst aufgenommen haben und mir stets mit Rat und Tat zur Seite standen. Mein besonderer Dank gilt dabei Claudia Stoffer, Yvonne Meyer, Dr. Andreas Groh, Dr. Martin Riplinger, Dr. Gaël Rigaud, Prof. Dr. Bernadette Hahn, Dr. Holger Kohr und Dr. Aref Lakhal.

Bei den Arbeitsgruppen von Herrn Univ.-Prof. Dr. Thomas Schuster und Herrn Univ.-Prof. Dr. Sergej Rjasanow bedank ich mich für die angenehme Arbeitsatmosphäre und Zusammenarbeit, insbesondere bei Dr. Anne Wald, Dr. Steffen Weißer, Dr. Christian Michel, Dimitri Rothermel, Rebecca Klein, und ganz besonders bei Prof. Thomas Schuster und Prof. Sergej Rjasanow für die Unterstützung.

Für die angenehme und freundschaftliche Zusammenarbeit mit Herrn Dr. Christian Schorr bedanke ich mich ebenfalls herzlich.

Ein ganz besonderes Dankeschön geht an Dr. Andreas Groh, der mich stets ermutigt hat und an mich geglaubt hat.

Zuletzt, aber dafür umso mehr, bedanke ich mich aus tiefstem Herzen bei meinen Eltern Gudrun und Robert Vogelgesang, meinem Bruder Jann, meinem Neffen und Patensohn Elias, und bei meinen Freunden Jan Amann und Joscha Meinck für die unendliche Unterstützung. Ohne diese Unterstützung und Euren Rückhalt wäre diese Arbeit nicht möglich gewesen.

Chapter 1

Introduction

Computerized Tomography (CT) is a very important imaging modality in analyzing the inner structure of a certain object without damaging the inspected specimen. In medical imaging, CT applications provide powerful non-invasive techniques to have insights in the human body, e.g. to create diagnoses without the need of surgery, as a preliminary step or even during surgeries. In non-destructive testing (NDT), a possible application could be the determination of porosity and air inclusions in the inspected specimen [Hah+13], determining cracks in printed circuit boards [VS16], fibers in fiber-reinforced plastics [VS17] production, etc.

Typically, a CT measurement setup in NDT consists of the X-ray source and the X-ray detector serving as the counterpart measuring the X-ray intensity. Most likely, a rotation table is located between the source and the detector. During the measurement X-rays are sent from the X-ray source through the object which is placed on the rotation table to the detector measuring the intensity. Knowing the initial intensity of the rays at the X-ray source the intensity loss can be determined. Some applications suffer from incomplete data caused by the dimensions of the inspected object. For example large objects or high magnification ratios prevent a full rotation of the object due to a risk of collision with the scanning device. Moreover, some applications make it also inevitable to use a different scanning setup as for example the inspection of large objects with extremely differing diameters in transversal and longitudinal direction. A more general but related scanning setup is used in Computed Laminography (CL). In contrast to the CT scanning setup, the central ray of the CL scanning device is not perpendicular to the rotation axis of the object. Per definition this concept leads to limited data problems.

Mathematically, these applications need a special treatment since many conventional methods are not readily applicable, for example due to the non-regularity of the utilized scanning curves, extremely under-determined problems [SM13], and so on. A quite widely used approach is to model the underlying scanning process as a fully-discretized matrix vector multiplication with a matrix A describing the scanning procedure. The arising finite-dimensional linear system

$$Ax = b$$

is then solved for some measured data described by the vector b. Classical methods to solve these finite dimensional linear systems are for example the algebraic reconstruction techniques with its presumably most prominent example ART (Algebraic Reconstruction Technique) [GBH70], sometimes also referred to as Kaczmarz iteration, and the SART (Simultaneous Algebraic Reconstruction Technique) [AK84]. In general, these methods yield good results and being extremely flexible to handle thus allowing to incorporate additional or prior knowledge into the reconstruction process. Though, a drawback of this fully-discretized model is the loss of the structure of the underlying problem and analytical properties of the underlying operator.

In this thesis, we propose a semi-discrete framework to overcome these drawbacks but keep the flexibility of the iteration methods. Our approach consists of three parts as follows:

(i) A semi-discrete data model,

(ii) formulating a semi-discrete reconstruction problem and

(iii) solving the semi-discrete problem iteratively.

Step (ii) and (iii) will be referred to as *semi-discrete iteration methods*. In the following, these steps are briefly explained.

Semi-discrete data model

The problem describing the reconstruction process is classically formulated as

$$\mathcal{A}f = g$$

where $\mathcal{A}$ describes the continuous model such as the Radon transform, the X-ray transform or the Cone Beam transform and the right-hand side g denotes the data. For applying analytical methods [Lou16], methods of filtered back-projection type as the FDK [FDK84] or the method of the approximate inverse, cf. [Lou03] and [LWT08], the data g is usually assumed to be continuous on the detector. Moreover, there must be certain conditions on the data acquisition fulfill such as the Tuy condition [Tuy83] or the Louis condition [Lou16]. In limited data applications, in particular the CL applications, these conditions are not fulfilled. On the other side of the reconstruction method spectrum there are the algebraic methods or iterative methods based on fully-discrete data.

We will proceed with an approach that assumes the data g to be given for a discrete set of X-ray source positions but continuously on the detector. For the scanning system above, we assume that the data is given as

$$g(a_i, \eta_l) \quad \text{for } \{a_i\}_{i\in I} \subset \Gamma \text{ and } \{\eta_l\}_l \subset E_{a_i}$$

where Γ usually denotes a great circle describing the positions of the X-ray source and E_{a_i} denotes the detector in dependence of the X-ray source positions a_i, $i \in I$. Throughout the thesis, I is of finite dimension. Our data model will be as follows: Instead of a prescribed path on a curve Γ we assume that the data is given for arbitrary discrete source positions $a_i \in \mathbb{R}^3$. At the same time, we assume that the data is given continuously on the detector. This yields a system of linear operator equations,

$$\mathcal{A}_i f = g_i \qquad i \in I$$

with $g_i(\eta) := g(a_i, \eta)$. In other words, every X-ray source position is considered as a separately taken measurement. On one hand, we obtain a model which is completely independent of a given source curve Γ but on the other hand still includes the characteristics of the underlying transforms.

Semi-discrete operator model

In a second step, we consider a semi-discrete model of the operators $\mathcal{A}_i$ by approximating the elements in the solution space, i.e., the operator domain by a finite dimensional space. In particular, these finite dimensional spaces are generated by a set of locally supported basis functions $\{b_j\}_{j\in J}$ such that

$$f \approx \sum_j f_j b_j. \tag{1.1}$$

Due to the linearity of the considered operators $\mathcal{A}$, the operator can immediately be transferred to the basis functions

$$\mathcal{A}f \approx \sum_j f_j \mathcal{A}b_j$$

such that we obtain a mapping on the coefficient space of the basis representation (1.1). In the context of this thesis there are two important basis functions:

(i) Voxel basis function (characteristic function),

(ii) Lewitt-Blob basis function (Generalized Kaiser-Bessel windows functions), cf. [Lew90].

Whereas the Voxel (resp. Pixel) basis function describes the classical image basis, being orthogonal and providing fast algorithms for its use in image reconstruction and computer graphics, the Blob basis function is designed and optimized for the application in image reconstruction problems, being rotationally invariant and providing closed formulas for its forward transform.

Iterative methods

We discuss iterative methods within this semi-discrete framework and their application in X-ray tomography. These iteration methods will basically consist of computing a virtual projection by applying the forward operator $\boldsymbol{A}_i$, and a correction step with applying a backward operator Ψ_i,

$$\boldsymbol{f}^{m+1} = \boldsymbol{f}^m + \Psi_i\left(g_i - \boldsymbol{A}_i \boldsymbol{f}^m\right) \qquad i \in I.$$

In particular, the

(i) the *Kaczmarz* method and

(ii) the *Landweber–Kaczmarz* method

will be considered. The Kaczmarz method, originally formulated in [Kac37] in the context of solving systems of linear equations in finite dimensions, has been found to be a powerful method in image reconstruction from tomographic data. It was independently introduced in image reconstruction by [GBH70] as the *Algebraic Reconstruction Technique* (ART) for solving the fully discretized integral equation and by [Hou73] where it served as reconstruction method in the first commercially available CT scanners (for more detailed information on Kaczmarz' method in image reconstruction, we refer to [Nat01] and the references therein). The Kaczmarz method will be defined for a positive relaxation factor $\lambda_k > 0$ by the backward operator

$$\Psi_k := \lambda_k \boldsymbol{A}_k^+.$$

Using theorem 2.21 the backward operator can be written as $\Psi_k = \lambda_k \boldsymbol{A}_k^*(\boldsymbol{A}_k \boldsymbol{A}_k^*)^+$ and particularly $\Psi_k = \lambda_k \boldsymbol{A}_k^*(\boldsymbol{A}_k \boldsymbol{A}_k^*)^{-1}$ for surjective operators $\boldsymbol{A}_k$. The classical defintion of the Kaczmarz method as used in [Nat01] and [NW01] thus coincides with the presented backward operator Ψ_k.

The Landweber-Kaczmarz method was proposed in the context of non-linear inverse problems in [KS02]. The backward operators Ψ_k are given by

$$\Psi_k := \lambda_k \boldsymbol{A}_k^*$$

for some positive relaxation factor $\lambda_k > 0$. The reconstruction problem is processed cyclically as it is done for the classical Kaczmarz method.

Necessary mathematical basics and results for the studies presented in this thesis are introduced in chapter 2. In particular, the fixed-point theory going back to Banach is introduced being a main argument in the convergence analysis of the proposed semi-discrete iteration methods. Further, the concept of weighted Hilbert spaces and the generalized inverse is introduced. Both concepts represent a major part of the semi-discrete framework which is introduced in chapter 4 and chapter 5.

In chapter 3, the definition of the classical Radon transform and the X-Ray transform and its closely related Cone Beam transforms for a fixed X-Ray source position resp. direction are recalled. We study the boundedness of the mentioned transforms with respect to weighted Hilbert spaces figuring out similarities for all these transforms.

The main theoretical concept of this work namely the semi-discrete iteration methods is introduced and analyzed in chapter 4 and chapter 5. Assuming the semi-discrete data model throughout the rest of this thesis, the semi-discrete iteration methods consist of two parts:

(i) The semi-discrete model is introduced and discussed in chapter 4. The approximation and convergence properties are analyzed in the context of the least-squares projection method.

(ii) An iteration scheme based on the semi-discrete forward operator and a backward operator is introduced in chapter 5. The convergence properties are investigated under general assumptions on the backward operator. In particular, the semi-discrete Landweber-Kaczmarz and the semi-discrete Kaczmarz methods are introduced and analyzed.

This concept is applied to X-Ray tomography in chapter 6. Based on the Voxel and the Lewitt-Blob basis a semi-discrete model for the application in X-Ray tomography is proposed and approximation properties investigated. The semi-discrete iteration methods are applied to the reconstruction problem for parallel scanning geometries and Cone Beam geometries with flat detectors, respectively, and convergence is shown. Finally, the iteration methods are applied for the parallel geometry to synthetic data generated for the Shepp-Logan head phantom [SL74] and measured data from a Synchrotron application. For the Cone Beam geometry the semi-discrete Landweber-Kaczmarz method is applied to measured data of a walnut [Häm+15a; Häm+15b].

Publications

The following articles were published during the work on this thesis.

[VS16] J. Vogelgesang and C. Schorr. “A Semi-Discrete Landweber-Kaczmarz Method for Cone Beam Tomography and Laminography Exploiting Geometric Prior Information”. *Sensing and Imaging* 17(1), 2016.

[Tra+17] P. Trampert, J. Vogelgesang, C. Schorr, M. Maisl, S. Bogachev, N. Marniok, A. Louis, T. Dahmen, and P. Slusallek. “Spherically symmetric volume elements as basis functions for image reconstructions in computed laminography”. *Journal of X-Ray Science and Technology* 25(4): 533–546, 2017.

[VS17] J. Vogelgesang and C. Schorr. “Iterative Region-of-Interest Reconstruction from Limited Data Using Prior Information”. *Sensing and Imaging* 18(1), 2017.

[Vog19] J. Vogelgesang. “A semi-discrete iteration method in X-ray tomography”. *Oberwolfach Reports.*, 2019.

Chapter 2

Mathematical Preliminaries

2.1 The Fourier transform

In this section, we briefly introduce the Fourier transform on the space of square-integrable functions $L_2(\mathbb{R}^d)$. The Fourier transform will play an important role in the analysis of the approximation quality of the basis functions and thus their efficiency. We will first have a short look at the Bessel function J_ν of the first kind and the modified Bessel function I_ν of the first kind. Both functions are intensively studied in literature and play an enormously important role in mathematical physics. In this thesis, the Bessel function appears as a key feature in the definition of the generalized Kaiser-Bessel window functions (Lewitt-Blobs) and the computation of their Fourier transform. As a general references for Bessel functions we give [AS65], [Wat95] and [AW05], for the Fourier transform we give [Wer18] and [Sne95]. The use of Bessel functions and the Fourier transform in the context of Computerized Tomography can be found in [Nat01].

Definition 2.1 (cf. [AS65, 9.6.10]). *Let $\nu \in \mathbb{R}$. The Bessel function (of the first kind) of the order ν is defined by the convergent series*

$$J_\nu(x) = \left(\frac{x}{2}\right)^\nu \sum_{l=0}^{\infty} \frac{(-1)^l}{l!\,\Gamma(\nu + l + 1)} \left(\frac{x}{2}\right)^{2l}$$

and the modified Bessel function (of the first kind) of the order ν by

$$I_\nu(x) = \left(\frac{x}{2}\right)^\nu \sum_{l=0}^{\infty} \frac{1}{l!\,\Gamma(\nu + l + 1)} \left(\frac{x}{2}\right)^{2l}.$$

We obtain the following properties of the Bessel function and the modified Bessel function.

Lemma 2.2. *(i) Let $m \in \mathbb{Z}$ and $\nu \in \mathbb{R}$. It holds*

$$J_{-m}(z) = (-1)^m J_m(z) \qquad \text{and} \qquad J_\nu(iz) = i^\nu I_\nu(z).$$

(ii) Let $d \in \mathbb{N} \setminus \{0\}$

$$J_{\frac{d}{2}-1}(\|x\|) = (2\pi)^{-\frac{d}{2}} \|x\|^{\frac{d}{2}-1} \int_{S^{d-1}} e^{ix^\top \omega}\, d\omega.$$

Proof. (i) See [AS65, Eqn. 9.1.5] and [AS65, Eqn. 9.6.3].

(ii) The result can be shown using the identity

$$\int_{S^{d-1}} \mathrm{e}^{i\sigma\theta^\top\omega}\, Y_l(\omega)\, d\omega = (2\pi)^{\frac{d}{2}}\, i^l\, \sigma^{-\left(\frac{d}{2}-1\right)}\, J_{l+\frac{d}{2}-1}(\sigma)\, Y_l(\theta) \qquad \theta \in S^{d-1}$$

as stated in [Nat01, VII, Eqn. (3.19)] where Y_l denotes spherical harmonics of degree l, see e.g. [Mül66; AW05]. For $l = 0$ it holds $Y_0 = 1$ and thus

$$J_{\frac{d}{2}-1}(\sigma) = (2\pi)^{-\frac{d}{2}} \sigma^{\left(\frac{d}{2}-1\right)} \int_{S^{d-1}} \mathrm{e}^{i\sigma\theta^\top\omega}\, d\omega.$$

For $x := \sigma\theta$, $\sigma = \|x\|$, follows the result.

□

Lemma 2.3. *(i) (Sonine's first finite integral). Let $m \in \mathbb{N}_0$. It holds,*

$$\left(\frac{2z}{\pi}\right)^{\frac{1}{2}} \int_0^{\frac{\pi}{2}} J_m(z\sin\theta)\, \sin^{m+1}\theta\, d\theta = J_{m+\frac{1}{2}}(z)$$

and

$$\left(\frac{2z}{\pi}\right)^{\frac{1}{2}} \int_0^{\frac{\pi}{2}} I_m(z\sin\theta)\, \sin^{m+1}\theta\, d\theta = I_{m+\frac{1}{2}}(z).$$

(ii) (Sonine's second finite integral). Let $\mathrm{Re}(\mu), \mathrm{Re}(\nu) > -1$. It holds,

$$\int_0^{\frac{\pi}{2}} \cos^{\nu+1}\theta\, \sin^{\mu+1}\theta\, J_\mu(z\sin\theta)\, J_\nu(Z\cos\theta)\, d\theta = \frac{z^\mu Z^\nu J_{\mu+\nu+1}\left(\sqrt{Z^2+z^2}\right)}{\left(\sqrt{Z^2+z^2}\right)^{\mu+\nu+1}}.$$

Proof. (i) Putting $\mu = -m$, we obtain

$$\left(\frac{2z}{\pi}\right)^{\frac{1}{2}} \int_0^{\frac{\pi}{2}} J_{-m}(z\sin\theta)\, \sin^{m+1}\theta\, d\theta = \mathcal{H}_{-(m+\frac{1}{2})}(z)$$

from lemma 2.2(i) and [Wat95, 12.11, p. 374, Eqn. (3)]. $\mathcal{H}_\nu$ denotes the Struve function, cf. [AS65, Chapt. 12]. With the identity

$$\mathcal{H}_{-(m+\frac{1}{2})}(z) = (-1)^m J_{m+\frac{1}{2}}(z)$$

from [AS65, Eqn. 12.1.15] and lemma 2.2 follows Sonine's first finite integral.

(ii) See [Wat95, 12.13, p. 376, Eqn. (1)].

□

Definition 2.4. *The Fourier Transform of $f \in \mathcal{S}(\mathbb{R}^d)$ is defined as*

$$\mathcal{F}f(\xi) = \hat{f}(\xi) = (2\pi)^{-\frac{d}{2}} \int_{\mathbb{R}^d} f(x)\, \mathrm{e}^{-ix^\top\xi}\, dx.$$

Theorem 2.5 ([Wer18, Thm. V.2.8]). *The Fourier transform $\mathcal{F} : \mathcal{S}(\mathbb{R}^d) \to \mathcal{S}(\mathbb{R}^d)$ is a bijection with*

$$\mathcal{F}^{-1} f(x) = (2\pi)^{-\frac{d}{2}} \int_{\mathbb{R}^d} f(\xi)\, \mathrm{e}^{ix^\top \xi}\, d\xi.$$

Further,

$$\langle \hat{f}, \hat{g} \rangle_{L_2(\mathbb{R}^d)} = \langle f, g \rangle_{L_2(\mathbb{R}^d)} \qquad \forall f, g, \in \mathcal{S}(\mathbb{R}^d).$$

Based on the denseness of the Schwartz space $\mathcal{S}(\mathbb{R})$ in $L_2(\mathbb{R}^d)$, cf. [Wer18, Lem. V.1.10], the Fourier transform can be continued due to Plancharel's equation as an isometry on $L_2(\mathbb{R}^d)$, i.e.,

$$\langle \hat{f}, \hat{g} \rangle_{L_2(\mathbb{R}^d)} = \langle f, g \rangle_{L_2(\mathbb{R}^d)} \qquad \forall f, g, \in L_2(\mathbb{R}^d).$$

In the following, we will identify the Fourier transform with its continuation on $L_2(\mathbb{R}^d)$.

Lemma 2.6. *The Fourier transform of a rotationally symmetric function $f \in L_2(\mathbb{R}^d)$ is computed as*

$$\hat{f}(\xi) = \|\xi\|^{1-\frac{d}{2}} \int_0^\infty r^{\frac{d}{2}} f(r) J_{\frac{d}{2}-1}(r\|\xi\|)\, dr.$$

The Fourier transform $\hat{f}$ is again rotationally symmetric.

Proof. Let $f \in L_2(\mathbb{R}^d)$ be rotationally symmetric. It

$$\begin{aligned}
\hat{f}(\xi) &= (2\pi)^{-\frac{d}{2}} \int_{\mathbb{R}^d} f(x)\, \mathrm{e}^{-ix^\top \xi}\, dx \\
&= (2\pi)^{-\frac{d}{2}} \int_0^\infty \int_{S^{d-1}} f(r)\, \mathrm{e}^{-ir\theta^\top \xi}\, r^{d-1}\, d\theta\, dr \\
&= (2\pi)^{-\frac{d}{2}} \int_0^\infty r^{d-1} f(r) \int_{S^{d-1}} \mathrm{e}^{-ir\theta^\top \xi}\, d\theta\, dr \\
&= \int_0^\infty r^{d-1} f(r)\, (r\|\xi\|)^{-\left(\frac{d}{2}-1\right)} J_{\frac{d}{2}-1}(r\|\xi\|)\, dr \\
&= \|\xi\|^{1-\frac{d}{2}} \int_0^\infty r^{\frac{d}{2}} f(r) J_{\frac{d}{2}-1}(r\|\xi\|)\, dr
\end{aligned}$$

where we used the identity of lemma 2.2(ii). □

Remark. *The Fourier transform of a rotationally symmetric function $f \in L_2(\mathbb{R}^d)$ is closely related to the Hankel transform defined by*

$$H_\nu f(\rho) = \int_0^\infty r f(r) J_\nu(\rho r)\, dr,$$

cf. [Sne95, Sec. 10]. In two dimensions, i.e. $d = 2$, the Fourier transform is equal to the Hankel transform $H_0 f$ of order 0, cf. [Sne95, Sec. 11].

2.2 Banach's fixed-point theorem

The classical fixed-point theorem of Banach and the closely related theorem of C. Neumann play both an important role for the convergence analysis of the studied iteration methods.

Definition 2.7 (Contraction, Lipschitz constant L). *Let $(\mathcal{M}, d)$ be a metricc space and $\Phi : \mathcal{M} \to \mathcal{M}$. Further, let $L < 1$ be a constant such that*

$$d(\Phi(x), \Phi(y)) \leq L\, d(x, y) \qquad \forall x, y \in \mathcal{M}.$$

Then, Φ is called a contraction.

We cite *Banach's fixed-point theorem* which is also referred to as *Contraction Theorem*.

Theorem 2.8 (Banach's fixed-point Theorem). *Let $(\mathcal{M}, d)$ be a complete metric space with $\mathcal{M} \neq \emptyset$ and let $\Phi : \mathcal{M} \to \mathcal{M}$ be a contraction with constant $L < 1$. Then, there exists a unique fixed-point $x^* \in \mathcal{M}$ of Φ and the fixed-point iteration*

$$x_{m+1} = \Phi(x_m)$$

converges for $m \to \infty$ to x^* for arbitrary initial values $x_0 \in \mathcal{M}$. The rate of convergence is linear and we obtain the following error estimates:

(i) A priori *error estimate:*

$$d(\boldsymbol{f}^m, \boldsymbol{f}^*) \leq \frac{L^m}{1-L}\, d(\boldsymbol{f}^1, \boldsymbol{f}^0).$$

(ii) A posteriori *error estimate:*

$$d(\boldsymbol{f}^m, \boldsymbol{f}^*) \leq \frac{L}{1-L}\, d(\boldsymbol{f}^m, \boldsymbol{f}^{m-1}).$$

Proof. A proof of this result can be found in various literature on calculus and functional analysis, see for example [Rud76, Thm. 9.23], [Kre78, Chapter 5.1] or [Wer18, Section IV.7]. For the error estimation, we find

$$\begin{aligned} d(\boldsymbol{f}^m, \boldsymbol{f}^*) &\leq d(\boldsymbol{f}^m, \Phi(\boldsymbol{f}^m)) + d(\Phi(\boldsymbol{f}^m), \boldsymbol{f}^*) \\ &= d(\Phi(\boldsymbol{f}^{m-1}), \Phi(\boldsymbol{f}^m)) + d(\Phi(\boldsymbol{f}^m), \Phi(\boldsymbol{f}^*)) \\ &\leq L \cdot d(\boldsymbol{f}^{m-1}, \boldsymbol{f}^m) + L \cdot d(\boldsymbol{f}^m, \boldsymbol{f}^*) \end{aligned}$$

and the *a posteriori* estimate follows immediately. The *a priori* estimate follows with

$$d(\boldsymbol{f}^m, \boldsymbol{f}^{m-1}) = d(\boldsymbol{G}^{m-1}(\boldsymbol{f}^1), \boldsymbol{G}^{m-1}(\boldsymbol{f}^0)) \leq L^{m-1} \cdot (\boldsymbol{f}^1, \boldsymbol{f}^0).$$

□

Additionally, we need the following result which is also referred to as *C. Neumann's Theorem*. We cite a slightly modified version adapted to our needs.

Theorem 2.9 (Theorem of C. Neumann). *Let $(\mathcal{X}, \|\cdot\|)$ be a Banach space and $T \in \mathcal{L}(\mathcal{X})$ be a bounded operator with $\|T\| < 1$. Then, the operator $\mathrm{id} - T$ has a unique bounded linear inverse which is given by the (convergent) Neumann series*

$$(\mathrm{id} - T^{-1}) = \sum_{k=0}^{\infty} T^k.$$

Further, the estimate

$$\|(\mathrm{id} - T)^{-1}\| \leq (1 - \|T\|)^{-1}$$

holds.

Proof. A proof can be found in [Wer18, Theorem II.1.12] and [Yos95, II.1, Thm. 2]. □

2.3 Weighted Hilbert spaces

Let X and Y be real Hilbert spaces equipped with the inner products $\langle\cdot,\cdot\rangle_X$ and $\langle\cdot,\cdot\rangle_Y$, respectively. The bounded linear operators from X to Y are denoted by $\mathcal{L}(X,Y)$ and we define $\mathcal{L}(X) \coloneqq \mathcal{L}(X,X)$

Further, we consider the direct sum of Hilbert spaces, cf. [Con94, I, §6] and [Aub00, Sect. 5.8]: For a set of real Hilbert spaces $\{H_i\}_{i\in I}$ its direct sum (or also orthogonal sum) is defined as

$$H \coloneqq \bigoplus_{i\in I} H_i = \left\{ g = (g_i)_{i\in I} \in (H_1 \times \ldots H_{|I|}) : \sum_{i\in I} \|g_i\|_{H_i}^2 < \infty \right\}.$$

Equipped with the inner product

$$\langle g, h\rangle_H \coloneqq \sum_{i\in I} \langle g_i, h_i\rangle_{H_i} \quad \forall g, h \in H \tag{2.1}$$

H is again a real Hilbert space, cf. [Con94]. The norm on H is induced by the inner product (2.1) and is thus given as

$$\|g\|_H \coloneqq \sqrt{\langle g, g\rangle_H} = \sqrt{\sum_{i\in I} \|g_i\|_{H_i}^2}. \tag{2.2}$$

We introduce the concept of positive operators on Hilbert spaces which represents the prototype of linear operators inducing weighted Hilbert spaces.

Definition 2.10 (Positive operator). *Let $T \in \mathcal{L}(X)$ be self-adjoint, i.e., $T^* = T$. The operator T is called* positive *if*

$$\langle x, Tx\rangle \geq 0 \quad \forall x \in X.$$

Theorem 2.11. *(i) For every positive operator T exists an unique positive operator $T^{\frac{1}{2}} \in \mathcal{L}(X)$ with*

$$(T^{\frac{1}{2}})^2 = T^{\frac{1}{2}} T^{\frac{1}{2}} = T.$$

If T is invertible then the square root operator $T^{\frac{1}{2}}$ is again invertible.

(ii) Every bijective positive operator $T \in \mathcal{L}(X)$ induces an inner product on X by

$$\langle \cdot, \cdot \rangle_T := \langle \cdot, T \cdot \rangle.$$

The Hilbert space X equipped with the weighted inner product $\langle \cdot, \cdot \rangle_T$ forms again a Hilbert space and the induced norm is given by

$$\| \cdot \|_T = \| T^{\frac{1}{2}} \cdot \|.$$

It is called weighted Hilbert space and denoted by $\left(X, \langle \cdot, \cdot \rangle_T\right)$.

Proof. (i) See [Con94, II. Theorem 7.16] and [Rud91, Theorem 12.33].

(ii) Let $T \in \mathcal{L}(X)$ be a bijective positive operator. Thus T is bounded, linear and self-adjoint by definition 2.10. The weighted inner product $\langle \cdot, \cdot \rangle_T$ fulfills the definition of an inner product on X, see e.g. [Con94] or [Wer18]. Following lemma 2.11(i), the unique square root operator of T exists and is positive. In particular, $T^{\frac{1}{2}}$ is self-adjoint. Thus, it yields

$$\| \cdot \|_T = \sqrt{\langle \cdot, T \cdot \rangle} = \sqrt{\left\langle T^{\frac{1}{2}} \cdot, T^{\frac{1}{2}} \cdot \right\rangle} = \| T^{\frac{1}{2}} \cdot \|.$$

Finally, it remains to show that X together with the weighted inner product $\langle \cdot, \cdot \rangle_T$ is again a Hilbert space. Since

$$\|x\|_T = \|T^{\frac{1}{2}} x\| \leq \|T^{\frac{1}{2}}\| \, \|x\|$$

holds true for all $x \in X$, the statement follows immediately from the fact that X is complete with respect to the induced norm $\| \cdot \|$.

□

We use the following notation. Let $T_X \in \mathcal{L}(X)$ and $T_Y \in \mathcal{L}(Y)$ be bijective positive operators. The operator norm of $A \in \mathcal{L}(X, Y)$ and in particular the weighted operator norm are given as

$$\|A\|_{X \to Y} = \sup_{x \neq 0} \frac{\|Ax\|_Y}{\|x\|_X} = \sup_{\|x\|_X = 1} \|Ax\|_Y$$

and

$$\|A\|_{(X, T_X) \to (Y, T_Y)} = \sup_{x \neq 0} \frac{\|Ax\|_{T_Y}}{\|x\|_{T_X}} = \sup_{\|x\|_{T_X} = 1} \|Ax\|_{T_Y},$$

respectively. We write $\|A\|$ if it is clear from the context which operator norm is used.

Lemma 2.12. *Let X and Y be real Hilbert spaces and let T_X and T_Y be bijective and positive operators on X and Y, respectively. For $A \in \mathcal{L}(X, Y)$ holds*

$$\|A\|_{(X, T_X) \to (Y, T_Y)} \leq \|T_Y^{\frac{1}{2}}\|_Y \, \|A\|_{X \to Y} \, \|T_X^{-\frac{1}{2}}\|_X.$$

Proof. Let $\varphi \in X$. Then,

$$\begin{aligned} \|A\varphi\|_{(Y, T_Y)} &= \|T_Y^{\frac{1}{2}} A\varphi\|_Y \\ &\leq \|T_Y^{\frac{1}{2}}\|_Y \, \|A\varphi\|_Y \\ &\leq \|T_Y^{\frac{1}{2}}\|_Y \, \|A\|_{X \to Y} \, \|\varphi\|_X \end{aligned}$$

$$
\begin{aligned}
&= \|T_Y^{\frac{1}{2}}\|_Y \, \|A\|_{X\to Y} \, \|T_X^{-\frac{1}{2}} T_X^{\frac{1}{2}} \varphi\|_X \\
&\leq \|T_Y^{\frac{1}{2}}\|_Y \, \|A\|_{X\to Y} \, \|T_Y^{-\frac{1}{2}}\|_Y \|T_X^{\frac{1}{2}} \varphi\|_X \\
&= \|T_Y^{\frac{1}{2}}\|_Y \, \|A\|_{X\to Y} \, \|T_Y^{-\frac{1}{2}}\|_Y \|\varphi\|_{(X,T_X)}.
\end{aligned}
$$

□

The condition number of a bounded linear operator $A \in \mathcal{L}(X,Y)$ with bounded inverse is defined as

$$\kappa(A) := \|A\| \|A^{-1}\|.$$

In section 2.4, the condition number is extended to a more general class of bounded linear operators. The condition number with respect to weighted norms will be indicated with a subscript, e.g. κ_T for the weighted norm $\|\cdot\|_T$.

Theorem 2.13. *Let $T : X \to X$ be bijective and positive. For the induced operator norms $\|\cdot\|$ and $\|\cdot\|_T$ holds:*

(i) Let $l \in \{\pm 1, \pm\frac{1}{2}\}$ be fixed. Then,

$$\|T^l\| = \|T^l\|_T.$$

(ii) The operator norms are equivalent with

$$\frac{1}{\kappa(T^{\frac{1}{2}})} \|A\|_T \leq \|A\| \leq \kappa(T^{\frac{1}{2}}) \|A\|_T$$

for all $A \in \mathcal{L}(X)$.

Proof. Since T is a bijective and positive operator, it follows from Theorem 2.11(ii) that T induces an inner product and thus a weighted norm on X by

$$\langle \cdot, \cdot \rangle_T = \langle \cdot, T \cdot \rangle \qquad \text{and} \qquad \|\cdot\|_T = \|T^{\frac{1}{2}} \cdot\|,$$

respectively. Further, T is bounded. The bounded inverse theorem, cf. [Rud91], now states the existence of the inverse operator T^{-1} and that T^{-1} is bounded. Thus, T^l is bounded for $l \in \{\pm 1, \pm\frac{1}{2}\}$.

(i) Together with lemma 2.11(i) follows

$$
\begin{aligned}
\|T^l\|_T &= \sup_{\|x\|_T = 1} \|T^l x\|_T \\
&= \sup_{\|T^{\frac{1}{2}} x\| = 1} \|T^{\frac{1}{2}} T^l x\| \\
&= \sup_{\|T^{\frac{1}{2}} x\| = 1} \|T^l T^{\frac{1}{2}} x\| \\
&= \sup_{\|x\| = 1} \|T^l x\| \\
&= \|T^l\|.
\end{aligned}
$$

(ii) Let $A \in \mathcal{L}(X)$ be a bounded operator on X. For $f \in X$ holds

$$\|Af\| = \|T^{-\frac{1}{2}} Af\|_T = \|T^{-\frac{1}{2}} A T^{\frac{1}{2}} T^{-\frac{1}{2}} f\|_T.$$

Thus,

$$\begin{aligned}\|A\| &= \sup_{\|f\|=1} \|Af\| \\ &= \sup_{\|f\|=1} \|T^{-\frac{1}{2}} A T^{\frac{1}{2}} T^{-\frac{1}{2}} f\|_T \\ &= \sup_{\|f\|_T=1} \|T^{-\frac{1}{2}} A T^{\frac{1}{2}} f\|_T \\ &= \|T^{-\frac{1}{2}} A T^{\frac{1}{2}}\|_T\end{aligned}$$

and with the submultiplicativity of the norm follows

$$\|A\| \leq \|T^{-\frac{1}{2}}\|_T \, \|T^{\frac{1}{2}}\|_T \, \|A\|_T = \kappa(T^{\frac{1}{2}}) \|A\|_T.$$

Analogously, it is

$$\|A\|_T \leq \|T^{-\frac{1}{2}}\| \, \|T^{\frac{1}{2}}\| \, \|A\| = \kappa(T^{\frac{1}{2}}) \|A\|$$

and the statement follows.

□

In the situation of finite dimensional spaces, we will mainly consider the Euclidean norm

$$\|x\|_2 := \sqrt{\langle x, x \rangle} = \sqrt{x^\top y} = \left(\sum_{j=1}^{n} x_j y_j \right)^{\frac{1}{2}} \qquad \forall x \in \mathbb{R}^n.$$

The Euclidean norm induces the spectral norm on $\mathbb{R}^n$ which is defined as

$$\|A\|_2 = \sup_{x \neq 0} \frac{\|Ax\|_2}{\|x\|_2} = \sup_{\|x\|_2=1} \|Ax\|_2 \qquad \forall x \in \mathbb{R}^n$$

for $A \in \mathbb{R}^{m \times n}$ being a $m \times n$-matrix. For the spectral norm holds

$$\|A\|_2 = \sqrt{\lambda_{\max}(A^* A)}$$

where $\lambda_{\max}(A^* A)$ denotes the largest Eigenvalue of $A^* A$, cf. [SK11]. For a symmetric and strictly positive definite matrix W the Euclidean norm and the induced weighted norms $\|\cdot\|_W := \|W^{\frac{1}{2}} \cdot\|$ are equivalent with

$$\frac{1}{\|W^{\frac{1}{2}}\|} \|\cdot\|_W \leq \|\cdot\| \leq \|W^{-\frac{1}{2}}\| \, \|\cdot\|_W.$$

In analogy to theorem 2.13 this follows immediately from the definition of the weighted Euclidean norm: For $x \in \mathbb{R}^n$ holds

$$\|x\| = \|W^{-\frac{1}{2}} W^{\frac{1}{2}} x\| \leq \|W^{-\frac{1}{2}}\| \, \|W^{\frac{1}{2}} x\| = \|W^{-\frac{1}{2}}\| \, \|x\|_W$$

and

$$\|x\|_W = \|W^{\frac{1}{2}} x\| \leq \|W^{\frac{1}{2}}\| \, \|x\|.$$

Corollary 2.14. *Let W be a symmetric and strictly positive definite matrix. The condition number with respect to the spectral norm $\|\cdot\|_2$ fulfills*

$$\kappa_2(W^{\frac{1}{2}}) = \sqrt{\kappa_2(W)}.$$

Proof. Since the weight matrix W is symmetric and positive definite it holds

$$(W^{\frac{1}{2}})^* W^{\frac{1}{2}} = W^{\frac{1}{2}} W^{\frac{1}{2}} = W = (W^2)^{\frac{1}{2}} = (W^* W)^{\frac{1}{2}}.$$

Thus,

$$\begin{aligned}
\kappa_2^2(W^{\frac{1}{2}}) &= \mu_{\max}((W^{\frac{1}{2}})^* W^{\frac{1}{2}})\, \mu_{\min}^{-1}((W^{\frac{1}{2}})^* W^{\frac{1}{2}}) \\
&= \mu_{\max}((W^* W)^{\frac{1}{2}})\, \mu_{\min}^{-1}((W^* W)^{\frac{1}{2}}) \\
&= (\mu_{\max}(W^* W)\, \mu_{\min}^{-1}(W^* W))^{\frac{1}{2}} \\
&= \kappa_2(W).
\end{aligned}$$

□

We give some examples of weighted Hilbert spaces.

Example 2.15. *(i) Let $X = \mathbb{R}^n$, $n \in \mathbb{N}_+$, equipped with the Euclidean inner product,*

$$\langle x, y \rangle = x^\top y = \sum_{j=1}^{n} x_j y_j.$$

In finite dimensions every symmetric and positive definite matrix W is regular (thus a bijective operator) and a positive operator in the sense of definition 2.10. The matrix W induces a weighted inner product on $\mathbb{R}^n$ by

$$\langle x, y \rangle_W = \langle x, Wy \rangle = \sum_{j=1}^{n} x_j (Wy)_j = \sum_{j=1}^{n} \left(W^{\frac{1}{2}} x\right)_j \left(W^{\frac{1}{2}} y\right)_j,$$

see theorem 2.11(ii).

(ii) Let $\Omega \subset \mathbb{R}^d$ be non-empty. The Lebesgue spaces of integrable functions on Ω are defined as

$$L_p(\Omega) := \left\{ f : \Omega \to \mathbb{R} \text{ measurable}, \ \|f\|_{L_p(\Omega)} := \left(\int_\Omega |f(x)|^p \, dx \right)^{\frac{1}{p}} < \infty \right\}.$$

For $p = 2$, the Lebesgue space $L_2(\Omega)$ equipped with the inner product

$$\langle f, g \rangle_{L_2(\Omega)} = \int_\Omega f(x) g(x) \, dx$$

forms a real Hilbert space, cf. [Yos95], [Wer18]. For $X = L_2(\Omega)$, the function $w \in L_1(\Omega)$ being positive almost-everywhere induces a weighted inner product on $L_2(\Omega)$ by

$$\langle f, g \rangle_w := \int_\Omega (fg)(x) w(x) \, dx.$$

(iii) *Now, let $X = L_2(\Omega)$ and $w \in L_\infty(\Omega)$ be an essentially bounded function on Ω being positive almost-everywhere. The function w induces a weighted inner product on $L_2(\Omega)$ by*

$$\langle f, g \rangle_w := \int_\Omega (fg)(x) w(x)\, dx.$$

This can be shown by means of the the multiplication operator $T_w : L_2(\Omega) \to L_2(\Omega)$ defined as point-wise multiplication with the weight function w,

$$T_w f(x) = (w\, f)(x),$$

and theorem 2.11(ii). First, we show that T_w is positive. Following [Con94, II, Thm. 1.5], the multiplication operator is a bounded linear operator on $L_2(\Omega)$. Additionally, T_w is self-adjoint, i.e.,

$$\left\langle f, T_w g \right\rangle_{L_2(\Omega)} = \int_\Omega f(x) g(x) w(x)\, dx = \left\langle T_w f, g \right\rangle_{L_2(\Omega)},$$

and it holds

$$\begin{aligned} \left\langle f, T_w f \right\rangle_{L_2(\Omega)} &= \int_\Omega f^2(x) w(x)\, dx \\ &= \int_\Omega (w f^2)(x)\, dx \\ &= \langle w^{\frac{1}{2}} f,\, w^{\frac{1}{2}} f \rangle_{L_2(\Omega)} \\ &= \| w^{\frac{1}{2}} f \|^2_{L_2(\Omega)} \geq 0 \qquad \forall f \in L_2(\Omega). \end{aligned}$$

Thus, T_w is positive on $L_2(\Omega)$ in the sense of definition 2.10. The bijectivity of T_w follows immediately from the positivity of the weight function w almost everywhere on Ω and that w is essentially bounded. Applying theorem 2.11(ii) now yields that

$$\langle f, g \rangle_w = \left\langle f, T_w g \right\rangle_{L_2(\Omega)} = \int_\Omega (fg)(x) w(x)\, dx$$

is a weighted inner product and that $L_2(\Omega)$ together with $\langle \cdot, \cdot \rangle_w$ forms a real Hilbert space.

2.4 The generalized inverse

Let $\mathcal{A} : \mathcal{X} \to \mathcal{Y}$ denote a bounded linear mapping between the real Hilbert spaces $\mathcal{X}$ and $\mathcal{Y}$ and let $g \in \mathcal{Y}$. Clearly, a solution of

$$\mathcal{A} f = g \tag{2.3}$$

exists only if g is an element of the range $\mathrm{R}(\mathcal{A})$. If the operator $\mathcal{A}$ is non-injective, i.e., the nullspace $\mathrm{N}(\mathcal{A})$ is non-trivial, and there are infinitely many solutions. We introduce the generalized inverse as a concept to extend the solvability of (2.3) to right-hand sides $g \in \mathcal{Y}$, see for example [Lou89], [EHN96], [Rie03].

Definition 2.16 (Generalized solution, [Lou89]). *The mapping*

$$\mathcal{A}^+ : \mathrm{D}(\mathcal{A}^+) := \mathrm{R}(\mathcal{A}) \oplus \mathrm{N}(\mathcal{A}^*) \subseteq \mathcal{Y} \to \mathcal{X}$$

characterized by

(i) $\mathcal{A}\mathcal{A}^+ = \mathrm{P}_{\overline{\mathrm{R}(\mathcal{A})}} g$ *and*

(ii) $\|\mathcal{A}^+ g\|_{\mathcal{X}} < \|u\|_{\mathcal{X}}$ *for all* $u \in \mathcal{X}$ *fulfilling*

$$\|\mathcal{A}\mathcal{A}^+ g - g\|_{\mathcal{X}} = \|\mathcal{A}u - g\| = \min \|\mathcal{A}f - g\|_{\mathcal{X}}$$

is called generalized inverse or pseudo inverse. The element $f^+ := \mathcal{A}^+ g$ *is called generalized solution of the problem* $Af = g$.

The generalized solution f^+ minimizes the defect $\mathcal{A}f - g$, i.e.,

$$\|\mathcal{A}f^+ - g\|_{\mathcal{Y}} \leq \|\mathcal{A}\varphi - g\|_{\mathcal{Y}} \qquad \forall \varphi \in \mathcal{X} \tag{2.4}$$

and marks the solution with minimal norm, i.e., for all $\varphi \neq f^+$ minimizing the defect (2.4) holds

$$\|f^+\|_{\mathcal{X}} < \|\varphi\|_{\mathcal{X}}.$$

Further, f^+ is determined as the unique solution of the normal equation

$$\mathcal{A}^*\mathcal{A}f = \mathcal{A}^* g$$

in $\mathrm{N}(\mathcal{A})^\perp$, cf. [Lou89]. If the exact solution of (2.3) exists, the generalized solution f^+ clearly coincides with the exact solution. Following [Rie03, Remark 2.1.7], the generalized solution can also be defined with respect to a given element $f_* \in \mathcal{X}$. Then, f^+ is defined as a minimizer of the defect (2.4) with minimal distance to f_*,

$$f_*^+ = \mathcal{A}^+ g + \mathrm{P}_{\mathrm{N}(\mathcal{A})} f_*. \tag{2.5}$$

The classical definition 2.16 is obtained for $f_* = 0$. The following theorem yields a criterion for the boundedness of the generalized inverse $\mathcal{A}^+$.

Theorem 2.17 ([Rie03, Theorem 2.1.8]). *The generalized inverse* $\mathcal{A}^+$ *is bounded if and only if the range of* $\mathcal{A}$ *is closed, i.e.,* $\mathrm{R}(\mathcal{A}) = \overline{\mathrm{R}(\mathcal{A})}$.

In particular, a criterion for the situation of finite dimensional spaces is needed. Therefore, we use a classical result known as Picard criterion:

Theorem 2.18 (Picard criterion, [Lou89; Rie03]). *Let* $\mathcal{A} \in \mathcal{L}(\mathcal{X}, \mathcal{Y})$ *be a compact operator with singular value system* $\{\sigma_n; v_n, u_n\}_{n\geq 0}$. *The range of* $\mathcal{A}$ *is closed if and only if*

$$\sum_{n\geq 0} \frac{\left|\langle g, u_n\rangle_{\mathcal{Y}}\right|^2}{\sigma_n^2} < \infty \qquad \forall g \in \overline{\mathrm{R}(\mathcal{A})}.$$

Corollary 2.19. *In finite dimensions the range of* $\mathcal{A}$ *is always closed, i.e.,* $\mathrm{R}(\mathcal{A}) = \overline{\mathrm{R}(\mathcal{A})}$ *and the generalized inverse* $\mathcal{A}^+$ *is bounded.*

Proof. In finite dimensions, the operator $\mathcal{A} \in \mathcal{L}(\mathcal{X}, \mathcal{Y})$ is compact. Thus, the singular system $\{\sigma_n; v_n, u_n\}_{n\geq 0}$ of $\mathcal{A}$ exists with $\sigma_n \equiv 0$ for n greater than the dimension of the finite dimensional space. The Picard criterion 2.18 is thus always fulfilled and $\mathrm{R}(\mathcal{A})$ is closed. With theorem 2.17 follows the boundedness of $\mathcal{A}^+$. □

The Moore–Penrose axioms provide a helpful tool to derive representations of the generalized inverse in terms of the operator $\mathcal{A}$.

Theorem 2.20 (Moore–Penrose axioms, [EHN96], [Rie03]). *The generalized inverse $\mathcal{A}^+$ is uniquely determined by the Moore–Penrose axioms:*

(i) $\mathcal{A} = \mathcal{A}\mathcal{A}^+\mathcal{A}$

(ii) $\mathcal{A}^+ = \mathcal{A}^+\mathcal{A}\mathcal{A}^+$

(iii) $\mathcal{A}^+\mathcal{A} = \mathrm{P}_{\mathrm{N}(\mathcal{A})^\perp}$

(iv) $\mathcal{A}\mathcal{A}^+ = \mathrm{P}_{\overline{\mathrm{R}(\mathcal{A})}}$

Corollary 2.21. *It holds $\mathcal{A}^+ = \mathcal{A}^*(\mathcal{A}\mathcal{A}^*)^+$. If $\mathcal{A}$ is surjective, then $\mathcal{A}^+ = \mathcal{A}^*(\mathcal{A}\mathcal{A}^*)^{-1}$.*

Proof. Since the Moore–Penrose Axioms are fulfilled, it holds $\mathcal{A}^* = \mathrm{P}_{\mathrm{N}(\mathcal{A})^\perp}\mathcal{A}^* = \mathcal{A}^+\mathcal{A}\mathcal{A}^*$ and thus

$$\mathcal{A}^*(\mathcal{A}\mathcal{A}^*)^+ = \mathcal{A}^+(\mathcal{A}\mathcal{A}^*)(\mathcal{A}\mathcal{A}^*)^+ = \mathcal{A}^+.$$

If $\mathcal{A}$ is surjective, the adjoint $\mathcal{A}^*$ is injective and also $\mathcal{A}\mathcal{A}^*$ is injective. Thus $(\mathcal{A}\mathcal{A}^*)^{-1}$ exists and

$$(\mathcal{A}\mathcal{A}^*)^+ = (\mathcal{A}\mathcal{A}^*)^{-1}.$$

□

The following representation of the operator norm follows directly from the definition of the operator norm.

Lemma 2.22. *Let $\mathcal{A} \in \mathcal{L}(\mathcal{X}, \mathcal{Y})$ with $\mathcal{A}^+$ being bounded. Then*

$$\|\mathcal{A}^+\| = \sup_{\varphi \in \mathrm{N}(\mathcal{A})^\perp,\, \|\mathcal{A}\varphi\|_{\mathcal{Y}}=1} \|\varphi\|_{\mathcal{X}}.$$

Chapter 3

Transforms in X-Ray tomography

The mathematical model of Computerized Tomography is given by the Radon transform and its related Ray transforms namely the X-ray transform and the Cone Beam transform. We follow [Nat01] to introduce the transforms as linear integral operators on the Schwartz space of rapidly decreasing functions

$$\mathcal{S}(\mathbb{R}^d) := \left\{ f \in C^\infty(\mathbb{R}^d) : \sup_{x\in\mathbb{R}^d} |x^\alpha D^\beta f(x)| < \infty \ \ \forall \alpha, \beta \in \mathbb{N}^d \right\}.$$

This guarantees the existence of all integrals and thus well-definedness of all integral operators. Since the Schwartz space of rapidly decreasing functions is dense in L_2, cf. [Wer18], the operators are then extended to L_2-spaces. For all discussed transforms and operators we consider a fixed source-detector setup.

The Radon transform is studied in a variety of publications as for example [Rad17], [Lou84], and [Hel99]. For the X-ray and Cone (resp. Fan) Beam transform we refer to [Ham+80]. As a general references for this chapter, we give [Nat01] and [NW01].

In the following, $\Omega \subset \mathbb{R}^d$ denotes the d-dimensional unit ball

$$\Omega := B_1(0) := \{x \in \mathbb{R}^d : \|x\| \leq 1\}$$

and $\mathcal{S}^{d-1}$ denotes the d-dimensional unit sphere in $\mathbb{R}^d$ given by $\mathcal{S}^{d-1} := \partial\Omega = \{x \in \mathbb{R}^d : \|x\| = 1\}$.

3.1 The Radon transform

Let $\theta \in \mathcal{S}^{d-1}$ and $s \in \mathbb{R}$. The d-dimensional hyperplane $H(\theta, s)$ is defined as

$$\begin{aligned} H(\theta, s) :=& \{x \in \mathbb{R}^d : \langle x, \theta\rangle = s\} \\ =& \{x \in \mathbb{R}^d : x = s\theta + t\theta^\perp,\ t \in \mathbb{R}\}. \end{aligned}$$

Definition 3.1. *The d-dimensional Radon transform of $f \in \mathcal{S}(\mathbb{R}^d)$ at $(\theta, s) \in (\mathcal{S}^{d-1} \times \mathbb{R})$ is defined as*

$$\begin{aligned} \mathcal{R}f(\theta, s) &= \int_{H(\theta,s)} f(x)\, dx \\ &= \int_{\mathbb{R}^d} f(x)\delta(s - x^\top\theta)\, dx. \end{aligned}$$

For a fixed direction $\theta \in \mathcal{S}^{d-1}$ we write $\mathcal{R}_\theta f(s) := \mathcal{R}f(\theta, s)$.

Proposition 3.2. *Let $f \in \mathcal{S}(\mathbb{R}^d)$ and $\theta \in \mathbb{S}^{d-1}$.*

(i) For $a \in \mathbb{R}^d$ holds

$$\mathcal{R}_\theta(f(\cdot - a))(s) = \mathcal{R}_\theta f(s - a^\top \theta).$$

(ii) For $U \in \mathbb{R}^{d\times d}$ being orthogonal holds

$$\mathcal{R}_\theta(f(U\cdot))(s) = \mathcal{R}_{U\theta} f(s).$$

Proof. (i) With the definition of the Radon transform follows

$$\begin{aligned}\mathcal{R}_\theta(f(\cdot - a))(s) &= \int_{\mathbb{R}^d} f(x-a)\delta(s - x^\top\theta)\,dx \\ &= \int_{\mathbb{R}^d} f(y)\delta\big((s - a^\top\theta) - y^\top\theta\big)\,dy \\ &= \mathcal{R}_\theta f(s - a^\top\theta).\end{aligned}$$

(ii) Since U is orthogonal, substituting $y := Ux$ yields

$$\begin{aligned}\mathcal{R}(f(U\cdot))(\theta, s) &= \int_{\mathbb{R}^d} f(Ux)\delta(s - x^\top\theta)\,dx \\ &= \int_{\mathbb{R}^d} f(y)\delta(s - y^\top U\theta)\,dy \\ &= \mathcal{R}f(U\theta, s).\end{aligned}$$

□

Example 3.3 (Radon transform of the unit ball Ω). *We cite an example from [Hel99, I.5.9(c)] regarding the Radon transform of the d-dimensional unit ball Ω. Therefore, let χ_Ω denote the characteristic function of Ω, i.e.,*

$$\chi_\Omega(s) = \begin{cases} 1, & \text{if } \|x\| \le 1 \\ 0, & \text{else.}\end{cases}$$

The Radon transform of χ_Ω is computed as

$$\mathcal{R}_\theta\chi_\Omega(s) = \frac{|\mathbb{S}^{d-2}|}{d-1}(1-s^2)^{\frac{d-1}{2}}.$$

Note that since χ_Ω is rotationally invariant the Radon transform is again rotationally invariant, cf. proposition 3.2.

The following theorem justifies the continuation of the Radon transform as a bounded linear operator on L_2-spaces. Let w_1 and w_2 be the weight functions

$$w_1(s) := \frac{1}{\mathcal{R}_\theta\chi_\Omega(s)} \qquad \text{and} \qquad w_2(s) \equiv 1.$$

Theorem 3.4. *The d-dimensional Radon transform*

$$\mathcal{R} : L_2(\Omega) \to L_2\big(\mathbb{S}^{d-1} \times [-1,1],\, w\big)$$

is bounded for $w = w_1$ and $w = w_2$, respectively.

Proof. Let $\tilde{w} := \big(1-s^2\big)^{-\frac{d-1}{2}}$. Then, $\mathcal{R} : L_2(\Omega) \to L_2\big(\mathbb{S}^{d-1} \times [-1,1],\, \tilde{w}\big)$ is a bounded operator as shown in [Nat01, Thm. II.1.6]. Together with the Radon transform of the unit ball, cf. example 3.3, follows

$$w_1(s) = \left(\frac{|\mathbb{S}^{d-2}|}{d-1}(1-s^2)^{\frac{d-1}{2}}\right)^{-1} = \frac{d-1}{|\mathbb{S}^{d-2}|}(1-s^2)^{-\frac{d-1}{2}} = \frac{d-1}{|\mathbb{S}^{d-2}|}\,\tilde{w}(s)$$

such that w_1 is a scaled version of $\tilde{w}$. Consequently, the Radon transform is bounded for the weight w_1. For w_2, the result follows immediately with $w_2 \leq \tilde{w}$, see [Lou89, Thm. 6.1.1]. □

Proposition 3.5. *Let $\theta \in \mathbb{S}^{d-1}$ be a fixed direction.*

(i) The adjoint operator $\mathcal{R}_\theta^* : L_2\big([-1,1],\, w\big) \to L_2(\Omega)$ is computed as

$$\mathcal{R}_\theta^* g(x) = (wg)(x^\top \theta).$$

(ii) For $w = w_1$, the generalized inverse $\mathcal{R}_\theta^+ : \mathrm{D}(\mathcal{R}_\theta^+) \subset L_2\big([-1,1],\, w_1\big) \to L_2(\Omega)$ is bounded and given as

$$\mathcal{R}_\theta^+ = \mathcal{R}_\theta^*.$$

Further, it holds

$$\|\mathcal{R}_\theta\|_{L_2(\Omega) \to L_2([-1,1],\, w_1)} = \|\mathcal{R}_\theta^+\|_{L_2([-1,1],\, w_1) \to L_2(\Omega)} = 1.$$

Proof. (i) Let $f \in L_2(\Omega)$ and $g \in L_2\big([-1,1],\, w\big)$. It holds

$$\begin{aligned}
\langle \mathcal{R}_\theta f,\, g \rangle_{L_2\left([-1,1],\, w\right)} &= \int_{[-1,1]} \mathcal{R}_\theta f(s) g(s) w(s)\, ds \\
&= \int_{[-1,1]} \int_{H(\theta,s)\cap\Omega} f(y)\, dy\, g(s) w(s)\, ds \\
&= \int_{[-1,1]} \int_{H(\theta,s)\cap\Omega} f(y)\, (wg)(s)\, dy\, ds \\
&= \int_{\Omega} f(x)\, (wg)(x^\top\theta)\, dx.
\end{aligned}$$

The adjoint operator is thus given by

$$\mathcal{R}_\theta^* g(x) = (wg)(x^\top \theta).$$

(ii) The representation of the generalized inverse $\mathcal{R}_\theta^+$ can be shown by means of corollary 2.21. First, we show the surjectivity of $\mathcal{R}_\theta$ for a fixed angle $\theta \in \mathbb{S}^{d-1}$. Analogously to [Nat01, Section V.4.3.], this can be shown by considering $\phi \in L_2\big([-1,1],\, w_1\big)$ and $\varphi \in L_2(\Omega)$ defined as

$$\varphi(x) := \mathcal{R}_\theta^* \phi(x) = (w_1 \phi)(x^\top \theta).$$

It follows $\mathcal{R}_\theta \varphi = \mathcal{R}_\theta \mathcal{R}_\theta^* \phi = \phi$ for every $\phi \in L_2\big([-1,1],\, w\big)$ and thus the surjectivity of $\mathcal{R}_\theta$. Further, it is

$$\begin{aligned}
\mathcal{R}_\theta \mathcal{R}_\theta^* \phi(s) &= \int_{H(\theta,s)\cap\Omega} \mathcal{R}_\theta^* \phi(y)\, dy \\
&= \int_{H(\theta,s)\cap\Omega} (w_1 \phi)(y^\top \theta)\, dy \\
&= \underbrace{\int_{H(\theta,s)\cap\Omega} dy}_{=w_1(s)^{-1}} (w_1 \phi)(s) \\
&= \phi(s).
\end{aligned}$$

Hence, $\mathcal{R}_\theta \mathcal{R}_\theta^*$ coincides with the identity on $L_2\big([-1,1],\, w_1\big)$ and with theorem 2.21 follows

$$\mathcal{R}_\theta^+ = \mathcal{R}_\theta^* \big(\mathcal{R}_\theta \mathcal{R}_\theta^*\big)^{-1} = \mathcal{R}_\theta^*.$$

The norm estimation of $\mathcal{R}_\theta$ is obtained with Hölder's inequality in analogy to [Nat01, Theorem II.1.6]. Let $\varphi \in \mathcal{S}(\mathbb{R}^d)$ be compactly supported with $\operatorname{supp} \varphi \subset \Omega$. Then,

$$\begin{aligned}
\left| \int_{H(\theta,s)\cap\Omega} \varphi(y)\, dy \right|^2 &\leq \underbrace{\int_{H(\theta,s)\cap\Omega} dy}_{=w_1(s)^{-1}} \int_{H(\theta,s)\cap\Omega} |\varphi(y)|^2\, dy \\
&= w_1(s)^{-1} \int_{H(\theta,s)\cap\Omega} |\varphi(y)|^2\, dy,
\end{aligned}$$

and thus,

$$\begin{aligned}
\|\mathcal{R}_\theta \varphi\|^2_{L_2([-1,1],\, w_1)} &= \int_{[-1,1]} |\mathcal{R}_\theta \varphi(s)|^2\, w_1(s)\, ds \\
&= \int_{[-1,1]} \left| \int_{H(\theta,s)\cap\Omega} \varphi(y)\, dy \right|^2 w_1(s)\, ds \\
&\leq \int_{[-1,1]} w_1(s)^{-1} \int_{H(\theta,s)\cap\Omega} |\varphi(y)|^2\, dy\, w_1(s)\, ds \\
&= \int_{[-1,1]} \int_{H(\theta,s)\cap\Omega} |\varphi(y)|^2\, dy\, ds \\
&= \int_\Omega |\varphi(x)|^2\, dx \\
&= \|\varphi\|^2_{L_2(\Omega)}.
\end{aligned}$$

Since the continuity of $\mathcal{R}_\theta$ implies the continuity of its adjoint operator $\mathcal{R}_\theta^*$, cf. [Wer18], it yields

$$\|\mathcal{R}_\theta\| = \|\mathcal{R}_\theta^*\| = \|\mathcal{R}_\theta^+\| \leq 1.$$

With the Moore–Penrose axioms 2.20 follows

$$1 = \|\mathrm{P}_{\overline{\mathrm{R}(\mathcal{R}_\theta)}}\| = \|\mathcal{R}_\theta \mathcal{R}_\theta^+\| \leq \|\mathcal{R}_\theta\| \|\mathcal{R}_\theta^+\| \leq 1$$

and thus the result $\|\mathcal{R}_\theta\| = \|\mathcal{R}_\theta^+\| = 1$.

□

3.2 The X-Ray transform

For $\theta \in \mathbb{S}^{d-1}$ and $x \in \theta^\perp$ let

$$L(\theta, x) \coloneqq \{y \in \mathbb{R}^d : y = x + t\theta, t \in \mathbb{R}\}.$$

Definition 3.6. *The d-dimensional X-ray transform of $f \in \mathcal{S}(\mathbb{R}^d)$ at $(\theta, x) \in (\mathbb{S}^{d-1} \times \theta^\perp)$ is defined as*

$$\begin{aligned}\mathcal{P}f(\theta, x) &= \int_{L(\theta,x)} f(y)\, dy \\ &= \int_{\mathbb{R}} f(x + t\theta)\, dt.\end{aligned}$$

For a fixed direction $\theta \in \mathbb{S}^{d-1}$ we write $\mathcal{P}_\theta f(x) \coloneqq \mathcal{P}f(\theta, x)$.

In two dimensions, i.e., $d = 2$, the X-ray transform thus coincides with the Radon transform up to parameterization.

Proposition 3.7. *Let $\theta \in \mathbb{S}^{d-1}$ be fixed and $f \in \mathcal{S}(\mathbb{R}^d)$.*

(i) For fixed $x_0 \in \mathbb{R}^d$ holds

$$\mathcal{P}_\theta\big(f(\cdot - x_0)\big)(x) = \mathcal{P}_\theta f\big(x - \mathrm{P}_{\theta^\perp} x_0\big).$$

(ii) For $U \in \mathbb{R}^{d\times d}$ being orthogonal holds

$$\mathcal{P}_\theta\big(f(U\cdot)\big)(x) = \mathcal{P}_{U\theta} f\big(Ux\big).$$

Proof. (i) For fixed $x_0 \in \mathbb{R}^d$ and $x \in \theta^\perp$ holds

$$\begin{aligned}\mathcal{P}_\theta(f(\cdot - x_0))(x) &= \int_{\mathbb{R}} f(x + t\theta - x_0)\, dt \\ &= \int_{\mathbb{R}} f(x - \mathrm{P}_{\theta^\perp} x_0 + (t - x_0^\top \theta)\theta)\, dt \\ &= \int_{\mathbb{R}} f(x - \mathrm{P}_{\theta^\perp} x_0 + t\theta)\, dt \\ &= \mathcal{P}_\theta f(x - \mathrm{P}_{\theta^\perp} x_0).\end{aligned}$$

(ii) For $U \in \mathbb{R}^{d\times d}$ being orthogonal follows

$$\mathcal{P}_\theta(f(U\cdot))(x) = \int_{\mathbb{R}} f(U(x + t\theta))\, dt = \int_{\mathbb{R}} f(Ux + tU\theta)\, dt = \mathcal{P}f(U\theta, Ux).$$

□

Lemma 3.8. *For $\theta \in \mathcal{S}^{d-1}$ being a fixed direction, the X-Ray transform of a radially symmetric function $\varphi \in \mathcal{S}(\mathbb{R}^d)$ is given by*

$$\mathcal{P}_\theta \varphi(x) = 2 \int_0^\infty \varphi\left(\sqrt{\|x\|^2 + t^2}\right) dt \qquad \forall x \in \theta^\perp.$$

Proof. Let $\varphi \in \mathcal{S}(\mathbb{R}^d)$ be radially symmetric, i.e., there exists a function $\tilde{\varphi} \in \mathcal{S}(\mathbb{R})$ such that

$$\varphi(y) = \tilde{\varphi}(\|y\|) \qquad \forall y \in \mathbb{R}^d.$$

For a fixed direction $\theta \in \mathcal{S}^{d-1}$ holds

$$\mathcal{P}_\theta \varphi(x) = \int_{\mathbb{R}} \varphi(x + t\theta)\, dt = \int_{\mathbb{R}} \tilde{\varphi}(\|x + t\theta\|)\, dt \qquad \forall x \in \theta^\perp.$$

For $x \in \theta^\perp$ follows $\langle x, \theta \rangle = 0$ and thus $\|x + t\theta\| = \sqrt{\|x\|^2 + |t|\|\theta\|^2}$ for $x \in \theta^\perp$. Thus

$$\mathcal{P}_\theta \varphi(x) = \int_{\mathbb{R}} \tilde{\varphi}\left(\sqrt{\|x\|^2 + |t|}\right) dt = 2 \int_0^\infty \tilde{\varphi}\left(\sqrt{\|x\|^2 + |t|}\right) dt.$$

□

Example 3.9. *The X-ray transform of the characteristic function of the d-dimensional ball $B_r(0)$ with radius $r > 0$ centered around the origin is computed as*

$$\mathcal{P}_\theta \chi_{B_r(0)}(x) = 2\sqrt{r^2 - \|x\|^2} \qquad x \in \theta^\perp.$$

This follows directly from lemma 3.8 with

$$\begin{aligned} \mathcal{P}_\theta \chi_{B_r(0)}(x) &= 2 \int_0^\infty \chi_{B_r(0)}\left(\sqrt{\|x\|^2 + t^2}\right) dt \\ &= 2 \int_0^{\sqrt{r^2 - \|x\|^2}} dt \\ &= 2\sqrt{r^2 - \|x\|^2}. \end{aligned}$$

As for the Radon transform in the previous section, we extend the X-ray transform as a bounded operator on L_2-spaces. Therefore, let the weight functions w_θ^1 and w_θ^2 be defined as

$$w_\theta^1(x) := \frac{1}{\mathcal{P}_\theta \chi_\Omega(x)} \quad \text{for } x \in \theta^\perp \quad \text{and} \quad w_\theta^2(x) \equiv 1 \quad \text{for } x \in \Omega.$$

Proposition 3.10. *The X-ray transform*

$$\mathcal{P}_\theta : L_2(\Omega) \to L_2\left(\theta^\perp, w_\theta\right)$$

for fixed directions $\theta \in \mathcal{S}^{d-1}$ is a bounded and linear operator for $w_\theta = w_\theta^1$ and $w_\theta = w_\theta^2$, respectively. Its adjoint operator $\mathcal{P}_\theta^* : L_2\left(\theta^\perp, w_\theta\right) \to L_2(\Omega)$ is computed as

$$\mathcal{P}_\theta^* g(x) = (w_\theta g)(\mathrm{P}_{\theta^\perp} x).$$

For $w_\theta = w_\theta^1$, the generalized inverse $\mathcal{P}_\theta^+ : \mathrm{D}(\mathcal{P}_\theta^+) \subset L_2\big(\theta^\perp, w_\theta^1\big) \to L_2(\Omega)$ is given by its adjoint operator, i.e., $\mathcal{P}_\theta^+ = \mathcal{P}_\theta^*$, and the norm estimation

$$\|\mathcal{P}_\theta\|_{L_2(\Omega)\to L_2(\theta^\perp, w_\theta^1)} = \|\mathcal{P}_\theta^+\|_{L_2(\theta^\perp, w_\theta^1)\to L_2(\Omega)} = 1$$

holds.

Proof. Putting $r = 1$ in example 3.9, the weight $w_\theta^1(x)$ is computed as

$$w_\theta^1(x) = \frac{1}{\mathcal{P}_\theta \chi_\Omega(x)} = \frac{1}{2\sqrt{1 - \|x\|^2}} \qquad x \in \theta^\perp.$$

Since $\mathcal{P}_\theta : L_2(\Omega) \to L_2\big(\theta^\perp, w_\theta\big)$ is bounded for $w_\theta(x) = \tilde{w}_\theta(x) := \big(1 - \|x\|^2\big)^{-\frac{1}{2}}$, cf. [Nat01, Theorem II.1.6], the boundedness for $w_\theta = w_\theta^1$ is immediately induced. With

$$w_\theta^2(x) = 1 \le \frac{1}{\sqrt{1 - \|x\|^2}} = \tilde{w}_\theta(x) \qquad x \in \theta^\perp$$

the boundedness for w_θ^2 is also settled. The representation of the adjoint operator is computed for $f \in L_2(\Omega)$ and $g \in L_2\big(\theta^\perp, w_\theta\big)$ by

$$\begin{aligned}
\big\langle \mathcal{P}_\theta f, g \big\rangle_{L_2(\theta^\perp, w_\theta)} &= \int_{\theta^\perp} \mathcal{P}_\theta f(x)\, \big(w_\theta g\big)(x)\, dx \\
&= \int_{\theta^\perp} \mathcal{P}_\theta f(x)\, \big(w_\theta g\big)(\mathrm{P}|_{\theta^\perp} x)\, dx \\
&= \int_{\theta^\perp} \int_{x+t\theta\in\Omega} f(x + t\theta) \big(w_\theta g\big)(\mathrm{P}|_{\theta^\perp} x)\, dt\, dx
\end{aligned}$$

and with the substitution $x \mapsto x + t\theta$ follows

$$= \int_\Omega f(x) \big(w_\theta g\big)(\mathrm{P}|_{\theta^\perp} x)\, dx.$$

For $w_\theta = w_\theta^1$, it yields $\mathcal{P}_\theta \mathcal{P}_\theta^* = \mathrm{id}$ on $L_2\big(\theta^\perp, w_\theta^1\big)$ as can be seen by

$$\begin{aligned}
\mathcal{P}_\theta \mathcal{P}_\theta^* g(x) &= \int_{x+t\theta\in\Omega} \mathcal{P}_\theta^* g(x + t\theta)\, dx \\
&= \int_{x+t\theta\in\Omega} \big(w_\theta^1 g\big)\big(\mathrm{P}_{\theta^\perp}(x + t\theta)\big)\, dy \\
&= \big(w_\theta^1 g\big)(x) \int_{x+t\theta\in\Omega} dy \\
&= \big(w_\theta^1 g\big)(x)\, w_\theta^1(x)^{-1} \\
&= g(x)
\end{aligned} \tag{3.1}$$

for arbitrary $g \in L_2\big(\theta^\perp, w_\theta^1\big)$. Applying Hölder's inequality further yields

$$\|\mathcal{P}_\theta f\|^2_{L_2(\theta^\perp, w_\theta^1)} = \int_{\theta^\perp} |\mathcal{P}_\theta f(x)|^2\, w_\theta^1(x)\, dx$$

$$
\begin{aligned}
&= \int_{\theta^\perp} \left| \int_{L(\theta,x)\cap\Omega} f(y)\, dy \right|^2 w_\theta^1(x)\, dx \\
&\leq \int_{\theta^\perp} w_\theta^1(x)^{-1} \int_{L(\theta,x)\cap\Omega} |f(y)|^2\, dy\, w_\theta^1(x)\, dx \\
&= \|f\|_{L_2(\Omega)}^2,
\end{aligned}
$$

such that

$$1 = \|\mathcal{P}_\theta \mathcal{P}_\theta^*\| \leq \|\mathcal{P}_\theta\| \|\mathcal{P}_\theta^*\| \leq 1.$$

Thus, it holds $\|\mathcal{P}_\theta\| = \|\mathcal{P}_\theta^*\| = 1$. Finally, we apply theorem 2.21 to obtain the representation of the generalized inverse for $w_\theta = w_\theta^1$. The surjectivity of $\mathcal{P}_\theta$ can be shown analogously to proposition 3.5. From $\mathcal{P}_\theta^+ = \mathcal{P}_\theta^*(\mathcal{P}_\theta \mathcal{P}_\theta^*)^{-1}$ together with equation (3.1) follows $\mathcal{P}_\theta^+ = \mathcal{P}_\theta^*(\mathcal{P}_\theta \mathcal{P}_\theta^*)^{-1} = \mathcal{P}_\theta^*$. Hence, $\|\mathcal{P}_\theta\| = \|\mathcal{P}_\theta^+\| = 1$. □

3.3 The Cone Beam transforms

The Cone Beam transform is described by the integral of a function f supported in the reconstruction area Ω along lines starting from a point $a \in \mathbb{R}^d \setminus \Omega$ describing the X-ray source position through the object. We basically distinguish two different definitions of the Cone Beam transform based on the parameterization of the lines of integration:

(i) The classical Cone Beam transform, cf. [Ham+80], is defined by integrating the function f along lines

$$L_+(a,\theta) := \left\{ y \in \mathbb{R}^d : y = a + t\theta, t \in \mathbb{R}_+ \right\}$$

resulting in

$$\mathcal{D}f(a,\theta) = \int_{L_+(a,\theta)} f(x)\, dx.$$

for $a \in \mathbb{R}^d \setminus \Omega$ and $\theta \in \mathcal{S}^{d-1}$. Since the lines are parameterized by a starting position and the direction of integration this definition is used to describe a spherically shaped detector around the X-ray source position a. Therefore we will refer to this transform as the Cone Beam transform with spherically shaped detector, the classical Cone Beam transform, or simply the Cone Beam transform.

(ii) A slightly different approach is to parameterize the lines of integration by

$$L_+(a, \eta - a) = \{ y \in \mathbb{R}^d : y = a + t(\eta - a), t \in \mathbb{R}_+ \}$$

with $\eta \in E_a$ being a point on the hyperplane

$$E_a := E(\mathrm{n}_a, \mathrm{d}_a) = \left\{ \eta \in \mathbb{R}^d : \left\langle \eta - \mathrm{d}_a, \mathrm{n}_a \right\rangle = 0 \right\}$$

where n_a denotes the normal vector of E_a and d_a denotes the displacement vector, see figure 3.1. The hyperplane E_a can be interpreted as a flat detector plane and η as the position of the detector pixels. We define the flat detector Cone Beam transform as

$$\mathcal{X}f(a,\eta) = \int_{L_+(a,\eta-a)} f(x)\, dx, \qquad \eta \in E_a.$$

In general, we do not require the position vector of $a \in \mathbb{R}^d$ to be perpendicular to the detector plane E_a. This will allow us to cover more general measurement geometries as for example used in computed laminography applications.

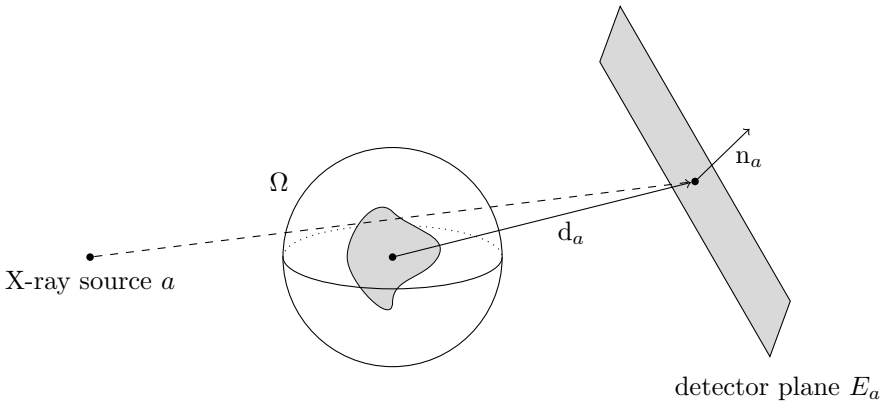

Figure 3.1: Scheme of the Cone Beam transform with a flat detector.

Definition 3.11. *Let* Γ *denote a curve of source positions fulfilling* $\operatorname{dist}(\Gamma, \overline{\Omega}) \geq 0$.

(i) The d-dimensional Cone Beam transform (with spherically shaped detectors) of $f \in \mathcal{S}(\mathbb{R}^d)$ *at the position* $(a, \theta) \in (\Gamma, \mathcal{S}^{d-1})$ *is defined as*

$$\mathcal{D}f(a,\theta) = \int_{L_+(a,\theta)} f(y)\, dy = \int_0^\infty f(a+t\theta)\, dt.$$

(ii) The d-dimensional (flat detector) Cone Beam transform of $f \in \mathcal{S}(\mathbb{R}^d)$ *at the position* $(a, \eta) \in (\Gamma, E_a)$ *is defined as*

$$\mathcal{X}f(a,\eta) = \int_{L_+(a,\eta-a)} f(y)\, dy = \int_0^\infty f(a+t(\eta-a))\, dt.$$

For a fixed source position $a \in \mathbb{R}^d \setminus \{\overline{\Omega}\}$ *we set*

$$\mathcal{D}_a f(\theta) := \mathcal{D}f(a,\theta) \qquad \text{and} \qquad \mathcal{X}_a f(\theta) := \mathcal{X}f(a,\theta),$$

respectively.

The properties of the source curve Γ plays an important role for the derivation of analytical inversion formulas for the Cone Beam transforms. A classical result usually referred to as Tuy's condition or Tuy–Kirillov condition stated in [Tuy83] requires a certain regularity on Γ. A less restrictive and therefore more general condition is referred to as Louis' condition and can be found in [Lou16]. However, many scanning geometries used in practical applications violate these conditions. To this end we consider the Cone Beam transform at fixed X-ray source positions not necessarily being sampled from a source curve Γ.

Theorem 3.12. *The Cone Beam transforms*

$$\mathcal{D}_a : L_2(\Omega) \to L_2(\mathcal{S}^{d-1}) \qquad \text{and} \qquad \mathcal{X}_a : L_2(\Omega) \to L_2(E_a)$$

for fixed source positions $a \in \mathbb{R}^d$ *with* $\operatorname{dist}(a, \overline{\Omega}) > 0$ *are bounded.*

Proof. For the boundedness of the classical Cone Beam transform $\mathcal{D}_a$ we refer to [Nat01, Theorem II.1.6]. Let $a \in \mathbb{R}^d$ be fixed with $\operatorname{dist}(a, \overline{\Omega}) > 0$ and $f \in \mathcal{S}(\mathbb{R}^d)$ supported in Ω. With Hölder's inequality follows for the flat detector Cone Beam transform

$$\begin{aligned}
|\mathcal{X}_a f(\eta)|^2 &= \left| \int_{L(a,\eta-a)\cap\Omega} f(y)\, dy \right|^2 \\
&\leq \underbrace{\int_{L(a,\eta-a)\cap\Omega} dy}_{\mathcal{X}_a\chi_\Omega(\eta)} \int_{L(a,\eta-a)\cap\Omega} |f(y)|^2\, dy \\
&= \mathcal{X}_a\chi_\Omega(\eta) \int_{L(a,\eta-a)\cap\Omega} |f(y)|^2\, dy \\
&\leq \max_{\eta\in E_a} \mathcal{X}_a\chi_\Omega(\eta) \int_{L(a,\eta-a)\cap\Omega} |f(y)|^2\, dy.
\end{aligned}$$

Thus,

$$\begin{aligned}
\|\mathcal{X}_a f\|^2_{L_2(E_a)} &= \int_{E_a} |\mathcal{X}_a f(\eta)|^2\, d\eta \\
&\leq \max_{\eta'\in E_a} \left(\mathcal{X}_a\chi_\Omega(\eta')\right) \int_{E_a} \int_{L(a,\eta-a)\cap\Omega} |f(y)|^2\, dy\, d\eta \\
&= \max_{\eta'\in E_a} \left(\mathcal{X}_a\chi_\Omega(\eta')\right) \int_{E_a} \int_{\{t\in\mathbb{R}\colon a+t(\eta-a)\in\Omega\}} |f\big(a+t(\eta-a)\big)|^2\, dt\, d\eta. \qquad (3.2)
\end{aligned}$$

To obtain an estimation of the integral on the right hand side we apply the substitution $x = a + t(\eta - a)$. With $\{\mathrm{e}_i\}_{i=1}^{d-1}$ being an orthonormal basis of the shifted detector plane $E_a - \mathrm{d}_a$ each element η of E_a has the representation as

$$\eta = \sum_{i=1}^{d-1} \eta_i\, \mathrm{e}_i + \mathrm{d}_a \qquad \text{with } \eta_i := \langle \eta - \mathrm{d}_a, \mathrm{e}_i \rangle.$$

The Jacobian determinant of the substitution results in

$$\begin{aligned}
\det \begin{vmatrix} \eta - a & t\,\mathrm{e}_1 & \cdots & t\,\mathrm{e}_{d-1} \end{vmatrix} &= t^{d-1} \det \begin{vmatrix} \left(\sum_{i=1}^{d-1} \eta_i\, \mathrm{e}_i + \mathrm{d}_a - a\right) & \mathrm{e}_1 & \cdots & \mathrm{e}_{d-1} \end{vmatrix} \\
&= t^{d-1} \underbrace{\det \begin{vmatrix} \sum_{i=1}^{d-1} \eta_i\, \mathrm{e}_i & \mathrm{e}_1 & \cdots & \mathrm{e}_{d-1} \end{vmatrix}}_{=0} \\
&\quad - t^{d-1} \underbrace{\det \begin{vmatrix} \mathrm{P}|_{(E_a-\mathrm{d}_a)}(a-\mathrm{d}_a) & \mathrm{e}_1 & \cdots & \mathrm{e}_{d-1} \end{vmatrix}}_{=0} \\
&\quad - t^{d-1} \det \begin{vmatrix} \mathrm{P}|_{(E_a-\mathrm{d}_a)^\perp}(a-\mathrm{d}_a) & \mathrm{e}_1 & \cdots & \mathrm{e}_{d-1} \end{vmatrix}.
\end{aligned}$$

Putting $\tilde{a} := \mathrm{P}|_{(E_a-\mathrm{d}_a)^\perp}(a-\mathrm{d}_a)$ yields

$$= -t^{d-1}\|\tilde{a}\| \underbrace{\det \begin{vmatrix} \frac{\tilde{a}}{\|\tilde{a}\|} & \mathrm{e}_1 & \cdots & \mathrm{e}_{d-1} \end{vmatrix}}_{=\pm 1}$$

$$= \pm t^{d-1} \|\tilde{a}\|.$$

Since

$$\langle \eta - a,\, \tilde{a} \rangle = \left\langle \sum_{i=1}^{d-1} \eta_i \, \mathrm{e}_i - (a - \mathrm{d}_a),\, \tilde{a} \right\rangle = \|\tilde{a}\|^2 \tag{3.3}$$

follows $t = \|\tilde{a}\|^{-2} \langle a - x, \tilde{a} \rangle$ and

$$dt\, d\eta = \|\tilde{a}\|^{-1} \left(\frac{|\langle a - x, \tilde{a} \rangle|}{\|\tilde{a}\|^2} \right)^{1-d} dx = \|\tilde{a}\|^{2d-3} (\langle a - x, \tilde{a} \rangle)^{1-d}\, dx. \tag{3.4}$$

We obtain the integral estimation

$$\begin{aligned} \int_{E_a} \int_{\{t \in \mathbb{R} \colon a + t(\eta - a) \in \Omega\}} |f(a + t(\eta - a))|^2 \, dt\, d\eta &= \|\tilde{a}\|^{2d-3} \int_\Omega |f(x)|^2 \, |\langle a - x, \tilde{a} \rangle|^{1-d} \, dx \\ &\leq \|\tilde{a}\|^{2d-3} \max_{x' \in \Omega} |\langle a - x', \tilde{a} \rangle|^{1-d} \int_\Omega |f(x)|^2 \, dx \\ &= \|\tilde{a}\|^{2d-3} \max_{x' \in \Omega} |\langle a - x', \tilde{a} \rangle|^{1-d} \, \|f\|^2_{L_2(\Omega)} \end{aligned} \tag{3.5}$$

Putting (3.5) into equation (3.2) finally yields

$$\begin{aligned} \|\mathcal{X}_a f\|^2_{L_2(E_a)} &\leq \max_{\eta' \in E_a} \mathcal{X}_a \chi_\Omega(\eta') \int_{E_a} \int_{\{t \in \mathbb{R} \colon a + t(\eta - a) \in \Omega\}} |f(a + t(\eta - a))|^2 \, dt\, d\eta \\ &\leq \|\tilde{a}\|^{2d-3} \max_{\eta' \in E_a} \mathcal{X}_a \chi_\Omega(\eta') \max_{x' \in \Omega} |\langle a - x', \tilde{a} \rangle|^{1-d} \, \|f\|^2_{L_2(\Omega)}. \end{aligned}$$

This states the boundedness of the flat detector Cone Beam transform $\mathcal{X}_a$ for a fixed X-ray source position. □

In analogy to the Radon transform and the X-ray transform, the operator norm of the Cone Beam transforms can be controlled by introducing weighted L_2-spaces. Therefore, we first note that for a given function $f \in \mathcal{S}(\mathbb{R}^d)$ supported in Ω holds

$$\mathcal{D}_a f(\theta) \equiv 0, \qquad \text{for } \theta \in \mathcal{S}^{d-1} \text{ with } L_+(a, \theta) \cap \Omega = \emptyset$$

as well as

$$\mathcal{X}_a f(\eta) \equiv 0, \qquad \text{for } \eta \in E_a \text{ with } L_+(a, \eta - a) \cap \Omega = \emptyset.$$

We thus have to restrict arguments on the detector and introduce the following operators. Again, $a \in \mathbb{R}^d$ shall denote a fixed X-ray source position with $\operatorname{dist}(a, \overline{\Omega}) > 0$.

(i) Let

$$\begin{aligned} \mathcal{S}_a^{d-1} &:= \left\{ \theta \in \mathcal{S}^{d-1} : \mathcal{D}_a \chi_\Omega(\theta) \neq 0 \right\} \\ &= \left\{ \theta \in \mathcal{S}^{d-1} : \{a + t\theta : t \in \mathbb{R}_+\} \cap \Omega \neq \emptyset \right\} \subset \mathcal{S}^{d-1} \end{aligned}$$

denote the restricted directions for the classical Cone Beam transform and let the weights $W_a : \Omega \to \mathbb{R}$ and $w_a : \mathcal{S}_a^{d-1} \to \mathbb{R}$ be defined as

$$W_a(x) = \frac{1}{\|x - a\|^{d-1}} \qquad \text{and} \qquad w_a(\theta) = \frac{1}{\mathcal{D}_a \chi_\Omega(\theta)}.$$

(ii) Let

$$\begin{aligned}\tilde{E}_a &:= \{\eta \in E_a : \mathcal{X}_a\chi_\Omega(\eta) \neq 0\} \\ &= \{\eta \in E_a : \{a + t(\eta - a) : t \in \mathbb{R}_+\} \cap \Omega \neq \emptyset\} \subset E_a.\end{aligned}$$

denote the restricted detector plane for the flat detector Cone Beam transform and let the weights $W_a : \Omega \to \mathbb{R}$ and $w_a : \tilde{E}_a \to \mathbb{R}$ be defined as

$$W_a(x) = \|\tilde{a}\|^{-1}\left(\frac{\|\tilde{a}\|^2}{\langle a - x, \tilde{a}\rangle}\right)^{d-1} = \|\tilde{a}\|^{2d-3}(\langle a - x, \tilde{a}\rangle)^{1-d} \qquad \text{and} \qquad w_a(\eta) = \frac{1}{\mathcal{X}\chi_\Omega(\eta)}.$$

Proposition 3.13. *Let $a \in \mathbb{R}^d \setminus \{\overline{\Omega}\}$. The Cone Beam operators*

$$\mathcal{D}_a : L_2(\Omega, W_a) \to L_2(S_a^{d-1}, w_a)$$

and

$$\mathcal{X}_a : L_2(\Omega, W_a) \to L_2(\tilde{E}_a, w_a)$$

are bounded with $\|\mathcal{D}_a\| = 1$ and $\|\mathcal{X}_a\| = 1$, respectively. The adjoint operators are computed as

$$\mathcal{D}_a^* g(x) = (w_a g)\left(\frac{x - a}{\|x - a\|}\right) \qquad \text{and} \qquad \mathcal{X}_a^* g(x) = (w_a g)\left(a + \frac{\|\tilde{a}\|^2}{\langle a - x, \tilde{a}\rangle}(x - a)\right)$$

where $\tilde{a} := \mathrm{P}|_{(\tilde{E}_a - \mathrm{d}_a)^\perp}(a - \mathrm{d}_a)$.

Proof. (i) Boundedness: For both operators, the boundedness follows with Hölder's inequality. Let $f \in \mathcal{S}(\mathbb{R}^d)$ be supported in Ω. Then,

$$\begin{aligned}|\mathcal{X}_a f(\eta)|^2 &= \left|\int_{L(a,\eta-a)\cap\Omega} f(y)\,dy\right|^2 \\ &\leq \underbrace{\int_{L(a,\eta-a)\cap\Omega} dy}_{\mathcal{X}_a\chi_\Omega(\eta) = w_a(\eta)^{-1}} \int_{L(a,\eta-a)\cap\Omega} |f(y)|^2\,dy \\ &= w_a(\eta)^{-1} \int_{L(a,\eta-a)\cap\Omega} |f(y)|^2\,dy\end{aligned}$$

and thus

$$\begin{aligned}\|\mathcal{X}_a f\|^2_{L_2(\tilde{E}_a, w_a)} &= \int_{\tilde{E}_a} |\mathcal{X}_a f(\eta)|^2 w_a(\eta)\,d\eta \\ &\leq \int_{\tilde{E}_a}\int_{L(a,\eta-a)\cap\Omega} |f(y)|^2\,dy\,d\eta \\ &= \int_{\tilde{E}_a}\int_{\{t\in\mathbb{R}:\, a+t(\eta-a)\in\Omega\}} |f(a + t(\eta - a))|^2\,dt\,d\eta.\end{aligned}$$

Substituting $x = a + t(\eta - a)$, cf. equation (3.4), yields

$$= \int_\Omega |f(x)|^2 \underbrace{\|\tilde{a}\|^{-1}\left(\frac{\|\tilde{a}\|^2}{\langle a - x, \tilde{a}\rangle}\right)^{d-1}}_{= W_a(x)} dx$$

$$= \|f\|^2_{L_2(\Omega, W_a)}.$$

For the classical Cone Beam transform the estimation is obtained analogously. With Hölder's inequality follows

$$|\mathcal{D}_a f(\theta)|^2 \leq w_a(\theta)^{-1} \int_{L(a,\theta)\cap\Omega} |f(y)|^2 \, dy.$$

Thus,

$$\begin{aligned}\|\mathcal{D}_a f\|^2_{L_2(S_a^{d-1}, w_a)} &= \int_{S_a^{d-1}} |\mathcal{D}_a f(\theta)|^2 w_a(\theta) \, d\theta \\ &\leq \int_{S_a^{d-1}} \int_{\{t\in\mathbb{R}: a+t\theta\in\Omega\}} |f(a+t\theta)|^2 \, dt \, d\theta.\end{aligned}$$

Substituting $x = a + t\theta,\ dt\, d\theta = \|x-a\|^{1-d}\, dx$, yields

$$\begin{aligned}&= \int_\Omega |f(x)|^2 \underbrace{\|x-a\|^{1-d}}_{=W_a(x)} \, dx \\ &= \|f\|^2_{L_2(\Omega, W_a)}.\end{aligned}$$

(ii) Adjoint operator: Since the weighted Cone Beam operators are bounded, the adjoint operators exist and are uniquely given. Let $f \in \mathcal{S}(\mathbb{R}^d)$ be supported in Ω and let $g \in L_2\big(S_a^{d-1}, w_a\big)$. Then,

$$\begin{aligned}\big\langle \mathcal{D}_a f, g\big\rangle_{L_2\left(S_a^{d-1}, w_a\right)} &= \int_{S_a^{d-1}} \mathcal{D}_a f(\theta) g(\theta) w_a(\theta) \, d\theta \\ &= \int_{S_a^{d-1}} \int_{L(a,\theta)\cap\Omega} f(y)\, dy \, g(\theta) w_a(\theta) \, d\theta \\ &= \int_{S_a^{d-1}} \int_{\left\{t\in\mathbb{R}_+ :\, a+t\theta\in\Omega\right\}} f(a+t\theta)\, dt \, g(\theta) w_a(\theta) \, d\theta.\end{aligned}$$

With the substitution $x = a + t\theta,\ dt\, d\theta = \|x-a\|^{1-d}\, dx$, follows

$$= \int_\Omega f(x) (w_a g)\left(\frac{x-a}{\|x-a\|}\right) \underbrace{\|x-a\|^{1-d}}_{=W_a(x)} \, dx$$

and the representation of the adjoint operator follows:

$$\mathcal{D}_a^* g(x) = (wg)\left(\frac{x-a}{\|x-a\|}\right).$$

Now, let $g \in L_2(\tilde{E}_a,\, w_a)$. Then,

$$\begin{aligned}\big\langle \mathcal{X}_a f, g\big\rangle_{L_2\left(\tilde{E}_a, w_a\right)} &= \int_{\tilde{E}_a} \mathcal{X}_a f(\eta) g(\eta) w_a(\eta) \, d\eta \\ &= \int_{E_a} \int_{\{t\in\mathbb{R}:\, a+t(\eta-a)\in\Omega\}} f(a+t(\eta-a)) \big(w_a g\big)(\eta) \, dt \, d\eta.\end{aligned}$$

Again, putting $x = a + t(\eta - a)$, see equation (3.4), yields

$$= \int_\Omega f(x)\big(w_a g\big)\left(a + \frac{\|\tilde{a}\|^2}{\langle a - x, \tilde{a}\rangle}(x-a)\right)\|\tilde{a}\|^{-1}\left(\frac{\langle a-x,\tilde{a}\rangle}{\|\tilde{a}\|^2}\right)^{1-d} dx$$
$$= \int_\Omega f(x)\big(w_a g\big)\left(a + \frac{\|\tilde{a}\|^2}{\langle a - x, \tilde{a}\rangle}(x-a)\right) W_a(x)\, dx.$$

Thus, we obtain the adjoint operator

$$\mathcal{X}_a^* g(x) = \big(w_a g\big)\left(a + \frac{\|\tilde{a}\|^2}{\langle a - x, \tilde{a}\rangle}(x-a)\right).$$

(iii) Norm estimate: For the determination of the operator norm, we make use of the relations $\|\mathcal{D}_a\| = \|\mathcal{D}_a^*\|$ and $\|\mathcal{D}_a\| = \|\mathcal{D}_a^*\|$. For $g \in L_2(\mathbb{S}_a^{d-1}, w_a)$ holds

$$\big\|\mathcal{D}_a^* g\big\|^2_{L_2(\Omega, W_a)} = \int_\Omega \big|\mathcal{D}_a^* g(x)\big|^2 \|x-a\|^{1-d}\, dx$$
$$= \int_\Omega \left|\big(w_a g\big)\left(\frac{x-a}{\|x-a\|}\right)\right|^2 \|x-a\|^{1-d}\, dx.$$

Substituting $x = a + t\theta,\ dt\, d\theta = \|x-a\|^{1-d}\, dx$, yields

$$= \int_{\mathbb{S}_a}\int_{\{t\in\mathbb{R}_+ :\, a+t(\eta-a)\in\Omega\}} \big|(w_a g)(\theta)\big|^2\, dt\, d\theta$$
$$= \int_{\mathbb{S}_a} \underbrace{\int_{\{t\in\mathbb{R}_+ :\, a+t(\eta-a)\in\Omega\}} dt}_{w_a(\theta)^{-1}\geq 0} \big|(w_a g)(\theta)\big|^2\, d\theta$$
$$= \int_{\mathbb{S}_a} |g(\theta)|^2\, w_a(\theta)\, d\theta$$
$$= \|g\|^2_{L_2(\mathbb{S}_a^{d-1}, w_a)}.$$

For $g \in L_2(\tilde{E}_a, w_a)$ further holds

$$\big\|\mathcal{X}_a^* g\big\|^2_{L_2(\Omega, W_a)} = \int_\Omega \big|\mathcal{X}_a^* g(x)\big|^2 \|\tilde{a}\|^{2d-3}\big(\langle a-x,\tilde{a}\rangle\big)^{1-d}\, dx$$
$$= \int_\Omega \left|\big(w_a g\big)\left(a + \frac{\|\tilde{a}\|^2}{\langle a - x, \tilde{a}\rangle}(x-a)\right)\right|^2 \|\tilde{a}\|^{2d-3}\big(\langle a-x,\tilde{a}\rangle\big)^{1-d}\, dx.$$

Substituting $x = a + t(\eta - a)$ with $dt\, d\eta = \|\tilde{a}\|^{2d-3}\big(\langle a-x,\tilde{a}\rangle\big)^{1-d}\, dx$ and $t = \|\tilde{a}\|^{-2}\langle a-x,\tilde{a}\rangle$, see equation (3.4), yields

$$= \int_{\tilde{E}_a}\int_{\{t\in\mathbb{R}:\, a+t(\eta-a)\in\Omega\}} \big|\big(w_a g\big)(\eta)\big|^2\, dt\, d\eta$$
$$= \int_{\tilde{E}_a} \underbrace{\int_{\{t\in\mathbb{R}:\, a+t(\eta-a)\in\Omega\}} dt}_{w_a(\eta)^{-1}\geq 0} \big|\big(w_a g\big)(\eta)\big|^2\, d\eta$$

$$= \int_{\tilde{E}_a} w_a(\eta)\, |g(\eta)|^2 \, d\eta$$
$$= \|g\|^2_{L_2(\tilde{E}_a, w_a)}.$$

□

Proposition 3.14. *The generalized inverse operators*

$$\mathcal{D}_a^+ : \mathrm{D}\big(\mathcal{D}_a^+\big) \subset L_2(\mathcal{S}_a^{d-1},\, w_a) \to L_2(\Omega,\, W_a)$$

and

$$\mathcal{X}_a^+ : \mathrm{D}\big(\mathcal{X}_a^+\big) \subset L_2(\tilde{E}_a,\, w_a) \to L_2(\Omega,\, W_a)$$

are given by the adjoint operators

$$\mathcal{D}_a^+ = \mathcal{D}_a^* \qquad \text{and} \qquad \mathcal{X}_a^+ = \mathcal{X}_a^*,$$

respectively. Further, it holds $\|\mathcal{D}_a^+\|_{L_2(\mathcal{S}_a^{d-1}, w_a) \to L_2(\Omega, W_a)} = 1$ *and* $\|\mathcal{X}_a^+\|_{L_2(\tilde{E}_a, w_a) \to L_2(\Omega, W_a)} = 1$.

Proof. The Cone Beam operators are surjective for fixed X-ray source positions $a \in \mathbb{R}^d \setminus \{\overline{\Omega}\}$. First, let $g \in L_2(\mathcal{S}_a^{d-1}, w_a)$ and $\varphi \in L_2(\Omega, W_a)$ be defined as

$$\varphi(x) \coloneqq \mathcal{D}_a^* g(x) = (w_a g)\left(\frac{x-a}{\|x-a\|}\right).$$

Then,

$$\begin{aligned}
\mathcal{D}_a \varphi(\theta) &= \int_{\left\{t \in \mathbb{R}_+ :\, a + t\theta \in \Omega\right\}} \varphi(a + t\theta)\, dt \\
&= \int_{\left\{t \in \mathbb{R}_+ :\, a + t\theta \in \Omega\right\}} (w_a g)(\theta)\, dt \\
&= \underbrace{\int_{\left\{t \in \mathbb{R}_+ :\, a + t\theta \in \Omega\right\}} dt}_{w_a(\theta)^{-1}} (w_a g)(\theta) \\
&= g(\theta).
\end{aligned}$$

Besides the surjectivity of $\mathcal{D}_a$ the identity $\mathcal{D}_a \mathcal{D}_a^* = \mathrm{id}|_{L_2(\mathcal{S}_a^{d-1}, w_a)}$ follows from

$$\mathcal{D}_a \mathcal{D}_a^* g(\theta) = \mathcal{D}_a \varphi(\theta) = g(\theta)$$

for all $g \in L_2(\mathcal{S}_a^{d-1}, w_a)$. Applying theorem 2.21 yields

$$\mathcal{D}_a^+ = \mathcal{D}_a^* (\mathcal{D}_a \mathcal{D}_a^*)^{-1} = \mathcal{D}_a^*$$

and with proposition 3.13 follows $\|\mathcal{D}_a\| = \|\mathcal{D}_a^+\| = 1$. For the flat detector Cone Beam transform we proceed analogously and define

$$\varphi(x) \coloneqq \mathcal{X}_a^* g(x) = \big(w_a g\big)\left(a + \frac{\|\tilde{a}\|^2}{\langle a - x, \tilde{a}\rangle}(x - a)\right)$$

for $g \in L_2(\tilde{E}_a, w_a)$. With equation (3.3) we obtain

$$\begin{aligned}\mathcal{X}_a\varphi(\eta) &= \int_{\left\{t\in\mathbb{R}_+ \colon a+t(\eta-a)\in\Omega\right\}} \varphi(a+t(\eta-a))\,dt \\ &= \underbrace{\int_{\left\{t\in\mathbb{R}_+ \colon a+t\theta\in\Omega\right\}} dt}_{w_a(\eta)^{-1}}\,(w_a g)(\eta) \\ &= g(\eta).\end{aligned}$$

The surjectivity follows immediately and further $\mathcal{X}_a\mathcal{X}_a^* = \mathrm{id}|_{g\in L_2(\tilde{E}_a,w_a)}$ since

$$\mathcal{X}_a\mathcal{X}_a^* g(x) = \mathcal{X}_a\varphi(\eta) = g(x).$$

Form theorem 2.21 follows the identity $\mathcal{D}_a^+ = \mathcal{D}_a^*$ and with $\|\mathcal{X}_a\| = \|\mathcal{X}_a^+\|$ follows the operator norm estimate from 3.13. □

3.4 Discussion

In this chapter we discussed the Radon transform, the X-ray transform and the related Cone Beam transforms for the situation of a fixed first argument, i.e., fixed scanning direction and fixed X-ray source positions, respectively, as bounded operators between weighted L_2-spaces. All these operators have in common that

(i) $\|T\| = 1$ and

(ii) $T^+ = T^*$ with $\|T^+\| = 1$,

for a suitable choice of weight functions, cf. proposition 3.5 for the Radon transform, proposition 3.10 for the X-ray transform and propositions 3.13 and 3.14 for the Cone Beam transforms. For the Radon transform, this is indirectly discussed in [Nat01, section V.4.3.] in the context of the Kaczmarz method. For the classical Cone Beam transform some results can be found in [Ham+80].

As a direct consequence, all of these operators are well-posed on the specified weighted spaces and the pseudo inverse can be directly computed via the adjoint operators. Moreover, it holds

$$TT^* = \mathrm{id} \qquad \text{and} \qquad T^*T = \mathrm{P}_{\mathrm{N}(T)^\perp}.$$

Having a closer look at the involved weight functions a certain pattern is observable. Let $T : L_2(\Omega, W) \to L_2(\Lambda, w)$ denote one of the above discussed operators.

(i) $T = \mathcal{R}_\theta$, $\Lambda = [-1, 1]$, with weights

$$W \equiv 1 \qquad \text{and} \qquad w_\theta(s) = \frac{1}{\mathcal{R}_\theta\chi_\Omega(s)}$$

(ii) $T = \mathcal{P}_\theta$, $\Lambda = \theta^\perp$, with weights

$$W \equiv 1 \qquad \text{and} \qquad w_\theta(x) = \frac{1}{\mathcal{P}_\theta\chi_\Omega(x)}$$

(iii) $T = \mathcal{D}_a$, $\Lambda = \mathcal{S}_a^{d-1}$, with weights

$$W_a(x) = \left\|x - a\right\|^{1-d} \qquad \text{and} \qquad w_a(\theta) = \frac{1}{\mathcal{D}_a \chi_\Omega(\theta)}$$

(iv) $T = \mathcal{X}_a$, $\Lambda = \tilde{E}_a$, with weights

$$W_a(x) = \|\tilde{a}\|^{2d-3}\big(\langle a - x, \tilde{a}\rangle\big)^{1-d} \qquad \text{and} \qquad w_a(\eta) = \frac{1}{\mathcal{X}\chi_\Omega(\eta)}$$

The weight functions w in the image domain are defined as the forward projection of the reconstruction area respectively the unit ball Ω. These weights compensate the ray length of the X-rays through the reconstruction area. The weights W in the operator domain are chosen as the Jacobian of the change of variables from Cartesian coordinates to the coordinates of the measurement geometry.

Chapter 4

A semi-discrete operator model

In this chapter, we derive a semi-discrete framework to solve finite dimensional systems of bounded linear operator equations with common domain. Let $\mathcal{X}$ be a real Hilbert space. Further, let $I \subset \mathbb{N}$ be a finite set of indices and let $\{\mathcal{Y}_i\}_{i\in I}$ be a set of real Hilbert spaces. The direct sum of $\{\mathcal{Y}_i\}_{i\in I}$ is defined as

$$\mathcal{Y} := \bigoplus_{i\in I} \mathcal{Y}_i.$$

By means of (2.1), $\mathcal{Y}$ is again a real Hilbert space with the inner product $\langle\cdot,\cdot\rangle_{\mathcal{Y}}$ defined by

$$\langle g, h\rangle_{\mathcal{Y}} := \sum_{i\in I} \langle g_i, h_i\rangle_{\mathcal{Y}_i} \qquad \forall g, h \in \mathcal{Y}.$$

We consider a set of linear operators $\{\mathcal{A}_i\}_{i\in I}$ where each operator is a bounded mapping

$$\mathcal{A}_i : \mathcal{X} \to \mathcal{Y}_i, \qquad \forall i \in I$$

and define the linear operator $\mathcal{A} : \mathcal{X} \to \mathcal{Y}$ as

$$(\mathcal{A}f)_i := \mathcal{A}_i f.$$

By means of equation (2.2), the boundedness of $\mathcal{A}$ follows with

$$\|\mathcal{A}f\|_{\mathcal{Y}}^2 = \sum_{i\in I} \|\mathcal{A}_i f\|_{\mathcal{Y}_i}^2 \le \left(\sum_{i\in I} \|\mathcal{A}_i\|^2\right)\|f\|^2$$

from the boundedness of the operators $\mathcal{A}_i$.

We consider the following prototype problem: For a given right-hand side $g \in \mathcal{Y}$, find $f \in \mathcal{X}$ such that

$$\mathcal{A}f = g.$$

This is clearly equivalent to solving the system

$$\mathcal{A}_i f = g_i (\forall i \in I) \tag{4.1}$$

since

$$\mathcal{A}f = \begin{pmatrix} \mathcal{A}_1 \\ \vdots \\ \mathcal{A}_{|I|} \end{pmatrix} f = \begin{pmatrix} \mathcal{A}_1 f \\ \vdots \\ \mathcal{A}_{|I|} f \end{pmatrix} \qquad \text{and} \qquad g = \begin{pmatrix} g_1 \\ \vdots \\ g_{|I|} \end{pmatrix}.$$

To solve this problem, we proceed as follows. First, we introduce a discretization scheme for the operator domain by approximation with a finite-dimensional set of basis elements $\{b_j\} \subset \mathcal{X}$. In a second step, the operators $\{\mathcal{A}_i\}_{i\in I}$ are restricted to a finite dimensional Hilbert space which we will use to compute an approximated solution to the reconstruction problem (5.2). Finally, the convergence of the finite dimensional solution to the solution of (4.1) is investigated.

4.1 Finite-dimensional approximation

Let $B \coloneqq \{b_j\}_{j\in J}$ a set of linearly independent elements $\{b_j\}_{j\in J} \subset \mathcal{X}$ for a finite dimensional set of indices $J \subset \mathbb{N}$. We call $B \subset \mathcal{X}$ a *basis* and its elements $b_j \in B$ the *basis elements*. The subspace

$$\mathcal{X}_B \coloneqq \operatorname{span} B \subseteq \mathcal{X}$$

is called the *generated subspace*. Together with the inner product $\langle\cdot,\cdot\rangle_{\mathcal{X}}$, $\mathcal{X}_B$ is a finite-dimensional real Hilbert space with dimension

$$\dim \mathcal{X}_B = |J|.$$

Every element $f \in \mathcal{X}_B$ has a unique representation in terms of B, i.e., for every $f \in \mathcal{X}_B$ exists the basis representation

$$f = \sum_{j\in J} f_j b_j, \tag{4.2}$$

where the coefficients $\{f_j\}_{j\in J}$ are uniquely determined, cf. [Lan87]. Thus, the mapping

$$f \mapsto \boldsymbol{f} = \begin{pmatrix} f_1 \\ \vdots \\ f_{|J|} \end{pmatrix} \in \mathbb{R}^{|J|} \tag{4.3}$$

which maps an element $f \in \mathcal{X}_B$ to its basis coefficient vector $\boldsymbol{f} \in \mathbb{R}^{|J|}$ is a bijection between $\mathcal{X}_B$ and the coefficient space $\mathbb{R}^{|J|}$.

Further, let W be a symmetric positive definite $|J|\times|J|$ matrix which we call weight matrix. Following example 2.15, the matrix W induces a weighted inner product and a weighted norm on $\mathbb{R}^{|J|}$ by

$$\langle\cdot,\cdot\rangle_W \coloneqq \langle\cdot, W\,\cdot\rangle \qquad \text{and} \qquad \|\cdot\|_W = \|W^{\frac{1}{2}}\,\cdot\|,$$

respectively, where $W^{\frac{1}{2}}$ denotes the square root of W, cf. theorem 2.11(i).

The following definition is used to extend linear operators to the coefficient space $\mathbb{R}^{|J|}$.

Definition 4.1. *The linear operator*

$$\mathcal{E}_B : \left(\mathbb{R}^{|J|}, \langle\cdot,\cdot\rangle_W\right) \to \mathcal{X}_B, \qquad \mathcal{E}_B\boldsymbol{f} \coloneqq \sum_{j\in J} \boldsymbol{f}_j b_j$$

is called (weighted) evaluation operator *for the basis B.*

Proposition 4.2. *The evaluation operator is bounded and its (weighted) adjoint operator*

$$\mathcal{E}_B^\sharp : \mathcal{X}_B \to (\mathbb{R}^{|J|}, \langle\cdot,\cdot\rangle_W)$$

is computed as

$$\mathcal{E}_B^\sharp\varphi = W^{-1}\begin{pmatrix} \langle b_1, \varphi\rangle_{\mathcal{X}} \\ \vdots \\ \langle b_{|J|}, \varphi\rangle_{\mathcal{X}} \end{pmatrix}.$$

Proof. Since $\mathcal{X}_B$ is finite dimensional the evaluation operator $\mathcal{E}_B$ is bounded as can be seen by the following estimation. For $\boldsymbol{f} \in \mathbb{R}^{|J|}$ holds

$$\begin{aligned}
\|\mathcal{E}_B \boldsymbol{f}\|_{\mathcal{X}_B} &= \left\| \sum_{j \in J} \boldsymbol{f}_j b_j \right\|_{\mathcal{X}_B} \\
&\leq \sum_{j \in J} |\boldsymbol{f}_j| \|b_j\|_{\mathcal{X}_B} \\
&\leq \max_{j \in J} \|b_j\|_{\mathcal{X}_B} \sum_{j \in J} |\boldsymbol{f}_j| \\
&\leq \max_{j \in J} \|b_j\|_{\mathcal{X}_B} \sqrt{|J|}\, \|\boldsymbol{f}\| \\
&\leq \max_{j \in J} \|b_j\|_{\mathcal{X}_B} \sqrt{|J|}\, \|W^{-\frac{1}{2}}\|\, \|\boldsymbol{f}\|_W,
\end{aligned}$$

where the equivalence of the Euclidean norm $\|\cdot\|_2$ and the norm $\|\cdot\|_1$ as well as the equivalence of the Euclidean norm and its weighted version $\|\cdot\|_W$ is used. To compute the weighted adjoint, let $\boldsymbol{f} \in \mathbb{R}^{|J|}$ and $\varphi \in \mathcal{X}_B$. We obtain

$$\begin{aligned}
\left\langle \mathcal{E}_B \boldsymbol{f},\, \varphi \right\rangle_{\mathcal{X}} &= \left\langle \sum_{j \in J} \boldsymbol{f}_j b_j \varphi \right\rangle_{\mathcal{X}} \\
&= \sum_{j \in J} \boldsymbol{f}_j \left\langle b_j,\, \varphi \right\rangle_{\mathcal{X}} \\
&= \left\langle \boldsymbol{f}, \begin{pmatrix} \langle b_1,\, \varphi \rangle_{\mathcal{X}} \\ \vdots \\ \langle b_{|J|},\, \varphi \rangle_{\mathcal{X}} \end{pmatrix} \right\rangle \\
&= \left\langle \boldsymbol{f}, W^{-1} \begin{pmatrix} \langle b_1, \varphi \rangle_{\mathcal{X}} \\ \vdots \\ \langle b_{|J|}, \varphi \rangle_{\mathcal{X}} \end{pmatrix} \right\rangle_W .
\end{aligned}$$

Thus the representation of the weighted adjoint $\mathcal{E}_B^\sharp$ follows. □

The evaluation operator $\mathcal{E}_B$ is defined as the inverse operator of (4.3), thus mapping a coefficient vector to its corresponding element in $\mathcal{X}_B$ by evaluating the representation (4.2).

It may also be of interest to recover the basis coefficients of a given element $f \in \mathcal{X}$, i.e., evaluating the mapping (4.3). To this end, we consider the normal equation

$$\mathcal{E}_B^\sharp \mathcal{E}_B \boldsymbol{f} = \mathcal{E}_B^\sharp f$$

which yields the interpolation problem

$$\Phi_B \boldsymbol{f} = \begin{pmatrix} \langle b_1, f \rangle_{\mathcal{X}} \\ \vdots \\ \langle b_{|J|}, f \rangle_{\mathcal{X}} \end{pmatrix}$$

where Φ_B is a regular $|J| \times |J|$ matrix given by

$$\Phi_B = \left(\langle b_j, b_k \rangle_{\mathcal{X}} \right)_{j,k \in J}.$$

For $f \in \mathcal{X}_B$, the interpolation problem is uniquely solvable since $\mathcal{E}_{B,k}$ and thus also its adjoint operators are bijections on $\mathcal{X}_B$. For the more general case $f \in \mathcal{X}$ the interpolation problem yields the basis coefficients of the best approximation in $\mathcal{X}_B$.

Assuming that B forms an orthonormal basis of $\mathcal{X}_B$, i.e.,

$$\langle b_i, b_j \rangle_{\mathcal{X}} = \delta_{ij} \qquad \forall i, j \in J$$

with δ_{ij} being the Kronecker delta, the interpolation matrix is equal to the identity matrix. The basis coefficients can thus be computed by evaluating the inner products $\langle f, b_j \rangle_{\mathcal{X}}$.

4.2 Semi-discrete operators

Let $f \in \mathcal{X}_B$ be fixed and let $\boldsymbol{f} \in \mathbb{R}^{|J|}$ denote its coefficient vector with respect to the basis B. For any bounded linear operator $\mathcal{T}$ defined on $\mathcal{X}$ holds

$$\mathcal{T}f = \mathcal{T}\mathcal{E}_B \boldsymbol{f} = \mathcal{T}\left(\sum_{j \in J} \boldsymbol{f}_j b_j \right) = \sum_{j \in J} \boldsymbol{f}_j \left(\mathcal{T} b_j \right)$$

with $\mathcal{E}_B$ being the evaluation operator for the basis B. Due to the bijection property of $\mathcal{E}_B$ the image of $\mathcal{T}|_{\mathcal{X}_B}$ is completely characterized by the image of the basis elements $\{\mathcal{T} b_j\}_{j \in J}$.

Let $\mathcal{A}$ and $\{\mathcal{A}_i\}_{i \in I}$ be defined as above: $\{\mathcal{A}_i\}_{i \in I}$ are bounded linear operators $\mathcal{A}_i : \mathcal{X} \to \mathcal{Y}_i$ and $\mathcal{A} : \mathcal{X} \to \mathcal{Y} = \bigoplus_{i \in I} \mathcal{Y}_i$ with $(\mathcal{A}f)_i = \mathcal{A}_i f$. The operator $\mathcal{A}$ is again bounded since

$$\|\mathcal{A}f\|_{\mathcal{Y}}^2 = \sum_{i \in I} \|\mathcal{A}_i f\|_{\mathcal{Y}_i}^2 \leq \sum_{k \in I} \|\mathcal{A}_i f\|_{\mathcal{Y}_i}^2$$

holds for all $f \in \mathcal{X}$. The adjoint operator $\mathcal{A}^* : \mathcal{Y} \to \mathcal{X}$ is computed by

$$\mathcal{A}^* \varphi = \sum_{i \in I} \mathcal{A}_i^* \varphi_i \tag{4.4}$$

as can be seen for $f \in \mathcal{X}$ and $\varphi \in \mathcal{Y}$ by

$$\begin{aligned} \langle \mathcal{A}f, \varphi \rangle_{\mathcal{Y}} &= \sum_{i \in I} \left\langle \mathcal{A}_i f, \varphi_i \right\rangle_{\mathcal{Y}_i} \\ &= \sum_{i \in I} \left\langle f, \mathcal{A}_i^* \varphi_i \right\rangle_{\mathcal{X}} = \left\langle f, \sum_{i \in I} \mathcal{A}_i^* \varphi_i \right\rangle_{\mathcal{X}}. \end{aligned}$$

Further, we introduce a partition P of the index set I, $P \coloneqq \{I_k\}_{k \in I_P}$, where the subsets I_k are mutually disjoint with

$$I = \bigcup_{k \in I_P} I_k \qquad \text{and} \qquad I_P \coloneqq \{1, \dots |P|\}.$$

The partitioned operators $\{A_k\}_{k \in I_P}$ with respect to the partition I_P are defined as

$$A_k : \mathcal{X} \to Y_k, \qquad A_k f \coloneqq \left(\mathcal{A}_i f \right)_{i \in I_k},$$

and the Hilbert spaces Y_k are defined by the orthogonal sum

$$Y_k := \bigoplus_{i \in I_k} \mathcal{Y}_i.$$

In analogy to equation (4.4), the adjoint partitioned operator A_k^* is computed as

$$A_k^* \varphi = \sum_{i \in I_k} \mathcal{A}_i^* \varphi_i \qquad \forall \varphi \in Y_k. \tag{4.5}$$

Definition 4.3. *The linear operator*

$$\boldsymbol{A}_{B,k} : \left(\mathbb{R}^{|J|}, \langle \cdot, \cdot \rangle_k\right) \to Y_k, \qquad \boldsymbol{A}_{B,k} \boldsymbol{f} := \left(A_k \mathcal{E}_{B,k}\right) \boldsymbol{f} = \sum_{j \in J} \boldsymbol{f}_j A_k b_j$$

is called the semi-discrete operator *of A_k with respect to the basis B.*

Proposition 4.4. *(i) $\boldsymbol{A}_{B,k}$ is bounded and its (weighted) adjoint operator*

$$\boldsymbol{A}_{B,k}^\sharp : Y_k \to \left(\mathbb{R}^{|J|}, \langle \cdot, \cdot \rangle_k\right)$$

is computed as

$$\boldsymbol{A}_{B,k}^\sharp \varphi = W_k^{-1} \sum_{i \in I_k} \begin{pmatrix} \langle \mathcal{A}_i b_1, \varphi_i \rangle_{\mathcal{Y}_i} \\ \vdots \\ \langle \mathcal{A}_i b_{|J|}, \varphi_i \rangle_{\mathcal{Y}_i} \end{pmatrix}.$$

(ii) The generalized inverse $\boldsymbol{A}_{B,k}^+ : \mathrm{D}(\boldsymbol{A}_{B,k}^+) = Y_k \to \left(\mathbb{R}^{|J|}, \langle \cdot, \cdot \rangle_k\right)$ is bounded.

Proof. (i) Since $\boldsymbol{A}_{B,k}$ is defined as the concatenation of the bounded linear operators A_k and $\mathcal{E}_{B,k}$, it is again bounded. Consequently, its adjoint operator exists and is uniquely determined. From the definition of $\boldsymbol{A}_{B,k}$ it yields

$$\boldsymbol{A}_{B,k}^\sharp = \left(A_k \mathcal{E}_{B,k}\right)^\sharp = \mathcal{E}_{B,k}^\sharp A_k^*.$$

Let $\varphi \in Y_k$. From proposition 4.2 follows

$$\begin{aligned} \boldsymbol{A}_{B,k}^\sharp \varphi = \mathcal{E}_{B,k}^\sharp A_k^* \varphi &= W_k^{-1} \begin{pmatrix} \langle b_1, A_k^* \varphi \rangle_{\mathcal{X}} \\ \vdots \\ \langle b_{|J|}, A_k^* \varphi \rangle_{\mathcal{X}} \end{pmatrix} \\ &\overset{(4.5)}{=} W_k^{-1} \begin{pmatrix} \langle b_1, \sum_{i \in I_k} \mathcal{A}_i^* \varphi_i \rangle_{\mathcal{X}} \\ \vdots \\ \langle b_{|J|}, \sum_{i \in I_k} \mathcal{A}_i^* \varphi_i \rangle_{\mathcal{X}} \end{pmatrix} \\ &= W_k^{-1} \sum_{i \in I_k} \begin{pmatrix} \langle b_1, \mathcal{A}_i^* \varphi_i \rangle_{\mathcal{X}} \\ \vdots \\ \langle b_{|J|}, \mathcal{A}_i^* \varphi_i \rangle_{\mathcal{X}} \end{pmatrix} \end{aligned}$$

$$= W_k^{-1} \sum_{i \in I_k} \begin{pmatrix} \langle \mathcal{A}_i b_1, \varphi_i \rangle_{\mathcal{Y}_i} \\ \vdots \\ \langle \mathcal{A}_i b_{|J|}, \varphi_i \rangle_{\mathcal{Y}_i} \end{pmatrix}.$$

(ii) This follows immediately from corollary 2.19.

□

The injectivity of the semi-discrete operators $\boldsymbol{A}_{B,k}$ plays an important role in the next chapter when analyzing iterative methods. The following lemma gives a characterization of $\boldsymbol{A}_{B,k}$ with respect to its injectivity.

Lemma 4.5. *The following statements are equivalent.*

(i) $\boldsymbol{A}_{B,k}$ *is injective,*

(ii) $\{A_k b_j\}_{j \in J}$ *is linearly independent,*

(iii) $\mathcal{X}_B \perp \mathrm{N}(A_k)$.

Proof. (i) $\Leftrightarrow$ (ii) Let $\boldsymbol{A}_{B,k}$ be injective. Then, the nullspace $\mathrm{N}(\boldsymbol{A}_{B,k})$ is trivial and it is

$$\boldsymbol{A}_{B,k} \boldsymbol{f} = \sum_{j \in J} \boldsymbol{f}_j A_k b_j = 0 \qquad \Leftrightarrow \qquad \boldsymbol{f} = 0.$$

This is equivalent to $\{A_k b_j\}_{j \in J}$ being mutually linearly independent.

(ii) $\Leftrightarrow$ (iii) Let $\{A_k b_j\}_{j \in J}$ be linearly independent. Thus,

$$\sum_{j \in J} \boldsymbol{f}_j A_k b_j = 0 \qquad \Leftrightarrow \qquad f_j \equiv 0 \quad \forall j \in J.$$

Since $\mathcal{E}_{B,k}$ is bijective, this is again equivalent to

$$A_k f = 0 \qquad \Leftrightarrow \qquad f = 0 \quad \forall f \in \mathcal{X}_B.$$

□

Lemma 4.6. *Let* $\alpha > 0$.

(i)

$$\left(\mathrm{id} - \alpha^2 \boldsymbol{A}_{B,k}^{\sharp} \boldsymbol{A}_{B,k}\right) \textit{ is positive semi-definite w.r.t. } \langle \cdot, \cdot \rangle_k \qquad \Leftrightarrow \qquad \|\boldsymbol{A}_{B,k}\|_{\mathrm{op}} \leq \frac{1}{\alpha}$$

(ii)

$$\left(\mathrm{id} - \alpha^2 \boldsymbol{A}_{B,k}^{\sharp} \boldsymbol{A}_{B,k}\right) \textit{ is negative semi-definite w.r.t. } \langle \cdot, \cdot \rangle_k$$
$$\Leftrightarrow \qquad \|\boldsymbol{A}_{B,k} \boldsymbol{f}\|_{Y_k} \geq \frac{1}{\alpha} \|\boldsymbol{f}\|_k \qquad \forall \boldsymbol{f} \in \mathrm{N}(\boldsymbol{A}_{B,k})^{\perp}$$

Both norm estimations hold strictly if and only if the operators are strictly definite.

Proof. For $\boldsymbol{f} \in \mathbb{R}^{|J|}$ holds

$$\left\langle \boldsymbol{f}, (\mathrm{id} - \alpha^2 \boldsymbol{A}_{B,k}^{\sharp} \boldsymbol{A}_{B,k}) \boldsymbol{f} \right\rangle_k = \|\boldsymbol{f}\|_k^2 - \alpha^2 \|\boldsymbol{A}_{B,k} \boldsymbol{f}\|_{Y_k}^2. \tag{4.6}$$

(i) First, let $(\mathrm{id} - \alpha^2 \boldsymbol{A}_{B,k}^{\sharp} \boldsymbol{A}_{B,k})$ be positive semi-definite with respect to $\langle \cdot, \cdot \rangle_k$. Using (4.6), this is equivalent to

$$\|\boldsymbol{A}_{B,k} \boldsymbol{f}\|_{Y_k} \leq \frac{1}{\alpha} \|\boldsymbol{f}\|_k$$

such that we obtain the norm estimation

$$\|\boldsymbol{A}_{B,k}\|_{\mathrm{op}} = \max_{\|\boldsymbol{f}\|_k = 1} \|\boldsymbol{A}_{B,k} \boldsymbol{f}\|_{Y_k} \leq \frac{1}{\alpha}.$$

Now, let $\|\boldsymbol{A}_{B,k}\|_{\mathrm{op}}$ be bounded by $\frac{1}{\alpha}$. From (4.6) follows

$$\begin{aligned} \|\boldsymbol{f}\|_k^2 - \alpha^2 \|\boldsymbol{A}_{B,k} \boldsymbol{f}\|_{Y_k}^2 &\geq \|\boldsymbol{f}\|_k^2 - \alpha^2 \|\boldsymbol{A}_{B,k}\|_{\mathrm{op}}^2 \|\boldsymbol{f}\|_k^2 \\ &= (1 - \alpha^2 \|\boldsymbol{A}_{B,k}\|_{\mathrm{op}}^2) \|\boldsymbol{f}\|_k^2 \\ &\geq 0. \end{aligned}$$

Thus $(\mathrm{id} - \alpha^2 \boldsymbol{A}_{B,k}^{\sharp} \boldsymbol{A}_{B,k})$ is positive semi-definite with respect to $\langle \cdot, \cdot \rangle_k$.

(ii) For $(\mathrm{id} - \alpha^2 \boldsymbol{A}_{B,k}^{\sharp} \boldsymbol{A}_{B,k})$ being negative semi-definite the statement follows immediately with equation (4.6) since

$$\|\boldsymbol{f}\|_k^2 - \alpha^2 \|\boldsymbol{A}_{B,k} \boldsymbol{f}\|_{Y_k}^2 \leq 0 \quad \Leftrightarrow \quad \frac{1}{\alpha} \|\boldsymbol{f}\|_k \leq \|\boldsymbol{A}_{B,k} \boldsymbol{f}\|_{Y_k}$$

for all $\boldsymbol{f} \in \mathrm{N}(\boldsymbol{A}_{B,k})^{\perp}$.

□

The parameter α in lemma 4.6 (ii) can be interpreted as a norm estimate for the inverse operator of $\boldsymbol{A}_{B,k}$ restricted to its range $\mathrm{R}(\boldsymbol{A}_{B,k}) \subseteq Y_k$.

Proposition 4.7. *The matrix representation of $\boldsymbol{A}_{B,k}^{\sharp} \boldsymbol{A}_{B,k}$ with respect to the canonical orthonormal basis in $\mathbb{R}^{|J|}$ is given by the symmetric and positive semi-definite $|J| \times |J|$-matrix*

$$\Phi_{B,k}^{W} = W_k^{-1} \sum_{i \in I_k} \left(\left\langle \mathcal{A}_i b_j, \mathcal{A}_i b_l \right\rangle_{\mathcal{Y}_i} \right)_{j,l=1}^{|J|}.$$

The matrix $\Phi_{B,k}^{W}$ is strictly positive definite with respect to the weighted inner product $\langle \cdot, \cdot \rangle_k$ if and only if $\boldsymbol{A}_{B,k}$ is injective.

Proof. For arbitrary $\boldsymbol{f} \in \mathbb{R}^{|J|}$ holds

$$\begin{aligned}
\boldsymbol{A}_{B,k}^{\sharp}\boldsymbol{A}_{B,k}\boldsymbol{f} &= W_k^{-1}\left(\left\langle A_k b_j, \sum_{l\in J} \boldsymbol{f}_l A_k b_l \right\rangle_{Y_k}\right)_{j\in J} \\
&= W_k^{-1}\left(\sum_{l\in J} \boldsymbol{f}_l \langle A_k b_j, A_k b_l\rangle_{Y_k}\right)_{j\in J} \\
&= W_k^{-1} \sum_{l\in J} \boldsymbol{f}_l \left(\langle A_k b_j, A_k b_l\rangle_{Y_k}\right)_{j\in J} \\
&= \sum_{l\in J} \boldsymbol{f}_l \cdot W_k^{-1}\left(\langle A_k b_j, A_k b_l\rangle_{Y_k}\right)_{j\in J} \\
&= \sum_{l\in J} \boldsymbol{f}_l \cdot W_k^{-1}\left(\sum_{i\in I_k} \langle \mathcal{A}_i b_j, \mathcal{A}_i b_l\rangle_{\mathcal{Y}_i}\right)_{j\in J} \\
&= \sum_{l\in J} \boldsymbol{f}_l \cdot W_k^{-1} \sum_{i\in I_k}\left(\langle \mathcal{A}_i b_j, \mathcal{A}_i b_l\rangle_{\mathcal{Y}_i}\right)_{j\in J} \\
&= \Phi_{B,k}^{W}\, \boldsymbol{f}.
\end{aligned}$$

The positive definiteness of $\Phi_{B,k}^{W}$ follows from

$$\left\langle \boldsymbol{f}, \Phi_{B,k}^{W}\boldsymbol{f}\right\rangle_k = \left\langle \boldsymbol{f}, \boldsymbol{A}_{B,k}^{\sharp}\boldsymbol{A}_{B,k}\boldsymbol{f}\right\rangle_k = \|\boldsymbol{A}_{B,k}\boldsymbol{f}\|_{Y_k}^2 \geq 0.$$

Moreover $\Phi_{B,k}^{W}$ is strictly positive definite if and only if $\boldsymbol{A}_{B,k}$ is injective.

□

To close this section, we give an example of suitable weight matrices which will be used later on. Therefore, we first introduce the concept of diagonally dominant matrices. For a detailed discussion on diagonally dominant matrices, see e.g. [Lan87].

Definition 4.8. *Let A be a quadratic real-valued $M\times M$ matrix. A is called* weakly *diagonally dominant if*

$$|a_{ii}| \geq \sum_{\substack{j=1\\ j\neq i}}^{M} |a_{ij}| \qquad \forall i \in \{1,\dots,M\}. \tag{4.7}$$

It is called strictly *diagonally dominant if* (4.7) *holds strictly for all $i \in \{1,\dots,M\}$.*

Lemma 4.9. *Let $A \in \mathbb{R}^{M\times M}$ be symmetric with non-negative diagonal. If A is (weakly) diagonally dominant then it is positive (semi-)definite.*

Proof. Let $x \in \mathbb{R}^M$. It holds,

$$\langle x, Ax\rangle = \sum_{j=1}^{M} x_j \sum_{k=1}^{M} a_{jk}x_k$$

$$
\begin{aligned}
&= \sum_{j=1}^{M} x_j \left(a_{jj} x_j + \sum_{\substack{k=1 \\ k \neq j}}^{M} a_{jk} x_k \right) \\
&= \sum_{j=1}^{M} a_{jj} x_j^2 + \sum_{j=1}^{M} \sum_{\substack{k=1 \\ k \neq j}}^{M} a_{jk} x_j x_k \\
&\geq \sum_{j=1}^{M} a_{jj} x_j^2 - \sum_{j=1}^{M} \sum_{\substack{k=1 \\ k \neq j}}^{M} |a_{jk}||x_j||x_k| \\
&\geq \sum_{j=1}^{M} a_{jj} x_j^2 - \frac{1}{2} \sum_{j=1}^{M} \sum_{\substack{k=1 \\ k \neq j}}^{M} |a_{jk}| \left(x_j^2 + x_k^2 \right) \\
&= \sum_{j=1}^{M} a_{jj} x_j^2 - \frac{1}{2} \sum_{j=1}^{M} \left(\sum_{\substack{k=1 \\ k \neq j}}^{M} |a_{jk}| \right) x_j^2 - \frac{1}{2} \sum_{j=1}^{M} \sum_{\substack{k=1 \\ k \neq j}}^{M} |a_{jk}| x_k^2
\end{aligned}
$$

and with the symmetry of A,

$$
= \sum_{j=1}^{M} a_{jj} x_j^2 - \sum_{j=1}^{M} \left(\sum_{\substack{k=1 \\ k \neq j}}^{M} |a_{jk}| \right) x_j^2 .
$$

We only consider the situation of A being weakly diagonally dominant. The result for strictly diagonally dominant matrices is shown analogously. Thus, let A be weakly diagonally dominant with non-negative diagonal elements, i.e.,

$$
|a_{jj}| = a_{jj} \geq \sum_{\substack{j=1 \\ j \neq k}}^{M} |a_{jk}| \qquad \forall j \in \{1, \dots, M\}.
$$

It follows

$$
\begin{aligned}
\langle x, Ax \rangle &\geq \sum_{j=1}^{M} a_{jj} x_j^2 - \sum_{j=1}^{M} \left(\sum_{\substack{k=1 \\ k \neq j}}^{M} |a_{jk}| \right) x_j^2 \\
&\geq \sum_{j=1}^{M} a_{jj} x_j^2 - \sum_{j=1}^{M} |a_{jj}| x_j^2 \\
&= 0,
\end{aligned}
$$

and A is positive semi-definite. □

Example 4.10. *(i) Let W_k be a diagonal matrix defined as*

$$
\left(W_k\right)_{jj} := \sum_{l \in J} \left| \left\langle A_k b_j, A_k b_l \right\rangle_{Y_k} \right| = \sum_{l \in J} \left| \sum_{i \in I_k} \left\langle \mathcal{A}_i b_j, \mathcal{A}_i b_l \right\rangle_{\mathcal{Y}_i} \right| \qquad \forall j \in J. \tag{4.8}
$$

Basically, lemma 4.6 is applied to obtain a norm estimation of the semi-discrete operators $\boldsymbol{A}_{B,k}$ *by showing that* $\mathrm{id} - \alpha^2 \boldsymbol{A}_{B,k}^{\sharp} \boldsymbol{A}_{B,k}$ *is positive (semi-)definite for some positive parameter* α*. With the matrix representation* $\Phi_{B,k}^{W}$ *of* $\boldsymbol{A}_{B,k}^{\sharp} \boldsymbol{A}_{B,k}$ *from proposition 4.7 we define the matrices*

$$\Phi_\alpha := (\mathrm{id} - \alpha^2 \Phi_{B,k}^{W}) \qquad \alpha > 0.$$

With lemma 4.6 follows the norm estimation $\|\boldsymbol{A}_{B,k}\|_{\mathrm{op}} \leq \alpha^{-1}$ *if* Φ_α *is diagonally dominant. Putting* $\alpha = 1$*, it follows*

$$\begin{aligned}
\left|(\Phi_1)_{jj}\right| &= \left|1 - \left(\Phi_{B,k}^{W}\right)_{jj}\right| \\
&= \Big|1 - (W_k)_{jj}^{-1} \underbrace{\langle A_k b_j, A_k b_j \rangle_{Y_k}}_{= \|A_k b_j\|_{Y_k}^2 \geq 0}\Big| \\
&= (W_k)_{jj}^{-1} \left|(W_k)_{jj} - \langle A_k b_j, A_k b_j \rangle_{Y_k}\right| \\
&= (W_k)_{jj}^{-1} \left|\sum_{l \neq j} \left|\langle A_k b_j, A_k b_l \rangle_{Y_k}\right|\right| \\
&= \sum_{l \neq j} (W_k)_{jj}^{-1} \left|\langle A_k b_j, A_k b_l \rangle_{Y_k}\right| \\
&= \sum_{l \neq j} \left|(W_k)_{jj}^{-1} \langle A_k b_j, A_k b_l \rangle_{Y_k}\right| \\
&= \sum_{l \neq j} \left|(\Phi_1)_{jl}\right|.
\end{aligned}$$

Hence, Φ_α *is weakly diagonally dominant and the norm estimation* $\|\boldsymbol{A}_{B,k}\|_{\mathrm{op}} \leq 1$ *follows.*

(ii) Assuming additionally

$$\left|\langle A_k b_j, A_k b_l \rangle_{Y_k}\right| = \langle A_k b_j, A_k b_l \rangle_{Y_k} \quad \forall j, l \in J$$

the weight matrices (4.8) are computed as

$$(W_k)_{jj} = \sum_{l \in J} \sum_{i \in I_k} \langle \mathcal{A}_i b_j, \mathcal{A}_i b_l \rangle_{\mathcal{Y}_i} = \sum_{i \in I_k} \left\langle \mathcal{A}_i b_j, \sum_{l \in J} \mathcal{A}_i b_l \right\rangle_{\mathcal{Y}_i}.$$

With the same argument as in (i), the matrix $-\Phi_1$ *is positive semi-definite with respect to* $\langle \cdot, \cdot \rangle_k$*. Thus for* $\boldsymbol{f} \in \mathbb{R}^{|J|}$ *holds*

$$-\left\langle \boldsymbol{f}, \left(\mathrm{id} - \Phi_{B,k}^{W}\right) \boldsymbol{f} \right\rangle_k \geq 0 \qquad \Leftrightarrow \qquad \|\boldsymbol{A}_{B,k} \boldsymbol{f}\|_{Y_k} \geq \|\boldsymbol{f}\|_k,$$

cf. lemma 4.6. Together with (i) follows

$$\|\boldsymbol{A}_{B,k}\|_{\mathrm{op}} \leq 1 \qquad \textit{and} \qquad \|\boldsymbol{A}_{B,k} \boldsymbol{f}\|_{Y_k} = \|\boldsymbol{f}\|_k \quad \forall \boldsymbol{f} \in \mathrm{N}(\boldsymbol{A}_{B,k})^{\perp}.$$

4.3 Convergence and regularization properties of the semi-discrete model

In the final section of this chapter, we treat the convergence and regularization properties of the semi-discrete operator model. The main question is under which conditions does the solution of the semi-discrete problem

$$\boldsymbol{A}_{B,k}\boldsymbol{f} = g_k \qquad k \in I_P$$

converges to the solution of the continuous problem $\mathcal{A}f = g$ for a given right-hand side $g \in Y$. Moreover, what impact does the presence of noise, i.e., only a disturbed version of the data g is available, have on the semi-discrete solution. To answer these questions, we will investigate the semi-discrete problem in the context of projection methods, in particular, the semi-discretization is treated within the scope of the least-squares projection method. Projection methods are widely-studied in literature. For an overview see [Kin16], [Lou89], [EHN96] and the references therein. We adapt the notation of [Nat77] and [Lou89].

Let $\mathcal{A} : \mathcal{X} \to Y$ be a bounded linear operator between the Hilbert spaces $\mathcal{X}$ and $\mathcal{Y}$. For $g \in \mathcal{Y}$, we aim at finding a solution of

$$\mathcal{A}f = g. \tag{4.9}$$

Since $\mathcal{A}$ is not further specified, we naturally consider the minimum-norm solution $f^\dagger \in \mathrm{N}(\mathcal{A})^\perp$. Further, we consider the sequences $\{\mathcal{X}_l\}_l \subset \mathcal{X}$ and $\{\mathcal{Y}_l\}_l \subset \mathcal{Y}$ of finite dimensional subspaces defining a projection method to solve (4.9). In other words, we solve the problem

$$f_l \in \mathcal{X}_l \cap \mathrm{N}(\mathcal{A})^\perp : \quad \langle \psi, \mathcal{A}f_l \rangle = \langle \psi, g \rangle \qquad \forall \psi \in \mathcal{Y}_l. \tag{4.10}$$

We are now confronted with the question under which conditions the solution of (4.10) does converge to f^+. To settle this question, we reformulate (4.10) as the following equivalent problem: Find $f_l \in \mathrm{N}(\mathcal{A}^l)^\perp$ such that

$$\mathcal{A}^l f_l = \mathrm{P}_{\mathcal{Y}_l} g$$

with $\mathcal{A}^l := \mathrm{P}_{\mathcal{Y}_l}\mathcal{A}\mathrm{P}_{\mathcal{X}_l}$ and $\mathrm{P}_{\mathcal{X}_l}$ and $\mathrm{P}_{\mathcal{Y}_l}$ denoting the orthogonal projectors onto $\mathcal{X}_l$ and $\mathcal{Y}_l$, respectively. The generalized inverse of $\mathcal{A}^l$ is denoted by $\mathcal{A}^{l,+}$. We obtain the following estimation which can be found e.g. in [Rie03, section 6.1.2].

Lemma 4.11. *It holds*

$$\|f^+ - f_l^+\|_{\mathcal{X}} \leq \left(1 + \|\mathcal{A}^{l,+}\mathrm{P}_{\mathcal{Y}_l}\mathcal{A}\|\right) \operatorname{dist}\left(f^+, \mathcal{X}_l\right) + \|\mathrm{P}_{\mathrm{N}(\mathcal{A}^l)} f^+\|_{\mathcal{X}}$$

with $f_l^+ := \mathcal{A}^{l,+}\mathrm{P}_{\mathcal{Y}_l} g$.

Proof. Since $\mathcal{X}_l$ and $\mathcal{Y}_l$ are finite dimensional subspaces, the generalized inverse $\mathcal{A}^{l,+}$ is bounded, cf. corollary 2.19, and with the boundedness of $\mathcal{A}$ follows $\|\mathcal{A}^{l,+}\mathrm{P}_{\mathcal{Y}_l}\mathcal{A}\| < \infty$. For arbitrary $\varphi \in \mathcal{X}_l$ follows

$$\mathcal{A}^{l,+}\mathrm{P}_{\mathcal{Y}_l}\mathcal{A}\varphi = \mathcal{A}^{l,+}\mathcal{A}_l\varphi = \mathrm{P}_{\mathrm{N}(\mathcal{A}^l)^\perp}\varphi \quad \Leftrightarrow \quad \left(\mathrm{P}_{\mathrm{N}(\mathcal{A}^l)^\perp} - \mathcal{A}^{l,+}\mathrm{P}_{\mathcal{Y}_l}\mathcal{A}\right)\varphi = 0.$$

Thus, it yields

$$\begin{aligned} f^+ - f_l^+ &= \left(\mathrm{id} - \mathcal{A}^{l,+}\mathrm{P}_{\mathcal{Y}_l}\mathcal{A}\right) f^+ \\ &= \left(\mathrm{P}_{\mathrm{N}(\mathcal{A}^l)^\perp} - \mathcal{A}^{l,+}\mathrm{P}_{\mathcal{Y}_l}\mathcal{A}\right) f^+ + \mathrm{P}_{\mathrm{N}(\mathcal{A}^l)} f^+ \end{aligned}$$

$$= \left(\mathrm{P}_{\mathrm{N}(\mathcal{A}^l)^\perp} - \mathcal{A}^{l,+}\mathrm{P}_{\mathcal{Y}_l}\mathcal{A}\right)\left(f^+ - \varphi\right) + \mathrm{P}_{\mathrm{N}(\mathcal{A}^l)}f^+$$

and further

$$\|f^+ - f_l^+\|_{\mathcal{X}} \leq \left(1 + \|\mathcal{A}^{l,+}\mathrm{P}_{\mathcal{Y}_l}\mathcal{A}\|\right)\|f^+ - \varphi\|_{\mathcal{X}} + \|\mathrm{P}_{\mathrm{N}(\mathcal{A}^l)}f^+\|_{\mathcal{X}} \qquad \forall \varphi \in \mathcal{X}_l.$$

In particular, this estimation still holds true when considering the infimum over all $\varphi \in \mathcal{X}_l$ of the right-hand side such that we obtain

$$\begin{aligned}\|f^+ - f_l^+\|_{\mathcal{X}} &\leq \left(1 + \|\mathcal{A}^{l,+}\mathrm{P}_{\mathcal{Y}_l}\mathcal{A}\|\right) \inf_{\varphi\in\mathcal{X}_l} \|f^+ - \varphi\|_{\mathcal{X}} + \|\mathrm{P}_{\mathrm{N}(\mathcal{A}^l)}f^+\|_{\mathcal{X}} \\ &= \left(1 + \|\mathcal{A}^{l,+}\mathrm{P}_{\mathcal{Y}_l}\mathcal{A}\|\right)\operatorname{dist}\left(f^+, \mathcal{X}_l\right) + \|\mathrm{P}_{\mathrm{N}(\mathcal{A}^l)}f^+\|_{\mathcal{X}}.\end{aligned}$$

□

With this lemma, we are able to formulate the following result which is basically an adaption of a result from [Nat77], see also [Lou89, theorem 4.5.4].

Theorem 4.12. *Let $\varepsilon > 0$. For $g, g^\varepsilon \in \mathcal{Y}$ with $\|g - g^\varepsilon\|_{\mathcal{Y}} < \varepsilon$ and $f_{l,\varepsilon}^+ = \mathcal{A}^{l,+}\mathrm{P}_{\mathcal{Y}_l}g^\varepsilon$ holds,*

$$\|f^+ - f_{l,\varepsilon}^+\|_{\mathcal{X}} \leq \left(1 + \|\mathcal{A}^{l,+}\mathrm{P}_{\mathcal{Y}_l}\mathcal{A}\|\right)\operatorname{dist}\left(f, \mathcal{X}_l\right) + \|\mathrm{P}_{\mathrm{N}(\mathcal{A}^l)}f^+\|_{\mathcal{X}} + \varepsilon\|\mathcal{A}^{l,+}\mathrm{P}_{\mathcal{Y}_l}\|.$$

Proof. The error can be split into an approximation error term and a data error term as

$$\|f^+ - f_{l,\varepsilon}^+\|_{\mathcal{X}} \leq \|f^+ - f_l^+\|_{\mathcal{X}} + \|f_l^+ - f_{l,\varepsilon}^+\|_{\mathcal{X}}.$$

Lemma 4.11 yields the estimation

$$\|f^+ - f_l^+\|_{\mathcal{X}} \leq \left(1 + \|\mathcal{A}^{l,+}\mathrm{P}_{\mathcal{Y}_l}\mathcal{A}\|\right)\operatorname{dist}\left(f, \mathcal{X}_l\right) + \|\mathrm{P}_{\mathrm{N}(\mathcal{A}^l)}f^+\|_{\mathcal{X}}$$

for the approximation error. The data error term is estimated with

$$\|f_l^+ - f_{l,\varepsilon}^+\|_{\mathcal{X}} = \|\mathcal{A}^{l,+}\mathrm{P}_{\mathcal{Y}_l}(g - g^\varepsilon)\|_{\mathcal{X}} \leq \|\mathcal{A}^{l,+}\mathrm{P}_{\mathcal{Y}_l}\|\|g - g^\varepsilon\|_{\mathcal{Y}} \leq \varepsilon\|\mathcal{A}^{l,+}\mathrm{P}_{\mathcal{Y}_l}\|$$

yielding the conclusion. □

We now have a closer look at the least squares projection method. Let $\{B_l\}_{l\in\mathbb{N}} \subseteq \mathcal{X}$ be a sequence of finite dimensional basis sets $B_l := \{b_j^l\}_{j\in J_l}$ denoting the sets of basis elements. The least-squares projection method is defined by the choice

$$\mathcal{X}_l := \operatorname*{span}_{l\in\mathbb{N}}\{B_l\} \qquad \text{and} \qquad \mathcal{Y}_l := \mathcal{A}\mathcal{X}_l = \operatorname*{span}_{l\in\mathbb{N}}\left\{\mathcal{A}b_j^l\right\}_{j\in J_l}.$$

To obtain convergence for the least squares method, we have to formulate the following denseness assumption of the basis sets $\{B_l\}_{l\in\mathbb{N}}$:

$$\lim_{l\to\infty} \operatorname{dist}\left(f, \mathcal{X}_l\right) = 0 \qquad \forall f \in \mathcal{X}. \tag{4.11}$$

Lemma 4.13. *For $\{B_l\}_{l\in\mathbb{N}} \subseteq \mathcal{X}$ fulfilling the denseness condition (4.11) holds*

$$\lim_{l\to\infty} \mathrm{P}_{\mathrm{N}(\mathcal{A}^l)^\perp}\varphi = 0 \qquad \forall \varphi \in \mathrm{N}(\mathcal{A})^\perp.$$

Proof. We first state that

$$\mathcal{A}^l = \mathrm{P}_{\mathcal{Y}_l}\mathcal{A}\mathrm{P}_{\mathcal{X}_l} = \mathcal{A}\mathrm{P}_{\mathcal{X}_l}.$$

Thus, the nullspace of $\mathcal{A}^l$ is given by

$$\begin{aligned}\mathrm{N}(\mathcal{A}^l) &= \{\varphi \in \mathcal{X} : \mathrm{P}_{\mathcal{X}_l}\varphi = 0\} \cup \{\varphi \in \mathcal{X}_l : \mathcal{A}\varphi = 0\} \\ &= \mathrm{N}(\mathrm{P}_{\mathcal{X}_l}) \cup \{\varphi \in \mathrm{N}(\mathrm{P}_{\mathcal{X}_l}) : \mathcal{A}\varphi = 0\} \\ &= \mathcal{X}_l^\perp \oplus (\mathcal{X}_l \cap \mathrm{N}(\mathcal{A})).\end{aligned}$$

For arbitrary $\varphi \in \mathrm{N}(\mathcal{A})^\perp$ follows

$$\mathrm{P}_{\mathrm{N}(\mathcal{A}^l)}\varphi = \mathrm{P}_{\mathcal{X}_l^\perp}\varphi + \mathrm{P}_{\mathcal{X}_l^\perp \cap \mathrm{N}(\mathcal{A})}\varphi = \mathrm{P}_{\mathcal{X}_l^\perp}\varphi = \varphi - \mathrm{P}_{\mathcal{X}_l}\varphi.$$

With condition (4.11) follows

$$\lim_{l\to\infty} \|\mathrm{P}_{\mathrm{N}(\mathcal{A}^l)}\varphi\|_{\mathcal{X}} = \lim_{l\to\infty} \|\varphi - \mathrm{P}_{\mathcal{X}_l}\varphi\|_{\mathcal{X}} = 0.$$

□

Lemma 4.14. *Let $|I| < \infty$. It holds:*

$$\|\mathcal{A}_i^+\| < \infty \quad \forall i \in I \qquad \Rightarrow \qquad \|\mathcal{A}^+\| < \infty \qquad \Rightarrow \qquad \|\mathcal{A}^{l,+}\| \le \|\mathcal{A}^+\| \quad \forall l \in l \in \mathbb{N}.$$

Proof. (i) Let the generalized inverse operators $\mathcal{A}_i^+$ be bounded for all $i \in I$. Thus, following theorem 2.17, the operators $\mathcal{A}_i$ have closed range, i.e.,

$$\mathrm{R}(\mathcal{A}_i) = \overline{\mathrm{R}(\mathcal{A}_i)} \qquad \forall i \in I.$$

Since $(\mathcal{A}f)_i = \mathcal{A}_i f$, it is

$$\mathrm{R}(\mathcal{A}) = \bigoplus_{i\in I} \mathrm{R}(\mathcal{A}_i) = \bigoplus_{i\in I} \overline{\mathrm{R}(\mathcal{A}_i)} = \overline{\bigoplus_{i\in I} \mathrm{R}(\mathcal{A}_i)}$$

and the range of $\mathcal{A}$ is closed. Theorem 2.17 now yields the boundedness of $\mathcal{A}^+$.

(ii) For arbitrary $l \in \mathbb{N}$ holds

$$\begin{aligned}\{\varphi \in \mathrm{N}(\mathcal{A}^l)^\perp : \|\mathcal{A}^l\varphi\|_{\mathcal{Y}} = 1\} &= \{\varphi \in \mathcal{X}_l \cap \mathrm{N}(\mathcal{A})^\perp : \|\mathcal{A}^l\varphi\|_{\mathcal{Y}} = \|\mathcal{A}\varphi\|_{\mathcal{Y}} = 1\} \\ &= \{\varphi \in \mathcal{X}_l : \|\mathcal{A}\varphi\|_{\mathcal{Y}} = 1\} \cap \{\varphi \in \mathrm{N}(\mathcal{A})^\perp : \|\mathcal{A}\varphi\|_{\mathcal{Y}} = 1\} \\ &\subseteq \{\varphi \in \mathrm{N}(\mathcal{A})^\perp : \|\mathcal{A}\varphi\|_{\mathcal{Y}} = 1\}.\end{aligned}$$

Thus, lemma 2.22 yields

$$\begin{aligned}\|\mathcal{A}^{l,+}\| &= \sup_{\varphi\in\mathrm{N}(\mathcal{A}^l)^\perp,\, \|\mathcal{A}^l\varphi\|_{\mathcal{Y}}=1} \|\varphi\|_{\mathcal{Y}} \\ &\le \sup_{\varphi\in\mathrm{N}(\mathcal{A})^\perp,\, \|\mathcal{A}\varphi\|_{\mathcal{Y}}=1} \|\varphi\|_{\mathcal{Y}} \\ &\le \|\mathcal{A}^+\|.\end{aligned}$$

□

Theorem 4.15. *Let $\{B_l\}_{l\in\mathbb{N}} \subseteq \mathcal{X}$ such that condition (4.11) is fulfilled and $g, g^\varepsilon \in \mathcal{Y}$ with $\|g - g^\varepsilon\|_{\mathcal{Y}} < \varepsilon$ for $\varepsilon > 0$. If the operator $\mathcal{A} = \left(\mathcal{A}_1, \dots, \mathcal{A}_{|I|}\right)^\top$ fulfills $\|(\mathcal{A}_i)^+\| < \infty$ for all $i \in I$, then*

$$\lim_{\substack{l\to\infty \\ \varepsilon\to 0}} \|f^+ - f^+_{l,\varepsilon}\|_{\mathcal{X}} = 0.$$

Proof. To show this result we use the norm estimation of theorem 4.12. It holds,

$$\|\mathcal{A}^{l,+}\| \leq \|\mathcal{A}^+\| \quad \forall l \in l \in \mathbb{N}$$

with $\|\mathcal{A}^+\| < \infty$, cf. lemma 4.14. It follows

$$\|\mathcal{A}^{l,+} \mathrm{P}_{\mathcal{Y}_l} \mathcal{A}\| = \|\mathcal{A}^+\| \|\mathcal{A}\| \quad \text{and} \quad \|\mathcal{A}^{l,+} \mathrm{P}_{\mathcal{Y}_l}\| \leq \|\mathcal{A}^+\|.$$

Applying the norm estimation from theorem 4.12 yields

$$\begin{aligned} \|f^+ - f^+_{l,\varepsilon}\|_{\mathcal{X}} &\leq \left(1 + \|\mathcal{A}^{l,+} \mathrm{P}_{\mathcal{Y}_l} \mathcal{A}\|\right) \operatorname{dist}\left(f, \mathcal{X}_l\right) + \|\mathrm{P}_{\mathrm{N}(\mathcal{A}^l)} f^+\|_{\mathcal{X}} + \varepsilon \|\mathcal{A}^{l,+} \mathrm{P}_{\mathcal{Y}_l}\| \\ &\leq \left(1 + \|\mathcal{A}^+\| \|\mathcal{A}\|\right) \operatorname{dist}\left(f, \mathcal{X}_l\right) + \|\mathrm{P}_{\mathrm{N}(\mathcal{A}^l)} f^+\|_{\mathcal{X}} + \varepsilon \|\mathcal{A}^+\|. \end{aligned}$$

Together with lemma 4.13, stating $\lim_{l\to\infty} \mathrm{P}_{\mathrm{N}(\mathcal{A})^\perp} \varphi = 0$ for $\varphi \in \mathrm{N}(\mathcal{A})^\perp$, and the approximation property (4.11) follows

$$\lim_{l\to\infty} \|f^+ - f^+_{l,\varepsilon}\|_{\mathcal{X}} \leq \varepsilon \|\mathcal{A}^+\| \quad \overset{\varepsilon\to 0}{\longrightarrow} \quad 0.$$

□

Chapter 5

Semi-discrete iteration methods

Let the operators

$$\mathcal{A} : \mathcal{X} \to \mathcal{Y} \qquad \text{and} \qquad \mathcal{A}_i : \mathcal{X} \to \mathcal{Y}_i \quad i \in I$$

be defined as bounded linear operators $\mathcal{A} \in \mathcal{L}(\mathcal{X}, \mathcal{Y})$ and $\mathcal{A}_i \in \mathcal{L}(\mathcal{X}, \mathcal{Y}_i)$, respectively. The Hilbert space $\mathcal{Y}$ is defined as the direct sum of the real Hilbert spaces $\{\mathcal{Y}_i\}_{i \in I}$, cf. chapter 4, for $I \subset \mathbb{N}$ being a finite set of indices. We further consider the basis B to be fixed throughout the rest of this chapter. For convenience, we will drop the subscript B in the notation. Let

$$\boldsymbol{A} := \begin{pmatrix} \boldsymbol{A}_1 \\ \vdots \\ \boldsymbol{A}_{|I_P|} \end{pmatrix} : \left(\mathbb{R}^{|J|}, \langle \cdot, \cdot \rangle_k\right) \to \mathcal{Y} \tag{5.1}$$

denote the semi-discrete operators of $A_k : \left(\mathbb{R}^{|J|}, \langle \cdot, \cdot \rangle_k\right) \to Y_k$, $k \in I_P$, with respect to the basis B.

In this chapter, we propose an iteration scheme to solve the inverse problem

$$\mathcal{A} f = g \qquad g \in \mathcal{Y} \tag{5.2}$$

by computing an approximation to f in $\mathcal{X}_B$ via solving the semi-discrete problem

$$\boldsymbol{A} f = g.$$

Together with the semi-discrete operator model (5.1), the iteration schemes are called *semi-discrete iteration methods* for solving problem (5.2). In particular, the following iteration scheme is considered: Let $\boldsymbol{f}^0 \in \mathbb{R}^{|J|}$ be an arbitrary initial value. For $m \geq 0$ compute

$$\begin{aligned} \boldsymbol{f}^{m,1} &:= \boldsymbol{f}^m \\ \boldsymbol{f}^{m,k+1} &= \boldsymbol{f}^{m,k} + \Psi_k\left(g_k - \boldsymbol{A}_k \boldsymbol{f}^{m,k}\right) \qquad \text{for } k \in I_P \\ \boldsymbol{f}^{m+1} &:= \boldsymbol{f}^{m,|I_P|+1}. \end{aligned} \tag{5.3}$$

The backward operators

$$\Psi_k : Y_k \to \left(\mathbb{R}^{|J|}, \langle \cdot, \cdot \rangle_k\right) \qquad k \in I_P$$

map from the data space Y_k to the coefficient space $\mathbb{R}^{|J|}$ and characterize the specific iteration methods. In particular we consider:

(i) The *Landweber-Kaczmarz* iteration

$$\Psi_k = \lambda_k \boldsymbol{A}_k^* \qquad \lambda_k > 0$$

(ii) The *Kaczmarz* iteration

$$\Psi_k = \lambda_k \boldsymbol{A}_k^+ \qquad \lambda_k > 0$$

The parameters $\{\lambda_k\}_{k\in I_p}$ are called relaxation parameter.

Before having a closer look at the convergence properties of the general iteration scheme (5.3) and the specific choices of Ψ_k we introduce some notation. Let $\boldsymbol{G}_k : \mathbb{R}^{|J|} \to \mathbb{R}^{|J|}$ be finite dimensional linear operators defined as

$$\boldsymbol{G}_k := \mathrm{id} - \Psi_k \boldsymbol{A}_k \qquad k \in I_P.$$

The operators $\boldsymbol{G}_k$ summarize all mappings applied to the coefficient vector $\boldsymbol{f}^{m,k}$ such that we can write the iteration steps as

$$\boldsymbol{f}^{m,k+1} = \boldsymbol{f}^{m,k} + \Psi_k\left(g_k - \boldsymbol{A}_k \boldsymbol{f}^{m,k}\right) = \boldsymbol{G}_k \boldsymbol{f}^{m,k} + \Psi_k g_k.$$

Lemma 5.1. *Let $p, q \in I_P$ with $p \le q$. It holds*

$$\boldsymbol{G}_q \circ \boldsymbol{G}_{q-1} \circ \cdots \circ \boldsymbol{G}_p = \mathrm{id} - \left(\Psi_q \boldsymbol{A}_q + \sum_{k=p}^{q-1} \left(\boldsymbol{G}_q \circ \cdots \circ \boldsymbol{G}_{k+1}\right)\Psi_k \boldsymbol{A}_k\right). \tag{5.4}$$

Proof. Let $p \in I_P$ be fixed. We show the result by induction over q. For $q = p$ the statement is trivial since the left-hand side of (5.4) reduces to $\boldsymbol{G}_q$ and the sum of the right-hand side is empty,

$$\boldsymbol{G}_q = \mathrm{id} - \left(\Psi_q \boldsymbol{A}_q + \underbrace{\sum_{k=q}^{q-1} \left(\boldsymbol{G}_q \circ \cdots \circ \boldsymbol{G}_{k+1}\right)\Psi_k \boldsymbol{A}_k}_{=0}\right) = \mathrm{id} - \Psi_q \boldsymbol{A}_q.$$

Now let $q > p$ and equation (5.4) be true for $(q-1)$, i.e.,

$$\boldsymbol{G}_{q-1} \circ \cdots \circ \boldsymbol{G}_p = \mathrm{id} - \left(\Psi_{q-1} \boldsymbol{A}_{q-1} + \sum_{k=p}^{q-2} \left(\boldsymbol{G}_{q-1} \circ \cdots \circ \boldsymbol{G}_{k+1}\right)\Psi_k \boldsymbol{A}_k\right). \tag{5.5}$$

It follows

$$\begin{aligned}
\boldsymbol{G}_q \circ \boldsymbol{G}_{q-1} \circ \cdots \circ \boldsymbol{G}_p &\overset{(5.5)}{=} \boldsymbol{G}_q \left(\mathrm{id} - \left(\Psi_{q-1} \boldsymbol{A}_{q-1} + \sum_{k=p}^{q-2} \left(\boldsymbol{G}_{q-1} \circ \cdots \circ \boldsymbol{G}_{k+1}\right)\Psi_k \boldsymbol{A}_k\right)\right) \\
&= \boldsymbol{G}_q - \left(\boldsymbol{G}_q \Psi_{q-1} \boldsymbol{A}_{q-1} + \sum_{k=p}^{q-2} \left(\boldsymbol{G}_q \circ \cdots \circ \boldsymbol{G}_{k+1}\right)\Psi_k \boldsymbol{A}_k\right) \\
&= \left(\mathrm{id} - \Psi_q \boldsymbol{A}_q\right) - \sum_{k=p}^{q-1} \left(\boldsymbol{G}_q \circ \cdots \circ \boldsymbol{G}_{k+1}\right)\Psi_k \boldsymbol{A}_k \\
&= \mathrm{id} - \left(\Psi_q \boldsymbol{A}_q + \sum_{k=p}^{q-1} \left(\boldsymbol{G}_q \circ \cdots \circ \boldsymbol{G}_{k+1}\right)\Psi_k \boldsymbol{A}_k\right)
\end{aligned}$$

where we made use of the linearity of $\boldsymbol{G}_k$. Thus, the representation of $\boldsymbol{G}_q \circ \boldsymbol{G}_{q-1} \circ \cdots \circ \boldsymbol{G}_p$ is shown for $q, p \in I_P$. □

To derive a closed form of the iteration scheme (5.3), we introduce the operators

$$\boldsymbol{Q}_k \coloneqq \boldsymbol{G}_{|I_P|} \circ \cdots \circ \boldsymbol{G}_{k+1} \quad \text{for } k = 0, \ldots, |I_P|$$

with $\boldsymbol{Q}_{|I_P|} \coloneqq \mathrm{id}$ and $\boldsymbol{G} \coloneqq \boldsymbol{G}_{|I_P|} \circ \cdots \circ \boldsymbol{G}_1$.

Lemma 5.2. *For $k \in I_P$ holds*

$$\boldsymbol{Q}_k = \mathrm{id} - \sum_{l=k+1}^{|I_P|} \boldsymbol{Q}_l \Psi_l \boldsymbol{A}_l \qquad \textit{and} \qquad \boldsymbol{G} = \mathrm{id} - \sum_{k \in I_P} \boldsymbol{Q}_k \Psi_k \boldsymbol{A}_k.$$

Proof. Putting $q = |I_P|$ and $p = k+1$ in lemma 5.1 yields

$$\begin{aligned}
\boldsymbol{Q}_k &= \boldsymbol{G}_{|I_P|} \circ \cdots \circ \boldsymbol{G}_{k+1} \\
&= \mathrm{id} - \left(\Psi_{|I_P|} \boldsymbol{A}_{|I_P|} + \sum_{l=k+1}^{|I_P|-1} \left(\boldsymbol{G}_{|I_P|} \circ \cdots \circ \boldsymbol{G}_{l+1} \right) \Psi_l \boldsymbol{A}_l \right) \\
&= \mathrm{id} - \left(\boldsymbol{Q}_{|I_P|} \Psi_{|I_P|} \boldsymbol{A}_{|I_P|} + \sum_{l=k+1}^{|I_P|-1} \boldsymbol{Q}_l \Psi_l \boldsymbol{A}_l \right) \\
&= \mathrm{id} - \sum_{l=k+1}^{|I_P|} \boldsymbol{Q}_l \Psi_l \boldsymbol{A}_l.
\end{aligned}$$

For $p = 0$ follows

$$\boldsymbol{G} = \boldsymbol{Q}_0 = \mathrm{id} - \sum_{k \in I_P} \boldsymbol{Q}_k \Psi_k \boldsymbol{A}_k.$$

□

We obtain the following closed form representations of the iteration scheme (5.3).

Proposition 5.3. *The following schemes are equivalent formulations of the iteration scheme* (5.3).

(i) (Closed form)

$$\boldsymbol{f}^{m+1} = \boldsymbol{f}^m + \sum_{k \in I_P} \boldsymbol{Q}_k \Psi_k \left(g_k - \boldsymbol{A}_k \boldsymbol{f}^m \right) \qquad m = 0, 1, \ldots$$

(ii) (Fixed-point form)

$$\boldsymbol{f}^{m+1} = \Phi \boldsymbol{f}^m \qquad m = 0, 1, \ldots$$

with the affine linear fixed-point operator

$$\Phi : \mathbb{R}^{|J|} \to \mathbb{R}^{|J|}, \qquad \Phi \boldsymbol{f} \coloneqq \boldsymbol{G} \boldsymbol{f} + \sum_{k \in I_P} \boldsymbol{Q}_k \Psi_k g_k.$$

(iii) (Direct form) It holds

$$f^m = G^m f^0 + \sum_{l=0}^{m-1} G^l \left(\sum_{k \in I_p} Q_k \Psi_k g_k \right) \qquad m = 1, 2, \ldots$$

with $G^0 := \mathrm{id}$.

Proof. (i) With f^{m+1} being defined as $f^{m+1} = f^{m,|I_P|+1}$, see (5.3), we have to verify

$$f^{m,|I_P|+1} = f^{m,0} + \sum_{k \in I_p} Q_k \Psi_k \left(g_k - A_k f^{m,0} \right).$$

We show by induction over the number of indices that

$$f^{m,l+1} = f^{m,0} + \sum_{0 \le k \le l} \left(G_l \circ \cdots \circ G_{k+1} \right) \Psi_k \left(g_k - A_k f^{m,0} \right)$$

holds for $l \ge 0$ where $\left(G_l \circ \cdots \circ G_p \right) := \mathrm{id}$ for $p > l$. For $l = 0$ the statement is trivially fulfilled. Now let the statement be true for some $l > 0$. We obtain

$$\begin{aligned}
f^{m,l+1} &= f^{m,l} + \Psi_l \left(g_l - A_l f^{m,l} \right) \\
&= G_l f^{m,l} + \Psi_l g_l \\
&= G_l \left(f^{m,0} + \sum_{0 \le k \le l-1} \left(G_{l-1} \circ \cdots \circ G_{k+1} \right) \Psi_k \left(g_k - A_k f^{m,0} \right) \right) + \Psi_l g_l \\
&= G_l f^{m,0} + \sum_{0 \le k \le l-1} \left(G_l \circ G_{l-1} \circ \cdots \circ G_{k+1} \right) \Psi_k \left(g_k - A_k f^{m,0} \right) + \Psi_l g_l \\
&= f^{m,0} + \sum_{0 \le k \le l-1} \left(G_l \circ \cdots \circ G_{k+1} \right) \Psi_k \left(g_k - A_k f^{m,0} \right) + \Psi_l \left(g_l - A_k f^{m,l} \right) \\
&= f^{m,0} + \sum_{0 \le k \le l} \left(G_l \circ \cdots \circ G_{k+1} \right) \Psi_k \left(g_k - A_k f^{m,0} \right).
\end{aligned}$$

The closed form follows by putting $l = |I_P|$.

(ii) Together with the closed form (i) and lemma 5.2 follows

$$\begin{aligned}
f^{m+1} &= f^m + \sum_{k \in I_p} Q_k \Psi_k \left(g_k - A_k f^m \right) \\
&= \left(\mathrm{id} - \sum_{k \in I_p} Q_k \Psi_k A_k \right) f^m + \sum_{k \in I_p} Q_k \Psi_k g_k \\
&= G f^m + \sum_{k \in I_p} Q_k \Psi_k g_k \\
&= \Phi f^m.
\end{aligned}$$

(iii) The direct form is shown by induction. For $m = 1$ the statement is trivially fulfilled as a consequence of the fixed-point form (ii). Let the statement be true for some $m > 0$. From the fixed-point formulation follows

$$f^{m+1} = G f^m + \sum_{k \in I_p} Q_k \Psi_k g_k$$

$$
\begin{aligned}
&= \boldsymbol{G}\left(\boldsymbol{G}^m \boldsymbol{f}^0 + \left(\sum_{l=0}^{m-1} \boldsymbol{G}^l \left(\sum_{k\in I_p} \boldsymbol{Q}_k \Psi_k g_k\right)\right)\right) + \sum_{k\in I_p} \boldsymbol{Q}_k \Psi_k g_k \\
&= \boldsymbol{G}^{m+1} \boldsymbol{f}^0 + \sum_{l=0}^{m-1} \boldsymbol{G}^{l+1} \left(\sum_{k\in I_p} \boldsymbol{Q}_k \Psi_k g_k\right) + \sum_{k\in I_p} \boldsymbol{Q}_k \Psi_k g_k \\
&= \boldsymbol{G}^{m+1} \boldsymbol{f}^0 + \sum_{l=0}^{m} \boldsymbol{G}^{l} \left(\sum_{k\in I_p} \boldsymbol{Q}_k \Psi_k g_k\right).
\end{aligned}
$$

□

5.1 Convergence properties

Let $|||\cdot|||$ denote an arbitrary vector norm on $\mathbb{R}^{|J|}$ as well as its induced operator norm, respectively. With the fixed-point formulation from proposition 5.3, we aim at showing convergence of the iteration scheme (5.3) by applying Banach's fixed-point theorem, cf. theorem 2.8: Whenever the fixed-point operator Φ is a contraction, i.e., there exists a constant $L \in [0, 1)$ such that

$$|||\Phi \boldsymbol{f}_1 - \Phi \boldsymbol{f}_2||| \leq L\, |||\boldsymbol{f}_1 - \boldsymbol{f}_2||| \qquad \forall \boldsymbol{f}_1, \boldsymbol{f}_2 \in \mathbb{R}^{|J|}$$

the iteration scheme converges to its uniquely determined fixed-point. The contraction condition on Φ can be directly passed to the operator $\boldsymbol{G}$ since

$$|||\Phi \boldsymbol{f}_1 - \Phi \boldsymbol{f}_2||| = |||\boldsymbol{G}\boldsymbol{f}_1 + \eta - (\boldsymbol{G}\boldsymbol{f}_2 + \eta)||| \leq |||\boldsymbol{G}|||\, |||\boldsymbol{f}_1 - \boldsymbol{f}_2|||$$

holds for all $\boldsymbol{f}_1, \boldsymbol{f}_2 \in \mathbb{R}^{|J|}$. It obviously follows that Φ is a contraction if $\boldsymbol{G}$ is bounded with $|||\boldsymbol{G}||| < 1$. We will therefore concentrate our convergence analysis on the operator norm of $\boldsymbol{G}$.

Proposition 5.4. *If $|||\boldsymbol{G}||| < 1$ then $\boldsymbol{A}$ is injective.*

Proof. We show the statement by contradiction: Let $|||\boldsymbol{G}||| < 1$ and assume that the operator $\boldsymbol{A}$ is non-injective. Thus, there exists a non-trivial element

$$0 \neq \tilde{\varphi} \in \mathrm{N}(\boldsymbol{A}) = \bigcap_{k\in I_p} \mathrm{N}\left(\boldsymbol{A}_k\right)$$

with $|||\tilde{\varphi}||| = 1$. With lemma 5.2 follows

$$\boldsymbol{G}\tilde{\varphi} = \left(\mathrm{id} - \sum_{k\in I_p} \boldsymbol{Q}_k \Psi_k \boldsymbol{A}_k\right)\tilde{\varphi} = \tilde{\varphi}$$

and therefore

$$|||\boldsymbol{G}||| = \max_{|||\varphi|||=1} |||\boldsymbol{G}\varphi||| \geq |||\boldsymbol{G}\tilde{\varphi}||| = |||\tilde{\varphi}||| = 1$$

This clearly contradicts the premiss $|||\boldsymbol{G}||| < 1$. Consequently, the operator $\boldsymbol{A}$ has to be injective. □

As a direct consequence from Banach's fixed-point theorem, the injectivity of $\boldsymbol{A}$ is necessary for the existence of a *unique* fixed-point of Φ and thus also for the convergence of the iteration scheme.

The situation becomes clearer when we assume for the moment that $\boldsymbol{A}$ is non-injective and that a fixed-point $\boldsymbol{f}^* \in \mathbb{R}^{|J|}$ of Φ exists. Then, $\boldsymbol{f}^* + \varphi_0$ with $\varphi \in \mathrm{N}(\mathrm{id} - \boldsymbol{G})$ (i.e. φ being a fixed-point of $\boldsymbol{G}$) is also a fixed-point of Φ since

$$\begin{aligned}\Phi(\boldsymbol{f}^* + \varphi) &= \boldsymbol{G}(\boldsymbol{f}^* + \varphi) + \sum_{k \in I_P} \boldsymbol{Q}_k \Psi_k g_k \\ &= \boldsymbol{G}\boldsymbol{f}^* + \sum_{k \in I_P} \boldsymbol{Q}_k \Psi_k g_k + \varphi \\ &= \Phi \boldsymbol{f}^* + \varphi \\ &= \boldsymbol{f}^* + \varphi.\end{aligned}$$

Further, the definition of $\boldsymbol{G}$ induces immediately that all elements of the nullspace of $\boldsymbol{A}$ are fixed-points of $\boldsymbol{G}$, i.e., $\mathrm{N}(\boldsymbol{A}) \subseteq \mathrm{N}(\mathrm{id} - \boldsymbol{G})$. More specifically, it holds

$$\mathrm{N}(\mathrm{id} - \boldsymbol{G}) = \mathrm{N}(\boldsymbol{A}) \oplus \mathrm{N}\left((\mathrm{id} - \boldsymbol{G})\mathrm{P}_{\mathrm{N}(\boldsymbol{A})^\perp}\right)$$

as can be seen with lemma 5.2 from

$$\mathrm{id} - \boldsymbol{G} = (\mathrm{id} - \boldsymbol{G})\mathrm{P}_{\mathrm{N}(\boldsymbol{A})} + (\mathrm{id} - \boldsymbol{G})\mathrm{P}_{\mathrm{N}(\boldsymbol{A})^\perp} = (\mathrm{id} - \boldsymbol{G})\mathrm{P}_{\mathrm{N}(\boldsymbol{A})^\perp}.$$

To establish convergence of the iteration scheme, we need to require additional assumptions on the restricted operator $\|\boldsymbol{G}\mathrm{P}_{\mathrm{N}(\boldsymbol{A})^\perp}\|$ and the specific backward operators Ψ_k.

Lemma 5.5. *Let* $\mathrm{R}(\Psi_k) \subseteq \mathrm{N}(\boldsymbol{A})^\perp$ *for all* $k \in I_P$. *Then,*

$$\mathrm{R}\left(\sum_{k \in I_P} \boldsymbol{Q}_k \Psi_k\right) \subseteq \mathrm{N}(\boldsymbol{A})^\perp.$$

Proof. Let $\phi \in \mathcal{Y}$. We show the statement recursively. For $k = |I_P|$ holds

$$\boldsymbol{Q}_{|I_P|}\Psi_{|I_P|}\phi_{|I_P|} = \Psi_{|I_P|}\phi_{|I_P|} \in \mathrm{N}(\boldsymbol{A})^\perp.$$

Let the statement be true for some k with $2 \leq k \leq |I_P|$. With lemma 5.2 we have

$$\begin{aligned}\boldsymbol{Q}_{k-1}\Psi_{k-1}\phi_{k-1} &= \left(\mathrm{id} - \sum_{l=k}^{|I_P|} \boldsymbol{Q}_l \Psi_l \boldsymbol{A}_l\right)\Psi_{k-1}\phi_{k-1} \\ &= \Psi_{k-1}\phi_{k-1} - \sum_{l=k}^{|I_P|} \boldsymbol{Q}_l \Psi_l \boldsymbol{A}_l \Psi_{k-1}\phi_{k-1} \qquad \in \mathrm{N}(\boldsymbol{A})^\perp\end{aligned}$$

since both terms are elements of $\mathrm{N}(\boldsymbol{A})^\perp$. Consequently, it is $\boldsymbol{Q}_k\Psi_k\phi_k \in \mathrm{N}(\boldsymbol{A})^\perp$ for all $k \in I_P$. For $\phi \in \mathcal{Y}$ follows

$$\sum_{k \in I_P} \boldsymbol{Q}_k \Psi_k \phi_k \in \mathrm{N}(\boldsymbol{A})^\perp.$$

□

The previous lemma gives a sufficient condition for $\boldsymbol{G}\mathrm{P}_{\mathrm{N}(\boldsymbol{A})^\perp}$ being a mapping from $\mathbb{R}^{|J|}$ to $\mathrm{N}(\boldsymbol{A})^\perp$, i.e.,

$$\boldsymbol{G}\mathrm{P}_{\mathrm{N}(\boldsymbol{A})^\perp} : \mathbb{R}^{|J|} \to \mathrm{R}(\boldsymbol{G}\mathrm{P}_{\mathrm{N}(\boldsymbol{A})^\perp}) \subseteq \mathrm{N}(\boldsymbol{A})^\perp. \tag{5.6}$$

We are now able to show the convergence of the iteration scheme for $m \to \infty$.

Theorem 5.6. *Let the backward operators $\{\Psi_k\}_{k\in I_p}$ be given such that $\mathrm{R}(\Psi_k) \subseteq \mathrm{N}(\boldsymbol{A})^\perp$ for all $k \in I_p$ and that*

$$\|\boldsymbol{G}\mathrm{P}_{\mathrm{N}(\boldsymbol{A})^\perp}\| < 1. \tag{5.7}$$

For $m \to \infty$, the iteration scheme (5.3) converges linearly with

$$\tilde{\boldsymbol{f}} = \mathrm{P}_{\mathrm{N}(\boldsymbol{A})}\boldsymbol{f}^0 + \left(\sum_{k\in I_p} \boldsymbol{Q}_k\Psi_k\boldsymbol{A}_k\right)^{-1}\left(\sum_{k\in I_p} \boldsymbol{Q}_k\Psi_k g_k\right).$$

The rate of convergence is bounded by $L := \|\boldsymbol{G}\mathrm{P}_{\mathrm{N}(\boldsymbol{A})^\perp}\|$ and the following error estimates hold:

(i) (Prior estimate)

$$\|\boldsymbol{f}^m - \tilde{\boldsymbol{f}}\| \le \frac{L^m}{1-L}\|\boldsymbol{f}^0 - \boldsymbol{f}^1\| + \frac{1}{1-L}\|\mathrm{P}_{\mathrm{N}(\boldsymbol{A})^\perp}\boldsymbol{f}^0\| \tag{5.8}$$

(ii) (Posterior estimate)

$$\|\boldsymbol{f}^m - \tilde{\boldsymbol{f}}\| \le \frac{L}{1-L}\|\boldsymbol{f}^{m-1} - \boldsymbol{f}^m\| + \frac{1}{1-L}\|\mathrm{P}_{\mathrm{N}(\boldsymbol{A})^\perp}\boldsymbol{f}^0\| \tag{5.9}$$

Proof. First, we verify that $\boldsymbol{G}\mathrm{P}_{\mathrm{N}(\boldsymbol{A})^\perp}$ is a contraction on $\mathrm{P}_{\mathrm{N}(\boldsymbol{A})^\perp}$. With lemma 5.5 follows

$$\boldsymbol{G}\mathrm{P}_{\mathrm{N}(\boldsymbol{A})^\perp}\varphi = \mathrm{P}_{\mathrm{N}(\boldsymbol{A})^\perp}\varphi - \sum_{k\in I_p}\boldsymbol{Q}_k\Psi_k\boldsymbol{A}_k\varphi \in \mathrm{N}(\boldsymbol{A})^\perp \qquad \forall\varphi \in \mathbb{R}^{|J|}$$

cf. equation (5.6). Together with assumption (5.7), the restricted operator $G\mathrm{P}_{\mathrm{N}(\boldsymbol{A})^\perp}$ is a contraction on $\mathrm{P}_{\mathrm{N}(\boldsymbol{A})^\perp}$. From the direct form of proposition 5.3(iii) follows

$$\begin{aligned}
\boldsymbol{f}^m &= \boldsymbol{G}^m\boldsymbol{f}^0 + \sum_{l=0}^{m-1}\boldsymbol{G}^l\left(\sum_{k\in I_p}\boldsymbol{Q}_k\Psi_k g_k\right)\\
&= \boldsymbol{G}^m\mathrm{P}_{\mathrm{N}(\boldsymbol{A})}\boldsymbol{f}^0 + \boldsymbol{G}^m\mathrm{P}_{\mathrm{N}(\boldsymbol{A})^\perp}\boldsymbol{f}^0 + \sum_{l=0}^{m-1}\boldsymbol{G}^l\left(\sum_{k\in I_p}\boldsymbol{Q}_k\Psi_k g_k\right)\\
&= \mathrm{P}_{\mathrm{N}(\boldsymbol{A})}\boldsymbol{f}^0 + \boldsymbol{G}^m\mathrm{P}_{\mathrm{N}(\boldsymbol{A})^\perp}\boldsymbol{f}^0 + \sum_{l=0}^{m-1}\boldsymbol{G}^l\left(\sum_{k\in I_p}\boldsymbol{Q}_k\Psi_k g_k\right)\\
&= \mathrm{P}_{\mathrm{N}(\boldsymbol{A})}\boldsymbol{f}^0 + \left(\boldsymbol{G}\mathrm{P}_{\mathrm{N}(\boldsymbol{A})^\perp}\right)^m\boldsymbol{f}^0 + \sum_{l=0}^{m-1}\left(\boldsymbol{G}\mathrm{P}_{\mathrm{N}(\boldsymbol{A})^\perp}\right)^l\left(\sum_{k\in I_p}\boldsymbol{Q}_k\Psi_k g_k\right).
\end{aligned} \tag{5.10}$$

Banach's fixed-point Theorem 2.8 yields the convergence of $\left(\boldsymbol{G}\mathrm{P}_{\mathrm{N}(\boldsymbol{A})^\perp}\right)^m\boldsymbol{f}^0$ for $m \to \infty$ to the unique fixed-point of $\boldsymbol{G}\mathrm{P}_{\mathrm{N}(\boldsymbol{A})^\perp}$. This fixed-point is given by $\boldsymbol{f}^* = 0$, since from the linearity of $\boldsymbol{G}$ follows directly

$$\boldsymbol{G}\mathrm{P}_{\mathrm{N}(\boldsymbol{A})^\perp}\boldsymbol{f}^* = 0.$$

Thus,

$$\lim_{m\to\infty} \left(\boldsymbol{G}\mathrm{P}_{\mathrm{N}(\boldsymbol{A})^\perp}\right)^m \boldsymbol{f}^0 = 0.$$

With C. Neumann's theorem, cf. theorem 2.9, follows for the second term on the right-hand side

$$\lim_{m\to\infty} \sum_{l=0}^{m} \left(\boldsymbol{G}\mathrm{P}_{\mathrm{N}(\boldsymbol{A})^\perp}\right)^l = \left(\mathrm{id}|_{\mathrm{N}(\boldsymbol{A})^\perp} - \boldsymbol{G}\mathrm{P}_{\mathrm{N}(\boldsymbol{A})^\perp}\right)^{-1}.$$

This settles also the the existence and boundedness of the inverse operator. Plugging both limits into (5.10) yields together with the representation of $\boldsymbol{G}$ from lemma 5.2 the convergence result

$$\begin{aligned}
\lim_{m\to\infty} \boldsymbol{f}^m &= \mathrm{P}_{\mathrm{N}(\boldsymbol{A})}\boldsymbol{f}^0 + \left(\mathrm{id}|_{\mathrm{N}(\boldsymbol{A})^\perp} - \boldsymbol{G}\mathrm{P}_{\mathrm{N}(\boldsymbol{A})^\perp}\right)^{-1}\left(\sum_{k\in I_p} \boldsymbol{Q}_k\Psi_k g_k\right) \\
&= \mathrm{P}_{\mathrm{N}(\boldsymbol{A})}\boldsymbol{f}^0 + \left(\mathrm{id}|_{\mathrm{N}(\boldsymbol{A})^\perp} - \left(\mathrm{id}|_{\mathrm{N}(\boldsymbol{A})^\perp} - \sum_{k\in I_p} \boldsymbol{Q}_k\Psi_k\boldsymbol{A}_k\right)\right)^{-1}\left(\sum_{k\in I_p} \boldsymbol{Q}_k\Psi_k g_k\right) \\
&= \mathrm{P}_{\mathrm{N}(\boldsymbol{A})}\boldsymbol{f}^0 + \left(\sum_{k\in I_p} \boldsymbol{Q}_k\Psi_k\boldsymbol{A}_k\right)^{-1}\left(\sum_{k\in I_p} \boldsymbol{Q}_k\Psi_k g_k\right).
\end{aligned}$$

Note, that $\left(\sum_{k\in I_p} \boldsymbol{Q}_k\Psi_k\boldsymbol{A}_k\right)^{-1}\left(\sum_{k\in I_p} \boldsymbol{Q}_k\Psi_k g_k\right) \in \mathrm{N}(\boldsymbol{A})^\perp$ holds, cf. 5.5 To show that the convergence rate is linear, we note that

$$\boldsymbol{f}^m - \tilde{\boldsymbol{f}} \in \mathrm{N}(\boldsymbol{A})^\perp$$

holds for all $m > 0$ as can be seen by

$$\begin{aligned}
\boldsymbol{f}^m - \tilde{\boldsymbol{f}} = \mathrm{P}_{\mathrm{N}(\boldsymbol{A})}\boldsymbol{f}^0 + \left(\boldsymbol{G}\mathrm{P}_{\mathrm{N}(\boldsymbol{A})^\perp}\right)^m \boldsymbol{f}^0 + \sum_{l=0}^{m-1} \left(\boldsymbol{G}\mathrm{P}_{\mathrm{N}(\boldsymbol{A})^\perp}\right)^l \left(\sum_{k\in I_p} \boldsymbol{Q}_k\Psi_k g_k\right) \\
- \left(\mathrm{P}_{\mathrm{N}(\boldsymbol{A})}\boldsymbol{f}^0 + \left(\sum_{k\in I_p} \boldsymbol{Q}_k\Psi_k\boldsymbol{A}_k\right)^{-1}\left(\sum_{k\in I_p} \boldsymbol{Q}_k\Psi_k g_k\right)\right) \\
= \left(\boldsymbol{G}\mathrm{P}_{\mathrm{N}(\boldsymbol{A})^\perp}\right)^m \boldsymbol{f}^0 + \sum_{l=0}^{m-1} \left(\boldsymbol{G}\mathrm{P}_{\mathrm{N}(\boldsymbol{A})^\perp}\right)^l \left(\sum_{k\in I_p} \boldsymbol{Q}_k\Psi_k g_k\right) - \left(\sum_{k\in I_p} \boldsymbol{Q}_k\Psi_k\boldsymbol{A}_k\right)^{-1}\left(\sum_{k\in I_p} \boldsymbol{Q}_k\Psi_k g_k\right).
\end{aligned}$$

Thus,

$$\begin{aligned}
\|\boldsymbol{f}^{m+1} - \tilde{\boldsymbol{f}}\| &= \|\Phi\boldsymbol{f}^m - \Phi\tilde{\boldsymbol{f}}\| \\
&= \|\boldsymbol{G}\left(\boldsymbol{f}^m - \tilde{\boldsymbol{f}}\right)\| \\
&= \|\boldsymbol{G}\mathrm{P}_{\mathrm{N}(\boldsymbol{A})^\perp}\left(\boldsymbol{f}^m - \tilde{\boldsymbol{f}}\right)\| \\
&\leq \|\boldsymbol{G}\mathrm{P}_{\mathrm{N}(\boldsymbol{A})^\perp}\|\,\|\boldsymbol{f}^m - \tilde{\boldsymbol{f}}\|
\end{aligned}$$

and it follows

$$\frac{\|\boldsymbol{f}^{m+1} - \tilde{\boldsymbol{f}}\|}{\|\boldsymbol{f}^m - \tilde{\boldsymbol{f}}\|} \leq \|\boldsymbol{G}\mathrm{P}_{\mathrm{N}(\boldsymbol{A})^\perp}\| < 1.$$

Accordingly, the convergence rate is linear and is bounded by $\|\boldsymbol{G}\mathrm{P}_{\mathrm{N}(\boldsymbol{A})^\perp}\|$. The error estimates follow with the representation

$$\boldsymbol{f}^m = \Phi^m\boldsymbol{f}^0 = \mathrm{P}_{\mathrm{N}(\boldsymbol{A})}\boldsymbol{f}^0 + \Phi^m\mathrm{P}_{\mathrm{N}(\boldsymbol{A})^\perp}\boldsymbol{f}^0$$

directly from Banach's fixed-point theorem. □

Corollary 5.7. *Let $\boldsymbol{A}$ be injective and let $\|\boldsymbol{G}\| < 1$. The iteration scheme (5.3) converges linearly for $m \longrightarrow \infty$ and the limit is given by*

$$\tilde{\boldsymbol{f}} = \left(\sum_{k \in I_p} \boldsymbol{Q}_k \Psi_k \boldsymbol{A}_k \right)^{-1} \left(\sum_{k \in I_p} \boldsymbol{Q}_k \Psi_k g_k \right).$$

Further, the error estimates of theorem 5.6 hold.

Proof. For $\boldsymbol{A}$ being injective, the nullspace of $\boldsymbol{A}$ is trivial, i.e., $\mathrm{N}(\boldsymbol{A}) = \{0\}$ it obviously holds $\boldsymbol{G}\mathrm{P}_{\mathrm{N}(\boldsymbol{A})^\perp} = \boldsymbol{G}$. The result follows immediately from theorem 5.6 since $\mathrm{R}\big(\Psi_k\big) \subset \mathrm{N}(\boldsymbol{A})^\perp = \mathbb{R}^{|J|}$ is naturally fulfilled. □

Now that the convergence of the iteration scheme is settled, we have a brief look at its limit $\tilde{\boldsymbol{f}}$ and give a result on its interpretation.

Proposition 5.8. *Let the requirements of theorem 5.6 be fulfilled and let $\tilde{\boldsymbol{f}}$ denote the limit of the iteration scheme (5.3) given as*

$$\tilde{\boldsymbol{f}} = \mathrm{P}_{\mathrm{N}(\boldsymbol{A})} \boldsymbol{f}^0 + \left(\sum_{k \in I_p} \boldsymbol{Q}_k \Psi_k \boldsymbol{A}_k \right)^{-1} \left(\sum_{k \in I_p} \boldsymbol{Q}_k \Psi_k g_k \right).$$

(i) If $\boldsymbol{A}\boldsymbol{f} = g$ is consistent, it holds

$$\tilde{\boldsymbol{f}} = \mathrm{P}_{\mathrm{N}(\boldsymbol{A})} \boldsymbol{f}^0 + \boldsymbol{f}^+.$$

(ii) If $\boldsymbol{A}\boldsymbol{f} = g$ is not consistent, the limit $\tilde{\boldsymbol{f}}$ is a solution of

$$\sum_{k \in I_p} \boldsymbol{Q}_k \Psi_k \big(g_k - \boldsymbol{A}_k \tilde{\boldsymbol{f}} \big) = 0$$

with $\mathrm{P}_{\mathrm{N}(\boldsymbol{A})^\perp} \tilde{\boldsymbol{f}}$ being uniquely determined.

Proof. First, we assume that $\boldsymbol{A}\boldsymbol{f} = g$ is consistent, i.e., there exists a solution for any given right-hand side $g \in \mathcal{Y}$. If there is more than one solution, all solutions are of the form

$$\boldsymbol{f} = \boldsymbol{f}^+ + \varphi_0$$

with $\boldsymbol{f}^+ \in \mathrm{N}(\boldsymbol{A})^\perp$ denoting the minimum-norm solution of $\boldsymbol{A}\boldsymbol{f} = g$ and $\varphi_0 \in \mathrm{N}(\boldsymbol{A})$ is arbitrary. If $\boldsymbol{A}$ is injective, the nullspace element φ_0 is equally zero and the solution is unique. Since $\boldsymbol{A}\boldsymbol{f} = g$ is consistent, the generalized solution $\boldsymbol{f}^+$ is also a solution of $\boldsymbol{A}_k \boldsymbol{f}^+ = g_k$ for $k \in I_P$. It follows

$$\begin{aligned}
\tilde{\boldsymbol{f}} &= \mathrm{P}_{\mathrm{N}(\boldsymbol{A})} \boldsymbol{f}^0 + \left(\sum_{k \in I_p} \lambda_k \boldsymbol{Q}_k \Psi_k \boldsymbol{A}_k \right)^{-1} \left(\sum_{k \in I_p} \lambda_k \boldsymbol{Q}_k \Psi_k \boldsymbol{A}_k \big(\boldsymbol{f}^+ + \varphi_0 \big) \right) \\
&= \mathrm{P}_{\mathrm{N}(\boldsymbol{A})} \boldsymbol{f}^0 + \left(\sum_{k \in I_p} \lambda_k \boldsymbol{Q}_k \Psi_k \boldsymbol{A}_k \right)^{-1} \left(\sum_{k \in I_p} \lambda_k \boldsymbol{Q}_k \Psi_k \boldsymbol{A}_k \right) \boldsymbol{f}^+ \\
&= \mathrm{P}_{\mathrm{N}(\boldsymbol{A})} \boldsymbol{f}^0 + \boldsymbol{f}^+.
\end{aligned}$$

Hence, the limit $\tilde{\boldsymbol{f}}$ of iteration scheme (5.3) is equal to the solution of $\boldsymbol{A}\boldsymbol{f} = g$ with minimal distance to the initial value $\boldsymbol{f}^0$, cf. equation(2.5).

If the system is inconsistent, there exists no exact solution for a given right-hand side $g \in \mathcal{Y}$. With lemma 5.2 and the fixed-point property of $\tilde{f}$ we obtain

$$\begin{aligned}\tilde{f} = \Phi\tilde{f} &= \boldsymbol{G}\tilde{f} + \sum_{k\in I_p} \lambda_k \boldsymbol{Q}_k \Psi_k g_k \\ &= \left(\mathrm{id} - \sum_{k\in I_p} \boldsymbol{Q}_k \Psi_k \boldsymbol{A}_k\right)\tilde{f} + \sum_{k\in I_p} \lambda_k \boldsymbol{Q}_k \Psi_k g_k \\ &= \tilde{f} - \sum_{k\in I_p} \boldsymbol{Q}_k \Psi_k \boldsymbol{A}_k \tilde{f} + \sum_{k\in I_p} \lambda_k \boldsymbol{Q}_k \Psi_k g_k.\end{aligned}$$

Hence, the limit $\tilde{f}$ is a solution of

$$\sum_{k\in I_p} \boldsymbol{Q}_k \Psi_k (g_k - \boldsymbol{A}_k \tilde{f}) = 0$$

with $\mathrm{P}_{\mathrm{N}(\boldsymbol{A})^\perp}\tilde{f}$ being uniquely determined.

□

Following theorem 5.6, the crucial point in verifying the convergence of the iteration scheme for specific choices of $\{\Psi_k\}_{k\in I_p}$ is the verification of the norm condition

$$\|\boldsymbol{G}\mathrm{P}_{\mathrm{N}(\boldsymbol{A})^\perp}\| < 1. \tag{5.11}$$

Especially for solving large systems $\mathcal{A}f = g$, i.e., a large number of operators $\mathcal{A}_i$, it may be difficult to verify this norm condition. To this end, we give a sufficient condition on the operator norm $\|\boldsymbol{G}_k\mathrm{P}_{\mathrm{N}(\boldsymbol{A})^\perp}\|$ to induce the norm condition (5.11). Assuming that the requirements of theorem 5.6 are fulfilled, i.e., $\mathrm{R}(\Psi_k) \subseteq \mathrm{N}(\boldsymbol{A})^\perp$ for all $k \in I_p$, we obtain

$$\boldsymbol{G}\mathrm{P}_{\mathrm{N}(\boldsymbol{A})^\perp} = \left(\boldsymbol{G}_{|I_p|} \circ \cdots \circ \boldsymbol{G}_1\right)\mathrm{P}_{\mathrm{N}(\boldsymbol{A})^\perp} = \left(\boldsymbol{G}_{|I_p|}\mathrm{P}_{\mathrm{N}(\boldsymbol{A})^\perp}\right) \circ \cdots \circ \left(\boldsymbol{G}_1\mathrm{P}_{\mathrm{N}(\boldsymbol{A})^\perp}\right).$$

and the estimation

$$\|\boldsymbol{G}\mathrm{P}_{\mathrm{N}(\boldsymbol{A})^\perp}\| \leq \prod_{k\in I_p} \|\boldsymbol{G}_k\mathrm{P}_{\mathrm{N}(\boldsymbol{A})^\perp}\| \tag{5.12}$$

follows immediately. Thus, equation (5.12) provides a sufficient condition.

Proposition 5.9. *Let* $\mathrm{N}(\boldsymbol{A}_k) \cap \mathrm{N}(\boldsymbol{A})^\perp$ *be non-trivial for all* $k \in I_p$. *Then*

$$\prod_{k\in I_p} \|\boldsymbol{G}_k\mathrm{P}_{\mathrm{N}(\boldsymbol{A})^\perp}\| \geq 1.$$

Proof. For $\mathrm{N}(\boldsymbol{A}_k) \cap \mathrm{N}(\boldsymbol{A})^\perp$ being non-trivial, there exists an element $\varphi_k \in \mathrm{N}(\boldsymbol{A}_k) \cap \mathrm{N}(\boldsymbol{A})^\perp$ with $\|\varphi_k\| = 1$ and

$$\boldsymbol{G}_k\mathrm{P}_{\mathrm{N}(\boldsymbol{A})^\perp}\varphi_k = \left(\mathrm{id} - \Psi_k\boldsymbol{A}_k\right)\mathrm{P}_{\mathrm{N}(\boldsymbol{A})^\perp}\varphi_k = \mathrm{P}_{\mathrm{N}(\boldsymbol{A})^\perp}\varphi_k.$$

It follows

$$\begin{aligned}\|\boldsymbol{G}_k\mathrm{P}_{\mathrm{N}(\boldsymbol{A})^\perp}\| &= \max_{\|\varphi\|=1} \|\boldsymbol{G}_k\mathrm{P}_{\mathrm{N}(\boldsymbol{A})^\perp}\varphi\| \\ &\geq \|\boldsymbol{G}_k\mathrm{P}_{\mathrm{N}(\boldsymbol{A})^\perp}\varphi_k\|\end{aligned}$$

$$
\begin{aligned}
&= \left\| \left(\mathrm{id} - \Psi_k \boldsymbol{A}_k \right) \varphi_k \right\| \\
&= \left\| \varphi_k \right\| \\
&= 1
\end{aligned}
$$

and thus $\prod_{k \in I_P} \left\| \boldsymbol{G}_k \mathrm{P}_{\mathrm{N}(\boldsymbol{A})^\perp} \right\| \geq 1$. □

Proposition 5.9 provides a necessary condition to conclude the norm condition $\left\| \boldsymbol{G} \mathrm{P}_{\mathrm{N}(\boldsymbol{A})^\perp} \right\| < 1$ from equation (5.12). The existence of an index $k \in I_P$ such that

$$\mathrm{N}\left(\boldsymbol{A}_k\right) \cap \mathrm{N}(\boldsymbol{A})^\perp = \{0\} \tag{5.13}$$

is required to obtain $\prod_{k \in I_P} \left\| \boldsymbol{G}_k \mathrm{P}_{\mathrm{N}(\boldsymbol{A})^\perp} \right\| < 1$. For the convergence study of specific choices of Ψ_k we summarize all indices satisfying (5.13) as

$$I_P^* := \left\{ l \in I_P : \mathrm{N}\left(\boldsymbol{A}_l\right) \cap \mathrm{N}(\boldsymbol{A})^\perp = \{0\} \right\} \subseteq I_P.$$

5.2 The Landweber-Kaczmarz method

In this section, we deal with the semi-discrete Landweber-Kaczmarz iteration scheme, defined by the backward operators

$$\Psi_k := \lambda_k \boldsymbol{A}_k^\sharp \qquad \forall k \in I_P$$

with strictly positive relaxation parameters $\{\lambda_k\}_{k \in I_P}$. $\{\boldsymbol{A}_k\}_{k \in I_P}$ denote the semi-discrete operators of $\mathcal{A}_k$ with respect to the basis B on the weighted coefficient spaces $\left(\mathbb{R}^{|J|}, \langle \cdot, \cdot \rangle_k\right)$. The weighted adjoint operators $\boldsymbol{A}_k^\sharp$ are given by

$$\boldsymbol{A}_k^\sharp \varphi = W_k^{-1} \sum_{i \in I_k} \begin{pmatrix} \left\langle \mathcal{A}_i b_1, \varphi_i \right\rangle_{\mathcal{Y}_i} \\ \vdots \\ \left\langle \mathcal{A}_i b_{|J|}, \varphi_i \right\rangle_{\mathcal{Y}_i} \end{pmatrix}$$

cf. proposition 4.4. The Landweber-Kaczmarz iteration scheme thus reads

$$
\begin{aligned}
\boldsymbol{f}^{m,1} &:= \boldsymbol{f}^m \\
\boldsymbol{f}^{m,k+1} &= \boldsymbol{f}^{m,k} + \lambda_k \boldsymbol{A}_k^\sharp \left(g_k - \boldsymbol{A}_k \boldsymbol{f}^{m,k} \right) \qquad \text{for } k \in I_P \\
\boldsymbol{f}^{m+1} &:= \boldsymbol{f}^{m,|I_P|+1}.
\end{aligned} \tag{5.14}
$$

Corollary 5.10. *The following schemes are equivalent formulations of the Landweber-Kaczmarz iteration scheme* (5.14).

(i) (Closed form)

$$\boldsymbol{f}^{m+1} = \boldsymbol{f}^m + \sum_{k \in I_P} \lambda_k \boldsymbol{Q}_k \boldsymbol{A}_k^\sharp \left(g_k - \boldsymbol{A}_k \boldsymbol{f}^m \right) \qquad m = 0, 1, \ldots$$

(ii) (Fixed-point form)

$$\boldsymbol{f}^{m+1} = \Phi \boldsymbol{f}^m \qquad m = 0, 1, \ldots$$

with the affine linear fixed-point operator

$$\Phi : \mathbb{R}^{|J|} \to \mathbb{R}^{|J|}, \qquad \Phi \boldsymbol{f} := \boldsymbol{G} \boldsymbol{f} + \sum_{k \in I_P} \lambda_k \boldsymbol{Q}_k \boldsymbol{A}_k^\sharp g_k.$$

(iii) (Direct form)

$$f^m = G^m f^0 + \sum_{l=0}^{m-1} G^l \left(\sum_{k \in I_P} \lambda_k Q_k A_k^\sharp g_k \right)$$

with $G^0 := \mathrm{id}$.

Proof. This result follows immediately from proposition 5.3 with $\Psi_k = \lambda_k A_k^\sharp$. □

For the following convergence analysis, we consider the spectral norm and the weighted spectral norm denoted by

$$\|G\| = \max_{\|f\|=1} \|Gf\| \qquad \text{and} \qquad \|G\|_k = \max_{\|f\|_k=1} \|Gf\|_k,$$

respectively, induced by the Euclidean norm $\|\cdot\| := \|\cdot\|_2$ and the weighted Euclidean norms $\|\cdot\|_k := \|W_k^{\frac{1}{2}} \cdot\|_2$ on $\mathbb{R}^{|J|}$. Further, we denote the weighted operator norm of A_k by

$$\|A_k\|_k = \max_{\|f\|_k=1} \|A_k f\|_{Y_k}.$$

Proposition 5.11. *(i) Let $k \in I_P^*$, i.e, $\mathrm{N}(A_k) \cap \mathrm{N}(A)^\perp = \{0\}$, and let $\beta_k > 0$ such that*

$$\frac{1}{\beta_k} \|f\|_k \leq \|A_k f\|_{Y_k} \tag{5.15}$$

holds for all $f \in \mathrm{N}(A)^\perp$. For the relaxation parameters

$$\lambda_k \in \left(\frac{1 - \left((C_k^2 - 1)\tau_k^4 + 1 \right)^{\frac{1}{2}}}{\tau_k^2 \|A_k\|_k^2}, \frac{1 + \left((C_k^2 - 1)\tau_k^4 + 1 \right)^{\frac{1}{2}}}{\tau_k^2 \|A_k\|_k^2} \right) \tag{5.16}$$

with $C_k \in \left(\sqrt{1 - \tau_k^{-4}}, 1 \right]$ and $\tau_k := \beta_k \|A_k\|_k$ follows

$$\|G_k \mathrm{P}_{\mathrm{N}(A)^\perp}\|_k < C_k.$$

(ii) Let $\mathrm{N}(A_k) \cap \mathrm{N}(A)^\perp \neq \{0\}$. For all relaxation parameters

$$\lambda_k \in \left(0, \frac{2}{\tau_k^2 \|A_k\|_k^2} \right)$$

holds

$$\|G_k \mathrm{P}_{\mathrm{N}(A)^\perp}\|_k = 1.$$

Proof. (i) With $\tilde{f} := \mathrm{P}_{\mathrm{N}(A)^\perp} f$ follows

$$\begin{aligned} \|G_k \mathrm{P}_{\mathrm{N}(A)^\perp} f\|_k^2 &= \|(\mathrm{id} - \lambda_k A_k^\sharp A_k)\tilde{f}\|_k^2 \\ &= \|\tilde{f}\|_k^2 - 2\lambda_k \left\langle \tilde{f}, A_k^\sharp A_k \tilde{f} \right\rangle_k + \lambda_k^2 \|A_k^\sharp A_k \tilde{f}\|_k^2 \\ &= \|\tilde{f}\|_k^2 - 2\lambda_k \|A_k \tilde{f}\|_{Y_k}^2 + \lambda_k^2 \|A_k^\sharp A_k \tilde{f}\|_k^2 \end{aligned}$$

$$\begin{aligned}
&\leq \|\tilde{f}\|_k^2 - 2\lambda_k \|A_k \tilde{f}\|_{Y_k}^2 + \lambda_k^2 \|A_k\|_k^4 \|\tilde{f}\|_k^2 \\
&\overset{(5.15)}{\leq} \|\tilde{f}\|_k^2 - 2\frac{\lambda_k}{\beta_k^2}\|\tilde{f}\|_k^2 + \lambda_k^2 \|A_k\|_k^4 \|\tilde{f}\|_k^2 \\
&= \left(\lambda_k^2 \|A_k\|_k^4 - 2\frac{\lambda_k}{\beta_k^2} + 1\right)\|\tilde{f}\|_k^2. \qquad (5.17)
\end{aligned}$$

For the relaxation parameter λ_k as specified in (5.16) the inequality

$$\lambda_k^2 \|A_k\|_k^4 - 2\frac{\lambda_k}{\beta_k^2} + 1 < C_k^2$$

is fulfilled. Hence, we obtain

$$\begin{aligned}
\|G_k P_{N(A)^\perp}\|_k &= \max_{\|f\|_k=1} \|G_k P_{N(A)^\perp} f\|_k \\
&= \max_{\substack{f \in N(A)^\perp \\ \|f\|_k=1}} \|G_k f\|_k \\
&< C_k \cdot \max_{\substack{f \in N(A)^\perp \\ \|f\|_k=1}} \|f\|_k \\
&= C_k.
\end{aligned}$$

(ii) Since $N(A_k) \cap N(A)^\perp \neq \{0\}$, it holds

$$G_k P_{N(A)^\perp} \varphi = (\mathrm{id} - \lambda_k A_k^\sharp A_k) P_{N(A)^\perp} \varphi = \varphi.$$

for all elements $\varphi \in N(A_k) \cap N(A)^\perp$ with $\|\varphi\|_k = 1$ and thus

$$\|G_k P_{N(A)^\perp} \varphi\|_k = \|\varphi\|_k.$$

The result follows together with (i).

□

We have a closer look at all relevant parameters of proposition 5.11.

- The parameter $\beta_k > 0$ can be regarded as a norm estimate of the generalized inverse A_k^+. Since the generalized inverse of A_k is bounded, see proposition 4.4, the norm

$$\|A_k^+\|_k = \max_{\|\phi\|_{Y_k}=1} \|A_k^+ \phi\|_k < \infty$$

exists. For $\phi = A_k f$ with $f \in N(A_k)^\perp$ follows

$$\|f\|_k = \|A_k^+ A_k f\|_k \leq \|A_k^+\|_k \|A_k f\|_{Y_k}.$$

By definition, the operator norm $\|A_k^+\|_k$ is equal to the smallest number such that this statement holds true. Thus,

$$\|A_k^+\|_k \leq \beta_k.$$

- τ_k can be regarded as an estimation of the condition number of the operator $\boldsymbol{A}_k$,

$$\kappa(\boldsymbol{A}_k) = \|\boldsymbol{A}_k^+\|_k \|\boldsymbol{A}_k\|_k \leq \beta_k \|\boldsymbol{A}_k\|_k = \tau_k.$$

  Since the condition number fulfills $\kappa(\boldsymbol{A}_k) > 1$ per definition, it holds

$$\tau_k \in [1, \infty).$$

- It is easy to see that

$$C_k \in \left(\sqrt{1-\tau_k^{-4}}, 1\right] \subseteq (0, 1]$$

  since $\lim_{\tau_k \to \infty} \sqrt{1-\tau_k^{-4}} = 1$. We assume for the moment that $\|\boldsymbol{A}_k^+\|_k$ is known exactly. Then, the condition number $\kappa(\boldsymbol{A}_k)$ is also known exactly and we can put $\tau_k = \kappa(\boldsymbol{A}_k)$. If $\boldsymbol{A}_k$ is well-conditioned, i.e. $\tau_k \approx 1$, C_k can be chosen close to zero which results in the operator norm of $\boldsymbol{G}_k$ being close to zero as well. On the other hand, if the operator is ill-conditioned, i.e., $\tau_k \gg 1$, the lower bound for C_k is close to 1 and so is the norm of $\boldsymbol{G}$. Consequently, the parameter C_k cannot be arbitrarily and depends heavily on the condition of the semi-discrete operators $\boldsymbol{A}_k$ and the chosen basis B.

- The feasible relaxation parameters λ_k for $k \in I_P^*$ as specified in (5.16) are symmetric in an interval around

$$\lambda_k^* := \frac{1}{\tau_k^2 \|\boldsymbol{A}_k\|_k^2}.$$

  and this interval is bounded by the interval $\left(0, \frac{2}{\tau_k^2 \|\boldsymbol{A}_k\|_k^2}\right)$, i.e.,

$$\left(\frac{1 - \left(\left(C_k^2 - 1\right)\tau_k^4 + 1\right)^{\frac{1}{2}}}{\tau_k^2 \|\boldsymbol{A}_k\|_k^2}, \frac{1 + \left(\left(C_k^2 - 1\right)\tau_k^4 + 1\right)^{\frac{1}{2}}}{\tau_k^2 \|\boldsymbol{A}_k\|_k^2}\right) \subseteq \left(0, \frac{2}{\tau_k^2 \|\boldsymbol{A}_k\|_k^2}\right).$$

  Equality of the interval boundaries holds for the maximum $C_k = 1$. The parameter choice $\lambda_k = \lambda_k^*$ is optimal in the sense of the minimal upper bound for $\|\boldsymbol{G}_k \mathrm{P}_{\mathrm{N}(\boldsymbol{A})^\perp}\|_k$. This can be seen by minimizing (5.17),

$$\|\boldsymbol{G}_k \mathrm{P}_{\mathrm{N}(\boldsymbol{A})^\perp} \boldsymbol{f}\|_k^2 \leq \underbrace{\left(\lambda_k^2 \|\boldsymbol{A}_k\|_k^4 - 2\frac{\lambda_k}{\beta_k^2} + 1\right)}_{=:F(\lambda_k)} \|\tilde{\boldsymbol{f}}\|_k^2$$

  with respect to the relaxation parameter λ_k. Since $F(\lambda_k)$ is a quadratic function with respect to λ_k, the minimum is uniquely given and obtained for

$$0 = F'(\lambda_k) = 2\lambda_k \|\boldsymbol{A}_k\|_k^4 - \frac{2}{\beta_k^2} \qquad \Leftrightarrow \qquad \lambda_k = \lambda_k^* = \frac{1}{\tau_k^2 \|\boldsymbol{A}_k\|_k^2}$$

  with $\sqrt{F(\lambda_k^*)} = \sqrt{1-\tau_k^4}$.

Theorem 5.12. *Let $I_P^* \neq \emptyset$ and the relaxation parameters λ_k be defined as follows:*

- *For $k \in I_P^*$ let*

$$\lambda_k \in \left(\frac{1 - \left((C_k^2 - 1)\tau_k^4 + 1 \right)^{\frac{1}{2}}}{\tau_k^2 \|\boldsymbol{A}_k\|_k^2}, \frac{1 + \left((C_k^2 - 1)\tau_k^4 + 1 \right)^{\frac{1}{2}}}{\tau_k^2 \|\boldsymbol{A}_k\|_k^2} \right)$$

  with C_k and τ_k being defined as in proposition 5.11 such that

$$\prod_{k \in I_P} \sqrt{\kappa(W_k)} \prod_{k \in I_P^*} C_k \leq 1.$$

- *For $k \in I_P \setminus I_P^*$ let*

$$\lambda_k \in \left(0, \frac{2}{\tau_k^2 \|\boldsymbol{A}_k\|_k^2} \right).$$

Then, the Landweber-Kaczmarz iteration (5.14) converges linearly for any initial value $\boldsymbol{f}^0 \in \mathbb{R}^{|J|}$ and the limit is given by

$$\boldsymbol{f}^* = \mathrm{P}_{\mathrm{N}(\boldsymbol{A})} \boldsymbol{f}^0 + \left(\sum_{k \in I_P} \lambda_k \boldsymbol{Q}_k \boldsymbol{A}_k^\sharp \boldsymbol{A}_k \right)^{-1} \left(\sum_{k \in I_P} \lambda_k \boldsymbol{Q}_k \boldsymbol{A}_k^\sharp g_k \right).$$

The rate of convergence is bounded by $\prod_{k \in I_P} \kappa_k(W_k) \prod_{k \in I_P^*} C_k$ and the error estimates (5.8) and (5.9) of theorem 5.6 hold.

Proof. Following the convergence theorem 5.6, we have to verify the range condition $\mathrm{R}(\Psi_k) \subseteq \mathrm{N}(\boldsymbol{A})^\perp$, $k \in I_P$, for $\Psi_k = \boldsymbol{A}_k^\sharp$ and the norm condition $\|\boldsymbol{G}\mathrm{P}_{\mathrm{N}(\boldsymbol{A})^\perp}\| < 1$. With $\boldsymbol{A}_k$ being defined on the finite dimensional coefficient space $\mathbb{R}^{|J|}$ we obtain

$$\mathrm{R}(\Psi_k) = \mathrm{R}(\boldsymbol{A}_k^\sharp) = \overline{\mathrm{R}(\boldsymbol{A}_k^\sharp)} = \mathrm{N}(\boldsymbol{A}_k)^\perp$$

from corollary 2.19. Since the relaxation parameters λ_k fulfill the requirements of proposition 5.11 it follows

$$\begin{aligned}
\|\boldsymbol{G}\mathrm{P}_{\mathrm{N}(\boldsymbol{A})^\perp}\| &\leq \prod_{k \in I_P} \|\boldsymbol{G}_k \mathrm{P}_{\mathrm{N}(\boldsymbol{A})^\perp}\| \\
&\leq \prod_{k \in I_P} \kappa(W_k^{\frac{1}{2}}) \|\boldsymbol{G}_k \mathrm{P}_{\mathrm{N}(\boldsymbol{A})^\perp}\|_k \\
&= \prod_{k \in I_P} \sqrt{\kappa(W_k)} \prod_{k \in I_P} \|\boldsymbol{G}_k \mathrm{P}_{\mathrm{N}(\boldsymbol{A})^\perp}\|_k \\
&< \prod_{k \in I_P} \sqrt{\kappa(W_k)} \prod_{k \in I_P^*} C_k \\
&\leq 1
\end{aligned}$$

such that the norm condition $\|\boldsymbol{G}\mathrm{P}_{\mathrm{N}(\boldsymbol{A})^\perp}\| \leq 1$ is fulfilled. The convergence $\boldsymbol{f}^m \to \boldsymbol{f}^*$ for $m \to \infty$ as well as the error estimates follow immediately from theorem 5.6. □

To end this section, we give an interpretation of the limit f^* in the sense of proposition 5.8. If the semi-discrete system $Af = g$ is consistent the limit f^* is given as

$$f^* = f^+ + \mathrm{P}_{\mathrm{N}(A)} f^0$$

where f^+ is uniquely determined in $\mathrm{N}(A)^\perp$. If the system is not consistent, the limit f^* is a solution of a modified normal equation

$$\sum_{k \in I_p} Q_k A_k^\sharp (g_k - A_k f^*) = 0$$

with $\mathrm{P}_{\mathrm{N}(A)^\perp} f^*$ being uniquely determined.

5.3 The Kaczmarz method

We will now analyze the semi-discrete Kaczmarz iteration methods defined by the backward operators

$$\Psi_k = \lambda_k A_k^+ \qquad k \in I_P \tag{5.18}$$

with strictly positive relaxation parameters $\{\lambda_k\}_{k \in I_p}$. As above, let A_k denote the semi-discrete operators of $\mathcal{A}_k$ with respect to the fixed basis B. The Kaczmarz iteration scheme is thus given by

$$\begin{aligned} f^{m,1} &:= f^m \\ f^{m,k+1} &= f^{m,k} + \lambda_k A_k^+ (g_k - A_k f^{m,k}) \qquad \text{for } k = 1, \ldots, |I_P| \\ f^{m+1} &:= f^{m,|I_P|+1}. \end{aligned} \tag{5.19}$$

In literature, the Kaczmarz iteration scheme is also defined by putting $\Psi_k = \lambda_k A_k^* (A_k A_k^*)^{-1}$ for A_k being surjective. Following theorem 2.21 this is identical to equation (5.18). In the intended application of the semi-discrete Kaczmarz method, the operators A_k are in general not surjective. Then, the inverse operator $(A_k A_k^*)^{-1}$ does not exist and we have to go over to the generalized inverse. Again with theorem 2.21, this is identical to (5.18).

Corollary 5.13. *The Kaczmarz iteration scheme* (5.19) *is equivalent to the following schemes.*

(i) (Closed form)

$$f^{m+1} = f^m + \sum_{k \in I_p} \lambda_k Q_k A_k^+ (g_k - A_k f^m) \qquad m = 0, 1, \ldots$$

(ii) (Fixed-point form)

$$f^{m+1} = \Phi f^m \qquad m = 0, 1, \ldots$$

with the affine linear fixed-point operator

$$\Phi : \mathbb{R}^{|J|} \to \mathbb{R}^{|J|}, \qquad \Phi f := G f + \sum_{k \in I_p} \lambda_k Q_k A_k^+ g_k.$$

(iii) (Direct form)

$$f^m = G^m f^0 + \sum_{l=0}^{m-1} G^l \left(\sum_{k \in I_p} \lambda_k Q_k A_k^+ g_k \right)$$

with $G^0 := \mathrm{id}$.

Proof. This result follows directly from proposition 5.3 with $\Psi_k = \lambda_k \boldsymbol{A}_k^+$. □

For the following convergence analysis, we consider again the spectral norm and the weighted spectral norm denoted by

$$\|\boldsymbol{G}\| = \max_{\|\boldsymbol{f}\|=1} \|\boldsymbol{G}\boldsymbol{f}\| \qquad \text{and} \qquad \|\boldsymbol{G}\|_k = \max_{\|\boldsymbol{f}\|_k=1} \|\boldsymbol{G}\boldsymbol{f}\|_k,$$

respectively, induced by the Euclidean norm $\|\cdot\| \coloneqq \|\cdot\|_2$ and the weighted Euclidean norms $\|\cdot\|_k \coloneqq \|W_k^{\frac{1}{2}}\cdot\|_2$ on $\mathbb{R}^{|J|}$.

Proposition 5.14. *(i) Let $k \in I_P^*$, i.e., $\mathrm{N}(\boldsymbol{A}_k) \cap \mathrm{N}(\boldsymbol{A})^\perp = \{0\}$. Then,*

$$\|\boldsymbol{G}_k \mathrm{P}_{\mathrm{N}(\boldsymbol{A})^\perp}\|_k = |1 - \lambda_k|.$$

(ii) Let $\mathrm{N}(\boldsymbol{A}_k) \cap \mathrm{N}(\boldsymbol{A})^\perp \neq \{0\}$. Then,

$$\|\boldsymbol{G}_k \mathrm{P}_{\mathrm{N}(\boldsymbol{A})^\perp}\|_k = \max\{1, |1 - \lambda_k|\}.$$

Proof. With the Moore–Penrose axioms, cf. theorem 2.20, follows

$$\boldsymbol{G}_k = \mathrm{id} - \lambda_k \boldsymbol{A}_k^+ \boldsymbol{A}_k = \mathrm{id} - \lambda_k \mathrm{P}|_{\mathrm{N}(\boldsymbol{A}_k)^\perp} = \mathrm{P}|_{\mathrm{N}(\boldsymbol{A}_k)} + (1 - \lambda_k)\mathrm{P}|_{\mathrm{N}(\boldsymbol{A}_k)^\perp}.$$

For $\varphi \in \mathrm{N}(\boldsymbol{A}_k)^\perp \cap \mathrm{N}(\boldsymbol{A})^\perp = \mathrm{N}(\boldsymbol{A}_k)^\perp$ we obtain

$$\begin{aligned}
\|\boldsymbol{G}_k \mathrm{P}_{\mathrm{N}(\boldsymbol{A})^\perp} \varphi\|_k &= \|\boldsymbol{G}_k \varphi\|_k \\
&= \|\big(\mathrm{P}|_{\mathrm{N}(\boldsymbol{A}_k)} + (1 - \lambda_k)\mathrm{P}|_{\mathrm{N}(\boldsymbol{A}_k)^\perp}\big)\varphi\|_k \\
&= \|(1 - \lambda_k)\mathrm{P}|_{\mathrm{N}(\boldsymbol{A}_k)^\perp} \varphi\|_k \\
&= |1 - \lambda_k| \|\varphi\|_k.
\end{aligned}$$

(i) For $\mathrm{N}(\boldsymbol{A}_k) \cap \mathrm{N}(\boldsymbol{A})^\perp = \{0\}$ follows

$$\|\boldsymbol{G}_k \mathrm{P}_{\mathrm{N}(\boldsymbol{A})^\perp}\|_k = |1 - \lambda_k|.$$

(ii) For $\mathrm{N}(\boldsymbol{A}_k) \cap \mathrm{N}(\boldsymbol{A})^\perp \neq \{0\}$, every element $\varphi \in \mathrm{N}(\boldsymbol{A}_k) \cap \mathrm{N}(\boldsymbol{A})^\perp$ with $\|\varphi\|_k = 1$ fulfills

$$\begin{aligned}
\|\boldsymbol{G}_k \mathrm{P}_{\mathrm{N}(\boldsymbol{A})^\perp} \varphi\|_k &= \|\big(\mathrm{P}|_{\mathrm{N}(\boldsymbol{A}_k)} + (1 - \lambda_k)\mathrm{P}|_{\mathrm{N}(\boldsymbol{A}_k)^\perp}\big)\mathrm{P}_{\mathrm{N}(\boldsymbol{A})^\perp} \varphi\|_k \\
&= \|\mathrm{P}|_{\mathrm{N}(\boldsymbol{A}_k)} \mathrm{P}_{\mathrm{N}(\boldsymbol{A})^\perp} \varphi\|_k \\
&= \|\varphi\|_k \\
&= 1.
\end{aligned}$$

With (i) follows

$$\|\boldsymbol{G}_k \mathrm{P}_{\mathrm{N}(\boldsymbol{A})^\perp}\|_k = \max\{1, |1 - \lambda_k|\}.$$

□

Theorem 5.15. *Let $I_P^* \neq \emptyset$ and the relaxation parameters $\{\lambda_k\}_{k\in I_P}$ be such that*

$$\prod_{k\in I_P^*} |1-\lambda_k| \prod_{k\in I_P\setminus I_P^*} \max\{1,|1-\lambda_k|\} < 1. \tag{5.20}$$

The Kaczmarz iteration (5.19) converges linearly for arbitrary initial values $\boldsymbol{f}^0 \in \mathbb{R}^{|J|}$ and the limit is given as

$$\boldsymbol{f}^* = \mathrm{P}_{\mathrm{N}(\boldsymbol{A})}\boldsymbol{f}^0 + \left(\sum_{k\in I_P} \lambda_k \boldsymbol{Q}_k \mathrm{P}_{\mathrm{N}(\boldsymbol{A})^\perp}\right)^{-1}\left(\sum_{k\in I_P} \lambda_k \boldsymbol{Q}_k \boldsymbol{A}_k^+ g_k\right).$$

The rate of convergence is bounded by $\prod_{k\in I_P^*} |1-\lambda_k| \prod_{k\in I_P\setminus I_P^*} \max\{1,|1-\lambda_k|\}$ and the error estimates (5.8) and (5.9) of theorem 5.6 hold.

Proof. Again, we have to verify the range condition $\mathrm{R}(\Psi_k) \subseteq \mathrm{N}(\boldsymbol{A})^\perp$, $k \in I_P$, for $\Psi_k = \boldsymbol{A}_k^+$ and the norm condition $\|\boldsymbol{G}\mathrm{P}_{\mathrm{N}(\boldsymbol{A})^\perp}\| < 1$. Then, the convergence result follows from theorem 5.6.

The range condition is trivially fulfilled since $\mathrm{R}(\Psi_k) = \mathrm{R}(\boldsymbol{A}_k^+) = \overline{\mathrm{R}(\boldsymbol{A}_k^+)} = \mathrm{N}(\boldsymbol{A}_k)^\perp$. Further we obtain with proposition 5.14,

$$\begin{aligned}
\|\boldsymbol{G}\mathrm{P}_{\mathrm{N}(\boldsymbol{A})^\perp}\| &\leq \prod_{k\in I_P} \|\boldsymbol{G}_k \mathrm{P}_{\mathrm{N}(\boldsymbol{A})^\perp}\|_k \\
&= \prod_{k\in I_P^*} \|\boldsymbol{G}_k \mathrm{P}_{\mathrm{N}(\boldsymbol{A})^\perp}\|_k \prod_{k\in I_P\setminus I_P^*} \|\boldsymbol{G}_k \mathrm{P}_{\mathrm{N}(\boldsymbol{A})^\perp}\|_k \\
&= \prod_{k\in I_P^*} |1-\lambda_k| \prod_{k\in I_P\setminus I_P^*} \max\{1,|1-\lambda_k|\} \\
&= \prod_{k\in I_P^*} |1-\lambda_k| \\
&< 1.
\end{aligned}$$

□

Condition (5.20) for the relaxation parameters λ_k is trivially fulfilled for

$$\lambda_k \in (0,2) \qquad \forall k \in I_P$$

since $|1-\lambda_k| < 1$ holds for all k. Further, the operator norm $\|\boldsymbol{G}\mathrm{P}_{\mathrm{N}(\boldsymbol{A})^\perp}\|_k$ is bounded and this estimation is independent of the chosen ceoefficient weight matrices W_k, cf. proposition 5.14.

Corollary 5.16. *Let $I_P^* \neq \emptyset$ and*

$$\lambda_k \in (0,2) \qquad \forall k \in I_P.$$

Then, the Kaczmarz iteration (5.19) converges linearly for arbitrary initial values $\boldsymbol{f}^0 \in \mathbb{R}^{|J|}$ and the limit is given as

$$\boldsymbol{f}^* = \mathrm{P}_{\mathrm{N}(\boldsymbol{A})}\boldsymbol{f}^0 + \left(\sum_{k\in I_P} \lambda_k \boldsymbol{Q}_k \mathrm{P}_{\mathrm{N}(\boldsymbol{A})^\perp}\right)^{-1}\left(\sum_{k\in I_P} \lambda_k \boldsymbol{Q}_k \boldsymbol{A}_k^+ g_k\right).$$

The rate of convergence is bounded by $\prod_{k\in I_P^*} |1-\lambda_k| < 1$.

According to proposition 5.8, the limit f^* can be interpreted as follows. If $Af = g$ is consistent, it clearly holds

$$f^* = f^+ + \mathrm{P}|_{\mathrm{N}(A)} f^0.$$

For the non-consistent case, we obtain

$$\sum_{k \in I_P} Q_k A_k^+ (g_k - A_k f^*) = \sum_{k \in I_P} Q_k \left(f_k^+ - \mathrm{P}|_{\mathrm{N}(A_k)^\perp} f^* \right) = 0.$$

To end this section we give a strategy to apply the semi-discrete Kaczmarz iteration scheme. To evaluate the iteration steps the generalized inverse A_k^+ has to be applied to the residual $g_k - A_k f$ explicitly. In general, we cannot assume that the generalized inverse A_k^+ is explicitly known or available for computation. Moreover, even if it is known its application may be numerically unstable. To apply the semi-discrete Kaczmarz method anyway we make use of an idea stemming from the method of the approximate inverse which was first proposed in [LM90]: Instead of applying the pseudo inverse operator directly the so-called auxiliary problem

$$A_k^\sharp \psi_{k,j} = \mathrm{e}_j$$

is solved for an orthonormal basis $\{\mathrm{e}_j\}_{j \in J} \in \mathbb{R}^{|J|}$. The solution of $A_k f = g_k$ can then be computed by evaluating the inner products $\langle g_k, \psi_{k,j} \rangle_{Y_k}$.

Definition 5.17. *Let $\{\mathrm{e}_j\}_{j \in J}$ be an orthonormal basis of $\mathbb{R}^{|J|}$. For a fixed index $k \in I_P$ the solutions $\psi_{k,j} \in \mathrm{N}(A_k^\sharp)^\perp$, $j \in J$, of the auxiliary problem*

$$A_k^\sharp \psi_{k,j} = \mathrm{P}|_{\mathrm{N}(A_k)^\perp} \mathrm{e}_j$$

are called the associated reconstruction kernels.

The following result shows how the application of the pseudo inverse can be evaluated by using reconstruction kernels.

Proposition 5.18. *Let $\{\mathrm{e}_j\}_{j \in J} \subset \mathbb{R}^{|J|}$ be an orthonormal basis with respect to $\langle \cdot, \cdot \rangle_k$ and $\{\psi_{k,j}\}_{j \in J}$ be the corresponding reconstruction kernels for a fixed $k \in I_P$. Then,*

$$A_k^+ \phi = \sum_{j \in J} \langle \psi_{k,j}, \phi \rangle_{Y_k} \mathrm{e}_j \qquad \text{for } \phi \in Y_k.$$

Proof. Let $\phi \in Y_k$ and

$$f_k^+ := A_k^+ \phi \in \mathrm{N}(A_k)^\perp.$$

denote the generalized solution of $A_k f = g_k$. By definition of the reconstruction kernels it is $\psi_{k,j} \in \mathrm{N}(A_k^\sharp)^\perp$ and thus

$$\langle \psi_{k,j}, \mathrm{P}|_{\mathrm{N}(A_k^\sharp)} \phi \rangle_{Y_k} = 0.$$

We obtain

$$\langle \psi_{k,j}, \phi \rangle_{Y_k} = \langle \psi_{k,j}, \mathrm{P}|_{\mathrm{R}(A_k)} \phi \rangle_{Y_k} + \langle \psi_{k,j}, \mathrm{P}|_{\mathrm{N}(A_k^\sharp)} \phi \rangle_{Y_k}$$

$$
\begin{aligned}
&= \left\langle \psi_{k,j}, \boldsymbol{A}_k \boldsymbol{f}_k^+ \right\rangle_{Y_k} \\
&= \left\langle \boldsymbol{A}_k^\sharp \psi_{k,j}, \boldsymbol{f}_k^+ \right\rangle_k \\
&= \left\langle \mathrm{P}|_{\mathrm{N}(\boldsymbol{A}_k)^\perp} \mathrm{e}_j, \boldsymbol{f}_k^+ \right\rangle_k \\
&= \left\langle \mathrm{e}_j, \boldsymbol{f}_k^+ \right\rangle_k .
\end{aligned}
$$

Since $\{\mathrm{e}_j\}_{j\in J}$ forms an orthonormal basis on $\mathbb{R}^{|J|}$ it follows

$$
\boldsymbol{A}_k^+ \phi = \boldsymbol{f}_k^+ = \sum_{j\in J} \left\langle \mathrm{e}_j, \boldsymbol{f}_k^+ \right\rangle_k \mathrm{e}_j = \sum_{j\in J} \left\langle \psi_{k,j}, \phi \right\rangle_{Y_k} \mathrm{e}_j \,.
$$

□

Example 5.19. *Let $\{\mathrm{e}_j\}_{j\in J}$ be the canonical basis of the coefficient space $\mathbb{R}^{|J|}$, i.e.,*

$$
\left(\mathrm{e}_j\right)_l = \delta_{jl} \qquad \forall j, l \in J.
$$

We obtain

$$
\boldsymbol{A}_k \mathrm{e}_j = \sum_{l\in J} \delta_{jl} A_k b_l = A_k b_j \qquad \text{and} \qquad \left\langle \boldsymbol{f}, \mathrm{e}_j \right\rangle = \boldsymbol{f}_j \quad \forall \boldsymbol{f} \in \mathbb{R}^{|J|}.
$$

With $\{\psi_{k,j}\}_{j\in J}$ being the associated reconstruction kernels of $\{\mathrm{e}_j\}_{j\in J}$, proposition 5.18 yields the representation

$$
\boldsymbol{A}_k^+ \phi = \sum_{j\in J} \left\langle \psi_{k,j}, \phi \right\rangle_{Y_k} \mathrm{e}_j = \left(\left\langle \psi_{k,j}, \phi \right\rangle_{Y_k} \right)_{j\in J}
$$

for the application of the generalized inverse $\boldsymbol{A}_k^+$.

With example 5.19 follows immediately:

Corollary 5.20. *Let $\{\mathrm{e}_j\}_{j\in J}$ be the canonical basis in $\mathbb{R}^{|J|}$ and $\{\psi_{k,j}\}_{j,k}$ the associated reconstruction kernels for all $k \in I_P$. The Kaczmarz iteration scheme (5.19) reads*

$$
\begin{aligned}
\boldsymbol{f}^{m,1} &:= \boldsymbol{f}^m \\
\boldsymbol{f}^{m,k+1} &= \boldsymbol{f}^{m,k} + \lambda_k \left(\left\langle \psi_{k,j}, g_k - \boldsymbol{A}_k \boldsymbol{f}^{m,k} \right\rangle_{Y_k} \right)_{j\in J} \qquad \text{for } k \in I_P \\
\boldsymbol{f}^{m+1} &:= \boldsymbol{f}^{m,|I_P|+1}.
\end{aligned}
$$

Chapter 6

Application in X-ray tomography

Let Ω be the n-dimensional unit ball and let $\mathbb{S}^{n-1} := \partial\Omega$ be the n-dimensional unit sphere. Further, we use ω and w to denote weight functions on the domain and the range of the operator, respectively. We focus on the Hilbert space setting of square-integrable functions on the unit ball Ω denoted by $L_2(\Omega)$. Using the notation of Chapter 4 the model operators are of the form

$$\mathcal{A}_i : L_2(\Omega, \omega) \to L_2(\Xi_i, w_i)$$

and

$$\mathcal{A} : L_2(\Omega, \omega) \to \mathcal{Y}$$

with I being a finite set of indices. The Hilbert space $\mathcal{Y}$ is given as the direct sum of weighted L_2 spaces,

$$\mathcal{Y} = \bigoplus_i L_2(\Xi_i, w_i).$$

The reconstruction problem is formulated as follows: For a given set of finitely many measurements $\{g_i\}_{i\in I}$, with $g_i \in L_2(\Xi_i, w_i)$ find $f \in L_2(\Omega, \omega)$ such that

$$\mathcal{A}_i f = g_i \qquad \forall i \in I.$$

6.1 Local basis functions

So far, we considered sets of mutually linearly independent basis elements $B \subset \mathcal{X}$. In the context of iterative reconstruction methods, we are interested in a fast evaluation of the forward projection of the basis elements as well as suitable approximation properties in the image space.

An important class of basis functions is thus the class of local (or locally supported) basis functions: Starting from a compactly supported initial function b the basis B is generated by scaling and shifting of the initial function b on a (regular) grid. We consider two important initial basis functions, namely, the Pixel resp. Voxel basis function and the Lewitt-Blob basis function. A comparison of both basis functions with respect to image quality of the reconstructions can be found in [Tra+17].

6.1.1 The Pixel and Voxel basis functions

Definition 6.1. *Let*

$$\square^d(x) := \chi_{[-\frac{1}{2},\frac{1}{2}]^d}(x) = \begin{cases} 1, & \text{if } \|x\|_\infty \le \frac{1}{2} \\ 0, & \text{else} \end{cases}$$

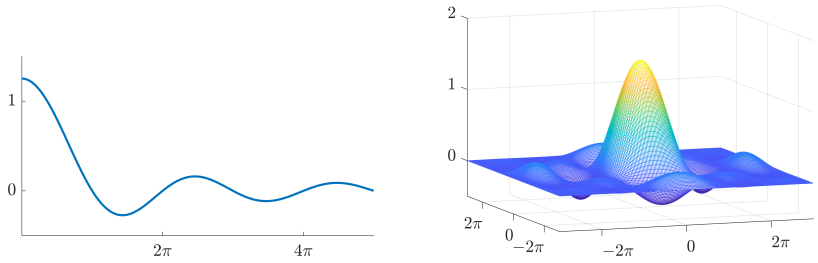

Figure 6.1: Fourier transform of the unit cube. Left: $\mathcal{F}\square^1$, right: $\mathcal{F}\square^2$.

denote the characteristic function of the d-dimensional unit cube centered around the origin. For $d = 2$ *we call* $\square^d$ *the* Pixel *basis function and for* $d = 3$ *the* Voxel *basis function.*

Proposition 6.2. *The Frourier transform of* $\square^d$ *is given by*

$$\mathcal{F}\square^d(\xi) = (2\pi)^{-\frac{d}{2}} \prod_{i=1}^{d} \operatorname{sinc}\left(\frac{\xi_i}{2}\right)$$

where $\operatorname{sinc} s = \frac{\sin s}{s}$ *for* $s \in \mathbb{R}$.

Proof. We start with the one-dimensional Fourier transform of the unit cube $\square^1$ in $\mathbb{R}$, i.e., the *box function*. For $\sigma \in \mathbb{R}$ it yields

$$\begin{aligned}
\mathcal{F}_1\square^1(\sigma) &= \frac{1}{\sqrt{2\pi}} \int_{\mathbb{R}} \square^1(s)\, \mathrm{e}^{-is\sigma}\, ds \\
&= \frac{1}{\sqrt{2\pi}} \int_{-\frac{1}{2}}^{\frac{1}{2}} \mathrm{e}^{-is\sigma}\, ds \\
&= \frac{1}{\sqrt{2\pi}} \left(\int_{-\frac{1}{2}}^{\frac{1}{2}} \cos(s\sigma)\, ds - i \underbrace{\int_{-\frac{1}{2}}^{\frac{1}{2}} \sin(s\sigma)\, ds}_{=0} \right) \\
&= \sqrt{\frac{2}{\pi}} \int_{0}^{\frac{1}{2}} \cos(s\sigma)\, ds \\
&= \frac{1}{\sqrt{2\pi}} \operatorname{sinc}\left(\frac{\sigma}{2}\right).
\end{aligned}$$

With this result we can compute the d-dimensional Fourier transform of the cube $\square^d$ as follows. For $\xi \in \mathbb{R}^d$ holds

$$\begin{aligned}
\mathcal{F}_d\square^d(\xi) &= (2\pi)^{-\frac{d}{2}} \int_{\mathbb{R}^d} \square^d(x)\, \mathrm{e}^{-ix^\top \xi}\, dx \\
&= (2\pi)^{-\frac{d}{2}} \int_{\left[-\frac{1}{2},\frac{1}{2}\right]^d} \mathrm{e}^{-ix^\top \xi}\, dx
\end{aligned}$$

$$
\begin{aligned}
&= (2\pi)^{-\frac{d}{2}} \int_{\left[-\frac{1}{2},\frac{1}{2}\right]^d} \prod_{i=1}^{d} \mathrm{e}^{-ix_i\xi_i}\, dx \\
&= (2\pi)^{-\frac{d}{2}} \prod_{i=1}^{d} \int_{-\frac{1}{2}}^{\frac{1}{2}} \mathrm{e}^{-ix_i\xi_i}\, dx_i \\
&= \prod_{i=1}^{d} \mathcal{F}_1 \square^1(\xi_i).
\end{aligned}
$$

Thus, the Fourier transform of the d-dimensional unit cube is given as

$$
\mathcal{F}_d \square^d(\xi) = \prod_{i=1}^{d} \frac{1}{\sqrt{2\pi}} \operatorname{sinc}\left(\frac{\xi_i}{2}\right) = (2\pi)^{-\frac{d}{2}} \prod_{i=1}^{d} \operatorname{sinc}\left(\frac{\xi_i}{2}\right).
$$

□

For the X-Ray transform of the unit cube, there is no closed expression. Instead, its X-Ray transform has to be evaluated separately for every given parameter combination of the angle $\theta \in \mathcal{S}^{d-1}$ and the position $x \in \theta^\perp$ on the detector. We use the fact that $\square^d$ is defined as the characteristic function of the unit cube, hence having constant value 1 inside the cube such that each line integral

$$
\mathcal{P}_\theta \square^d(x) = \int_{L(\theta,x)} \square^d(y)\, dy
$$

corresponds to the length of the intersection of $L(\theta, x)$ with the unit cube. We can thus formulate the computation of the X-ray transform as the geometrical problem

$$
\mathcal{P}_\theta \square^d(x) = \operatorname{length}\left(\left\{z \coloneqq x + t\theta : t \in \mathbb{R}\right\} \cap \left\{\|z\|_\infty < \frac{1}{2}\right\}\right).
$$

For the Pixel basis function in two dimensions ($d = 2$), we differentiate between two (non-trivial) cases. Let e_1 and e_2 be the canonical unit vectors in $\mathbb{R}^2$.

(i) $\langle\theta, \mathrm{e}_1\rangle = 0$ *or* $\langle\theta, \mathrm{e}_2\rangle = 0$: This is the case if the direction of integration θ is parallel to one of the edges. Then, the X-ray transform is equal to the edge length of the unit square, i.e.,

$$
\mathcal{P}_\theta \square^2(x) = 1.
$$

(ii) $\langle\theta, \mathrm{e}_1\rangle \neq 0 \neq \langle\theta, \mathrm{e}_2\rangle$:

a) Compute the intersection points $\mathcal{S}_2 \coloneqq \{x_{1,\pm}, x_{\pm,2}\}$ of

$$
L(\theta, x) = \{x + t\theta : t \in \mathbb{R}\}
$$

with the continued edges

$$
\Gamma_{1,\pm} \coloneqq \left\{ \pm \frac{1}{2}\mathrm{e}_1 + t\,\mathrm{e}_2 : t \in \mathbb{R}\right\} \quad \text{and} \quad \Gamma_{2,\pm} \coloneqq \left\{t\,\mathrm{e}_1 \pm \frac{1}{2}\mathrm{e}_2 : t \in \mathbb{R}\right\}.
$$

b) Define

$$
x^1_{\min} \coloneqq \min_{x \in \mathcal{S}_2} \|x\| \qquad \text{and} \qquad x^2_{\min} \coloneqq \min_{x \in \mathcal{S}_2 \setminus \{x^1_{\min}\}} \|x\|.
$$

The X-ray transform is now given as the distance between $x^1_{\min}$ and $x^2_{\min}$, i.e.,

$$
\mathcal{P}_\theta \square^2(x) = \|x^2_{\min} - x^1_{\min}\|.
$$

In three dimensions ($d = 3$), we have to take a third case into account to obtain the X-ray transform of the Voxel basis function. Let $\mathrm{e}_1, \mathrm{e}_2$ and e_3 denote the canonical unit vectors in $\mathbb{R}^3$.

(i) $\langle \theta, \mathrm{e}_i \rangle \neq 0$ for a single index $i^* \in \{1,2,3\}$: In this case, the direction of integration θ is parallel to e_{i^*} and thus parallel to one of the edges of the unit cube. The X-ray transform is thus given as the edge length of the unit cube, i.e.,

$$\mathcal{P}_\theta \square^3(x) = 1.$$

(ii) $\langle \theta, \mathrm{e}_i \rangle = 0$ for exactly one index $i^* \in \{1,2,3\}$: The direction θ is perpendicular to the unit vector e_{i^*} and is thus an element of the plane spanned by $\{\mathrm{e}_i\}_{i \in \{1,2,3\} \setminus \{i^*\}}$. Thus, the three-dimensional case reduces to the two-dimensional case described before,

$$\mathcal{P}_\theta \square^3(x) = \mathcal{P}_\theta \square^2(\tilde{x}),$$

where $\tilde{x} \in \mathbb{R}^2$ denotes the position of x on the hyperplane $\theta_{i^*}^\perp$.

(iii) $\langle \theta, \mathrm{e}_i \rangle \neq 0$ for all indices $i \in \{1,2,3\}$:

a) Compute the intersection points $\mathcal{S}_3 := \{x_{1,\pm}, x_{2,\pm}, x_{3,\pm}\}$ of the line of integration

$$L := \{x + t\theta : t \in \mathbb{R}\}$$

with the continued outer surfaces

$$\mathcal{M}_{1,\pm} := \left\{ \pm \frac{1}{2} \mathrm{e}_1 + t_2 \mathrm{e}_2 + t_3 \mathrm{e}_3 : t_2, t_3 \in \mathbb{R} \right\},$$

$$\mathcal{M}_{2,\pm} := \left\{ t_1 \mathrm{e}_1 \pm \frac{1}{2} \mathrm{e}_2 + t_3 \mathrm{e}_3 : t_1, t_3 \in \mathbb{R} \right\},$$

$$\mathcal{M}_{3,\pm} := \left\{ t_1 \mathrm{e}_1 + t_2 \mathrm{e}_2 \pm \frac{1}{2} \mathrm{e}_3 : t_1, t_2 \in \mathbb{R} \right\}.$$

b) With

$$x^1_{\min} := \min_{x \in \mathcal{S}_3} \|x\| \qquad \text{and} \qquad x^2_{\min} := \min_{x \in \mathcal{S}_3 \setminus \{x^1_{\min}\}} \|x\|$$

the X-ray transform is given as the distance between $x^1_{\min}$ and $x^2_{\min}$, i.e.,

$$\mathcal{P}_\theta \square^3(x) = \|x^2_{\min} - x^1_{\min}\|.$$

6.1.2 The Lewitt-Blob basis function

The generalized Kaiser-Bessel window functions also referred to as Lewitt-Blobs were proposed in [Lew90] as optimal basis functions being compactly supported and being efficiently band-limited. The Blobs were designed as an approximation to prolate spheroidal wave functions which were computed in [Sle65] as the optimum of functions having minimal support and minimal support in the Fourier domain at the same time.

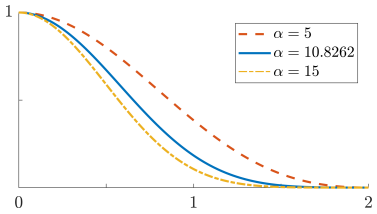

Figure 6.2: Radial plot of $b_{m,a,\alpha}$ for $m = 2$, $a = 2$ and different shaping parameter α.

Definition 6.3. *Let $a, \alpha > 0$ and $m \geq 0$. The function*

$$b_{m,a,\alpha}(x) := \begin{cases} I_m(\alpha)^{-1}\left(\sqrt{1-\left(\frac{\|x\|}{a}\right)^2}\right)^m I_m\left(\alpha\sqrt{1-\left(\frac{\|x\|}{a}\right)^2}\right), & \text{if } \|x\| \leq a \\ 0, & \text{else} \end{cases}$$

where I_m denotes the modified Bessel function of the first kind of order m is called generalized Kaiser-Bessel window function *or* (Lewitt-)Blob function.

We summarize basic properties of the Blob basis function.

Proposition 6.4. *Let $a, \alpha > 0$ and $m \geq 0$. The Lewitt-Blob basis function is*

(i) rotationally invariant, non-negative and compactly supported, i.e.,

$$\overline{\operatorname{supp}(b_{m,a,\alpha})} \Subset \mathbb{R}^d,$$

(ii) continuous on $\mathbb{R}^d$ for all $m \neq 0$,

(iii) $(m-1)$ - times continuously differentiable for $m \in \mathbb{N} \setminus \{0\}$, thus,

$$b_{m,a,\alpha} \in C_0^{m-1}(\mathbb{R}^d).$$

Proof. (i) Follows directly from the definition of the Blob function and the properties of the modified Bessel function I_m, where the non-negativity follows with the non-negativity of the modified Bessel function I_m as can be seen by the series representation in definition 2.1,

$$I_m(x) = \left(\frac{x}{2}\right)^m \sum_{k=0}^{\infty} \frac{(\frac{1}{2}x)^{2k}}{k!\,\Gamma(m+k+1)}. \tag{6.1}$$

(ii) Let $z \in \mathbb{R}^d$ with $\|z\| = a$. By definition, the Blob function at z is given as

$$b_{m,a,\alpha}(z) = I_m(\alpha)^{-1}\, I_m(0).$$

The series representation (6.1) yields

$$I_m(0) = 0^m \sum_{k=0}^{\infty} \frac{0^{2k}}{k!\,\Gamma(m+k+1)}$$

$$= 0^m \left(1 + \sum_{k=1}^{\infty} \frac{0^{2k}}{k!\,\Gamma(m+k+1)}\right)$$
$$= 0^m = \begin{cases} 1, & m = 0 \\ 0, & m > 0. \end{cases}$$

Hence, the Blob basis function is continuous on $\mathbb{R}^d$ for $m \neq 0$.

(iii) With the representation of the l-th derivative of the modified Bessel function

$$I_m^{(l)}(x) = \frac{1}{2^l} \sum_{j=0}^{l} \binom{l}{j} I_{m-l+2j}(x)$$
$$= \frac{1}{2^l} I_{m-l}(x) + \frac{1}{2^l} \sum_{j=1}^{l} \binom{l}{j} I_{m-l+2j}(x),$$

cf. [AS65, 9.6.29], and property (ii) follows the result.

□

Proposition 6.5 (Fourier transform). *The Fourier transform of the Blob basis function is given as*

$$\hat{b}^d_{m,a,\alpha}(\xi) = \frac{a^d \alpha^m}{I_m(\alpha)} \left(\sqrt{a^2\|\xi\|^2 - \alpha^2}\right)^{-(\frac{d}{2}+m)} J_{\frac{d}{2}+m}\left(\sqrt{a^2\|\xi\|^2 - \alpha^2}\right)$$

where $J_{\frac{d}{2}+m}$ denotes the Bessel function of the first kind of order $\frac{d}{2} + m$.

Proof. The proof follows [Lew90]. Note that a different definition of the Fourier transform is used. Let a, α and m be fixed and put $b := b_{m,a,\alpha}$. Since the Blob function is rotationally invariant, the Fourier transform of b^d is computed via

$$\hat{b}^d(\xi) = \|\xi\|^{1-\frac{d}{2}} \int_0^{\infty} r^{\frac{d}{2}}\, \varphi(r)\, J_{\frac{d}{2}-1}(r\|\xi\|)\, dr,$$

see lemma 2.6, where φ is defined as the radial part of the Blob, i.e., $b(x) = \varphi(\|x\|)$ for all $x \in \mathbb{R}^d$. Putting $t(r) := (1 - (\frac{r}{a})^2)^{\frac{1}{2}}$ and plugging in the definition of the Blob function yields

$$\hat{b}^d(\xi) = \frac{\|\xi\|^{1-\frac{d}{2}}}{I_m(\alpha)} \int_0^a r^{\frac{d}{2}}\, t^m(r)\, I_m(\alpha t(r))\, J_{\frac{d}{2}-1}(r\|\xi\|)\, dr$$
$$= \frac{i^{-m}\, \|\xi\|^{1-\frac{d}{2}}}{I_m(\alpha)} \int_0^a r^{\frac{d}{2}}\, t^m(r)\, J_m(i\alpha t(r))\, J_{\frac{d}{2}-1}(r\|\xi\|)\, dr$$

where we used the identity $I_m(z) = i^{-m} J_m(iz)$, cf. lemma 2.2, in the last step.

With the substitution $r = a\cos\theta$, $dr = -a\sin\theta\, d\theta$, follows

$$t(r) = t(a\cos\theta) = \sqrt{1 - \left(\frac{a\cos\theta}{a}\right)^2} = \sin\theta$$

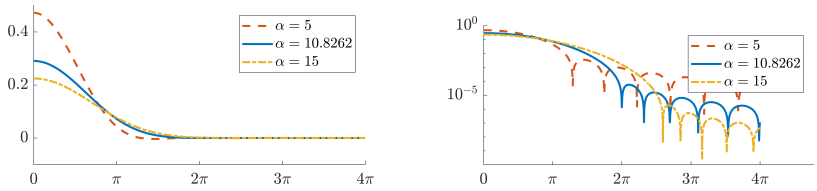

(a) $\hat{b}^2_{m,a,\alpha}$ (b) $\log|\hat{b}^2_{m,a,\alpha}|$

Figure 6.3: Radial plots of the Fourier transform $\hat{b}^d_{m,a,\alpha}$ for $m = 2$, $a = 2$ and the $\alpha \approx 10.8$.

and it yields

$$\hat{b}^d(\xi) = \frac{i^{-m}\,\|\xi\|^{1-\frac{d}{2}}\,a^{\frac{d}{2}+1}}{I_m(\alpha)} \int_0^{\frac{\pi}{2}} \cos^{\frac{d}{2}}\theta\,\sin^{m+1}\theta\,J_m(i\alpha\sin\theta)\,J_{\frac{d}{2}-1}(a\|\xi\|\cos\theta)\,d\theta.$$

To evaluate the integral on the right hand side, we use *Sonine's second finite integral* from lemma 2.3 with $\mu = m$, $\nu = {}^d\!/_2 - 1$, $z = i\alpha$ and $Z = a\|\xi\|$, yielding

$$\begin{aligned}\int_0^{\frac{\pi}{2}} &\cos^{\frac{d}{2}}\theta\,\sin^{m+1}\theta\,J_m(i\alpha\sin\theta)\,J_{\frac{d}{2}-1}(a\|\xi\|\cos\theta)\,d\theta \\ &= (i\alpha)^m(a\|\xi\|)^{\frac{d}{2}-1}\left(\sqrt{(a\|\xi\|)^2-\alpha^2}\right)^{-(m+\frac{d}{2})} J_{m+\frac{d}{2}}\left(\sqrt{(a\|\xi\|)^2-\alpha^2}\right).\end{aligned}$$

We finally obtain

$$\hat{b^d}(\xi) = \frac{a^d\alpha^m}{I_m(\alpha)}\left(\sqrt{(a\|\xi\|)^2-\alpha^2}\right)^{-(\frac{d}{2}+m)} J_{m+\frac{d}{2}}\left(\sqrt{(a\|\xi\|)^2-\alpha^2}\right).$$

□

Having a closer look at the Fourier transform of the Blob function, the argument of the Bessel function $J_{m+\frac{d}{2}}$ is complex valued whenever

$$a^2\|\xi\|^2 - \alpha^2 < 0.$$

In that case, it holds

$$\sqrt{a^2\|\xi\|^2-\alpha^2} = i\sqrt{|a^2\|\xi\|^2-\alpha^2|}$$

and with the identity $I_m(z) = i^{-m}J_m(iz)$ we obtain

$$\begin{aligned}&\left(\sqrt{a^2\|\xi\|^2-\alpha^2}\right)^{-(\frac{d}{2}+m)} J_{\frac{d}{2}+m}\left(\sqrt{a^2\|\xi\|^2-\alpha^2}\right) \\ &\quad= \left(\sqrt{|a^2\|\xi\|^2-\alpha^2|}\right)^{-(\frac{d}{2}+m)} i^{-(\frac{d}{2}+m)}\,J_{\frac{d}{2}+m}\left(i\sqrt{|a^2\|\xi\|^2-\alpha^2|}\right) \\ &\quad= \left(\sqrt{|a^2\|\xi\|^2-\alpha^2|}\right)^{-(\frac{d}{2}+m)} I_{\frac{d}{2}+m}\left(\sqrt{|a^2\|\xi\|^2-\alpha^2|}\right).\end{aligned}$$

Thus, we obtain

$$\mathcal{F}b^d_{m,a,\alpha}(\xi) = \frac{a^d\alpha^m}{I_m(\alpha)}\left(\sqrt{|a^2\|\xi\|^2-\alpha^2|}\right)^{-(\frac{d}{2}+m)}\begin{cases} I_{\frac{d}{2}+m}\left(\sqrt{|a^2\|\xi\|^2-\alpha^2|}\right), & a^2\|\xi\|^2 \le \alpha^2, \\ J_{\frac{d}{2}+m}\left(\sqrt{|a^2\|\xi\|^2-\alpha^2|}\right), & a^2\|\xi\|^2 \ge \alpha^2, \end{cases}$$

which is a more suitable formula for implementation.

Theorem 6.6 (X-Ray transform of the Blob function).

$$\mathcal{P}_\theta b_{m,a,\alpha}(x) = \begin{cases} \frac{a}{I_m(\alpha)}\sqrt{\frac{2\pi}{\alpha}}\left(\sqrt{1-a^{-2}\|x\|^2}\right)^{m+\frac{1}{2}} I_{m+\frac{1}{2}}\left(\alpha\sqrt{1-a^{-2}\|x\|^2}\right), & \|x\| \le a, \\ 0, & else. \end{cases}$$

Proof. The proof follows again [Lew90]. Let a, α and m be fixed and put $b := b_{m,a,\alpha}$. Since the Blob function is rotationally invariant, the X-Ray transform is computed by

$$\mathcal{P}_\theta b(x) = 2\int_0^\infty b\left(\sqrt{\|x\|^2+t^2}\right)dt$$

for $x \in \theta^\perp$, see lemma 3.8. With definition 6.3 of the Blob function follows,

$$\mathcal{P}_\theta b(x) = \frac{2}{I_m(\alpha)}\int_0^{\sqrt{a^2-\|x\|^2}}\left(\sqrt{1-\frac{\|x\|^2+t^2}{a^2}}\right)^m I_m\left(\alpha\sqrt{1-\frac{\|x\|^2+t^2}{a^2}}\right)dt.$$

Putting $t := \sqrt{a^2-\|x\|^2}\cos\phi,\ dt = -\sqrt{a^2-\|x\|^2}\sin\phi\, d\phi$, yields

$$\begin{aligned} 1-\frac{\|x\|^2+t^2}{a^2} &= 1-\frac{\|x\|^2+\left(a^2-\|x\|^2\right)\cos^2\phi}{a^2} \\ &= 1-\frac{\|x\|^2+\left(a^2-\|x\|^2\right)(1-\sin^2\phi)}{a^2} \\ &= 1-\frac{a^2-\left(a^2-\|x\|^2\right)\sin^2\phi}{a^2} \\ &= \frac{\left(a^2-\|x\|^2\right)\sin^2\phi}{a^2} \\ &= \left(1-\frac{\|x\|^2}{a^2}\right)\sin^2\phi \end{aligned}$$

and thus

$$\begin{aligned} \mathcal{P}_\theta b(x) &= \frac{2}{I_m(\alpha)}\int_0^{\frac{\pi}{2}}\left(\sqrt{1-a^{-2}\|x\|^2}\sin\phi\right)^m I_m\left(\alpha\sqrt{1-a^{-2}\|x\|^2}\sin\phi\right)\sqrt{a^2-\|x\|^2}\sin\phi\, d\phi \\ &= \frac{2}{I_m(\alpha)}\left(\sqrt{1-a^{-2}\|x\|^2}\right)^m\int_0^{\frac{\pi}{2}} I_m\left(\alpha\sqrt{1-a^{-2}\|x\|^2}\sin\phi\right)a\sqrt{1-a^{-2}\|x\|^2}\sin^{m+1}\phi\, d\phi \end{aligned}$$

$$= \frac{2a}{I_m(\alpha)}\left(\sqrt{1-a^{-2}\|x\|^2}\right)^{m+1}\int_0^{\frac{\pi}{2}} I_m\left(\alpha\sqrt{1-a^{-2}\|x\|^2}\sin\phi\right)\sin^{m+1}\phi\, d\phi.$$

Applying *Sonine's first finite integral* for the modified Bessel function I_m of the first kind, see lemma 2.3, given as

$$\sqrt{\frac{2}{\pi}}\left(\alpha\sqrt{1-a^{-2}\|x\|^2}\right)^{\frac{1}{2}}\int_0^{\frac{\pi}{2}} I_m\left(\alpha\sqrt{1-a^{-2}\|x\|^2}\sin\phi\right)\sin^{m+1}\phi\, d\phi = I_{m+\frac{1}{2}}\left(\alpha\sqrt{1-a^{-2}\|x\|^2}\right)$$

for $z = \alpha\sqrt{1-a^{-2}\|x\|^2}$, finally yields the X-Ray transform of the Blob function

$$\mathcal{P}_\theta b(x) = \frac{a}{I_m(\alpha)}\sqrt{\frac{2\pi}{\alpha}}\left(\sqrt{1-a^{-2}\|x\|^2}\right)^{m+\frac{1}{2}} I_{m+\frac{1}{2}}\left(\alpha\sqrt{1-a^{-2}\|x\|^2}\right).$$

□

6.1.3 Approximation properties

We will also have a look at the approximation properties of the Pixel/Voxel and the Blob basis functions. We define the translates of a fixed basis function b as

$$b_j := b(\cdot - x_j) \tag{6.2}$$

for a given set of centers $\{x_j\}_j$ depending on the underlying grid. For the Blob basis functions, different types of grids have been studied for two and three dimensions, see e.g. [ML95] and [ML96]. Nevertheless, we will restrict the approximation analysis to the canonical case of regular Cartesian grids, i.e., the centers in equation (6.2) are defined as $x_j \in \mathbb{Z}^d$. For a given grid size $h > 0$, we further define

$$x_j^h := h^{-1}x_j.$$

For compactly supported $\psi \in L_2(\mathbb{R}^d)$ and $\{w_j\}_{j\in\mathbb{Z}^d} \subset \mathbb{R}$ we define

$$S_\psi^h w(x) := h^{-\frac{d}{2}}\sum_{j\in\mathbb{Z}^d} w_j\psi\left(\frac{\cdot - x_j}{h}\right).$$

For our approximation considerations, we refer to the so-called Strang-Fix conditions introduced in [SF73] and broadly used in literature for example in [BJ85].

Theorem 6.7 ([SF73, Theorem 1]). *Let $\psi \in L_2(\mathbb{R}^d)$ be compactly supported. It is equivalent:*

(i) (Strang-Fix conditions) $\hat{\psi}(0) = 1$ and $\hat{\psi} = 0$ on $2\pi\mathbb{Z}^m \setminus \{0\}$

(ii) For each $u \in H^1(\mathbb{R}^d)$ there exists $\{w_j^h\}_{j\in\mathbb{Z}^d}$ such that

$$\|u - S_\psi^h w^h\|_{L_2(\mathbb{R}^d)} \le Ch\,\|u\|_{H^1(\mathbb{R}^d)} \qquad \text{and} \qquad \sum_{j\in\mathbb{Z}^d}|w_j^h|^2 \le c\|u\|^2_{L_2(\mathbb{R}^d)}$$

where $H^\nu(\mathbb{R}^d)$ denotes the Sobolev space of order ν associated to $L_2(\mathbb{R}^d)$,

$$H^\nu(\mathbb{R}^d) := \left\{f \in L_2(\mathbb{R}^d) :\ \|f\|_{H^\nu(\mathbb{R}^d)} := \left(\int_{\mathbb{R}^d}\left(1+\|\xi\|^2\right)^\nu |\hat{f}(\xi)|^2\, d\xi\right)^{\frac{1}{2}} < \infty\right\}.$$

For $\psi \in L_2(\mathbb{R}^d)$, the first part of the Strang-Fix condition (i) is obviously fulfilled by rescaling the basis function with the constant c_b defined as

$$c_b^{-1} := \hat{\psi}(0) = (2\pi)^{-\frac{d}{2}} \int_{\mathbb{R}^d} b(x)\, dx.$$

6.1.3.1 Strang-Fix condition for the Pixel/Voxel basis

The Strang-Fix conditions are trivially fulfilled for the Pixel/Voxel basis function $\square^d$ up to the scaling factor $c_\square^d := (2\pi)^{\frac{d}{2}}$. Following proposition 6.2, the Fourier transform of the Pixel basis function $\square^d$ is given as

$$\mathcal{F}\square^d(\xi) = (2\pi)^{-\frac{d}{2}} \prod_{i=1}^{d} \operatorname{sinc}\left(\frac{\xi_i}{2}\right).$$

with $\operatorname{sinc} x = \frac{\sin x}{x}$ for $x \in \mathbb{R}$. It holds:

(i)
$$\mathcal{F}\left(c_\square^d \square^d\right)(0) = c_\square^d \mathcal{F}\square^d(0) = 1,$$

(ii)
$$\mathcal{F}\square^d(2k\pi) = (2\pi)^{-\frac{d}{2}} \prod_{i=1}^{d} \operatorname{sinc}(k_i\pi) = 0 \qquad \forall k \in \mathbb{Z}^d.$$

6.1.3.2 Strang-Fix condition for the Lewitt-Blobs

For the Lewitt-Blob basis function $b_{m,a,\alpha}$ the situation looks different. We first recall that $b_{m,a,\alpha}$ is an $m-1$-times continuously differentiable function with compact support, see proposition 6.4, and thus obviously $b_{m,a,\alpha} \in L_2(\mathbb{R}^d)$. The diameter of its support is controlled via the parameter a while the shape of the Blob and thus its spectral behavior is controlled via the parameter α. While the parameters m and a are chosen according to the requirements of the application and the used algorithm, α remains a free parameter which has to be chosen with respect to m and a.

Optimizing the Blob parameters can already be found in [ML96]. The authors derive a criterion in the Fourier domain based on the partition-of-unity property to minimize $\hat{b}^d$ at 2π, i.e., for $k = 1$.

In [Nil+15, Theorem 2] a negative result is stated: The Strang-Fix conditions from theorem 6.7 cannot be fulfilled for compactly supported radially symmetric function. The authors showed this for the equivalent partition-of-unity condition and proposed a method to obtain optimal Blob parameters by mimimizing the ratio

$$\frac{\sum_{k\in\mathbb{Z}^d\setminus 0} \hat{b}^d_{m,a,\alpha}(2k\pi)}{\hat{b}^d_{m,a,\alpha}(0)}.$$

The following proposition characterizes the zeros of the Blob function in terms of the zeros of the Bessel function J.

Proposition 6.8. *The zeros of the radial part $\hat{b}^{d,R}_{m,a,\alpha}$ of the Fourier transform of the Blob basis function are given by*

$$\zeta_n = \frac{1}{a}\sqrt{\left(j_{\frac{d}{2}+m,n}\right)^2 + \alpha^2} \in \mathbb{R}_+ \qquad n \in \mathbb{N}_+$$

where $j_{\frac{d}{2}+m,n}$ denotes the n-th positive zero of the Bessel function $J_{\frac{d}{2}+m}$. All zeros ζ_n are simple.

Proof. According to proposition 6.5, the Fourier transform of $b_{m,a,\alpha}$ is given as

$$\hat{b}^d_{m,a,\alpha}(\xi) = \frac{a^d\alpha^m}{I_m(\alpha)}\left(\sqrt{a^2\|\xi\|^2 - \alpha^2}\right)^{-(\frac{d}{2}+m)} J_{\frac{d}{2}+m}\left(\sqrt{a^2\|\xi\|^2 - \alpha^2}\right).$$

Putting $\varphi(\sigma) \coloneqq \sqrt{(a\sigma)^2 - \alpha^2}$, the radial part is given as

$$\begin{aligned}\hat{b}^{d,R}_{m,a,\alpha}(\sigma) &= \frac{a^d\alpha^m}{I_m(\alpha)}\left(\sqrt{(a\sigma)^2 - \alpha^2}\right)^{-(\frac{d}{2}+m)} J_{\frac{d}{2}+m}\left(\sqrt{(a\sigma)^2 - \alpha^2}\right) \\ &= \frac{a^d\alpha^m}{I_m(\alpha)}\frac{J_{\frac{d}{2}+m}(\varphi(\sigma))}{\varphi(\sigma)^{\frac{d}{2}+m}}.\end{aligned}$$

From the theory of Bessel functions, cf. [Wat95; GR15], it is known that the non-zero zeros of the Bessel function J_ν are fully characterized by $j_{\frac{d}{2}+m,n}$, $n \in \mathbb{N}_+$. It follows immediately, that $\hat{b}^{d,R}_{m,a,\alpha}$ has infinitely many non-zero real zeros characterized by the zeros of the Bessel function as follows,

$$\varphi(\zeta_n) = \sqrt{(a\zeta_n)^2 - \alpha^2} = j_{\frac{d}{2}+m,n} \qquad \Leftrightarrow \qquad \zeta_n = \frac{1}{a}\sqrt{\left(j_{\frac{d}{2}+m,n}\right)^2 + \alpha^2}.$$

For $\nu > 0$, there may exist an additional non-simple zero exists at the origin ($\varphi(\sigma) = 0$). In the following we show for odd and even dimensions separately that there is no zero at the origin. For $\varphi(\sigma) \to 0$ we obtain for even dimensions d with L'Hospital's rule

$$\begin{aligned}\lim_{\varphi(\sigma)\to 0}\frac{J_{\frac{d}{2}+m}(\varphi(\sigma))}{\varphi(\sigma)^{\frac{d}{2}+m}} &= \lim_{\varphi(\sigma)\to 0}\frac{2^{-(\frac{d}{2}+m)}\sum_{l=0}^{\frac{d}{2}+m}(-1)^l\binom{k}{l}J_{2l}(\varphi(\sigma))}{(\frac{d}{2}+m)!} \\ &= \frac{1}{2^{(\frac{d}{2}+m)}(\frac{d}{2}+m)!}\lim_{\varphi(\sigma)\to 0}\sum_{l=0}^{\frac{d}{2}+m}(-1)^l\binom{k}{l}J_{2l}(\varphi(\sigma)) \\ &= \frac{1}{2^{(\frac{d}{2}+m)}(\frac{d}{2}+m)!}\lim_{\varphi(\sigma)\to 0}\left(J_0(\varphi(\sigma)) + \sum_{l=1}^{\frac{d}{2}+m}(-1)^l\binom{k}{l}J_{2l}(\varphi(\sigma))\right) \\ &= \frac{1}{2^{(\frac{d}{2}+m)}(\frac{d}{2}+m)!}.\end{aligned}$$

For d being odd we proceed analogously

$$\lim_{\varphi(\sigma)\to 0}\frac{J_{\frac{d}{2}+m}(\varphi(\sigma))}{\varphi(\sigma)^{\frac{d}{2}+m}} = \lim_{\varphi(\sigma)\to 0}\frac{2^{-(\frac{d-1}{2}+m)}\sum_{l=0}^{\frac{d-1}{2}+m}(-1)^l\binom{k}{l}J_{2l+\frac{1}{2}}(\varphi(\sigma))}{(\frac{d-1}{2}+m)!\sqrt{\varphi(\sigma)}}$$

$$= \frac{1}{2^{(\frac{d-1}{2}+m)}(\frac{d-1}{2}+m)!} \lim_{\varphi(\sigma)\to 0} \frac{\sum_{l=0}^{\frac{d-1}{2}+m}(-1)^l\binom{k}{l}J_{2l+\frac{1}{2}}(\varphi(\sigma))}{\sqrt{\varphi(\sigma)}}$$

$$= \frac{1}{2^{(\frac{d-1}{2}+m)}(\frac{d-1}{2}+m)!} \lim_{\varphi(\sigma)\to 0} \frac{J_{\frac{1}{2}}(\varphi(\sigma)) + \sum_{l=1}^{\frac{d-1}{2}+m}(-1)^l\binom{k}{l}J_{2l+\frac{1}{2}}(\varphi(\sigma))}{\sqrt{\varphi(\sigma)}}.$$

With

$$\Xi(\varphi(\sigma)) \coloneqq \sum_{l=1}^{\frac{d-1}{2}+m}(-1)^l\binom{k}{l}J_{2l+\frac{1}{2}}(\varphi(\sigma))$$

follows

$$\begin{aligned}
\lim_{\varphi(\sigma)\to 0} \frac{J_{\frac{d}{2}+m}(\varphi(\sigma))}{\varphi(\sigma)^{\frac{d}{2}+m}} &= \frac{1}{2^{(\frac{d-1}{2}+m)}(\frac{d-1}{2}+m)!} \lim_{\varphi(\sigma)\to 0} \frac{J_{\frac{1}{2}}(\varphi(\sigma)) + \Xi(\varphi(\sigma))}{\sqrt{\varphi(\sigma)}} \\
&= \frac{\sqrt{\pi}}{2^{(\frac{d}{2}+m)}(\frac{d-1}{2}+m)!} \lim_{\varphi(\sigma)\to 0} \frac{\varphi(\sigma)^{-\frac{1}{2}}\sin(\varphi(\sigma)) + \Xi(\varphi(\sigma))}{\sqrt{\varphi(\sigma)}} \\
&= \frac{\sqrt{\pi}}{2^{(\frac{d}{2}+m)}(\frac{d-1}{2}+m)!} \lim_{\varphi(\sigma)\to 0} \left(\frac{\sin(\varphi(\sigma))}{\varphi(\sigma)} + \frac{\Xi(\varphi(\sigma))}{\sqrt{\varphi(\sigma)}}\right) \\
&= \frac{\sqrt{\pi}}{2^{(\frac{d}{2}+m)}(\frac{d-1}{2}+m)!} \left(\operatorname{sinc}(0) + \lim_{\varphi(\sigma)\to 0} 2\sqrt{\varphi(\sigma)}\,\Xi'(\varphi(\sigma))\right)
\end{aligned}$$

where we again used L'Hospital's rule in the last step. Since $\Xi'(\varphi(\sigma)) \to 0$ for $\varphi(\sigma) \to 0$, we obtain

$$\lim_{\varphi(\sigma)\to 0} \frac{J_{\frac{d}{2}+m}(\varphi(\sigma))}{\varphi(\sigma)^{\frac{d}{2}+m}} = \frac{\sqrt{\pi}}{2^{(\frac{d}{2}+m)}(\frac{d-1}{2}+m)!}.$$

□

Due to preceding lemma, the zeros of the Fourier transform $\hat{b}^d_{m,a,\alpha}$ are fully characterized by the zeros of the Bessel functions of specific order. We obtain the following connection between $\hat{b}^d_{m,a,\alpha}(2\pi k)$ and its radial part $\hat{b}^{d,R}_{m,a,\alpha}(2\pi k)$,

$$\begin{aligned}
&\hat{b}^d_{m,a,\alpha}(2\pi k) = \hat{b}^d_{m,a,\alpha}\left(\sqrt{(2\pi a\|k\|)^2 - \alpha^2}\right) = 0 \quad \forall k \in \mathbb{Z}^d \setminus \{0\} \\
\Leftrightarrow \quad &\hat{b}^{d,R}_{m,a,\alpha}(2\pi k') = \hat{b}^{d,R}_{m,a,\alpha}\left(\sqrt{(2\pi a k')^2 - \alpha^2}\right) = 0 \quad \forall k' \in K' \coloneqq \left\{n \in \mathbb{N}_+ : n = \|k\|^2,\, k \in \mathbb{Z}^d\right\}.
\end{aligned}$$

Consequently the shaping parameter α should be chosen in such a way that

$$2\pi k' \in \{\zeta_n\}_n$$

is approximately fulfilled for all $k' \in K'$. Numerical experiments have shown that this condition can be approximately fulfilled in the sense that

$$\hat{b}^{d,R}_{m,a,\alpha}(2\pi k') \approx 0 \qquad \forall k' \in K' \tag{6.3}$$

for choosing of α as specified in [ML96] and [Nil+15].

6.2 Semi-discrete models for X-ray tomography

6.2.1 Parallel scanning geometry

The parallel scanning geometry in arbitrary dimensions is induced by the X-Ray transform. In the two-dimensional case, i.e., $d = 2$, the Radon transform coincides with the X-Ray transform up to parametrization. It holds,

$$\mathcal{R}f(\theta, s) = \mathcal{P}f(\theta^\perp, s\theta) \qquad \text{and} \qquad \mathcal{P}f(\theta, x) = \mathcal{R}f(\theta^\perp, x^\top\theta^\perp),$$

for $\theta \in \mathbb{S}^1$, $s \in \mathbb{R}$ and $x \in \theta^\perp$. To model the parallel scanning geometry, we will therefore consider the X-ray transform, i.e.,

$$\mathcal{A}_i := \mathcal{P}_{\theta_i} : L_2(\Omega) \to L_2(\theta_i^\perp, w_{\theta_i}),$$

with the weight functions

$$w^1_{\theta_i} \equiv 1 \qquad \text{and} \qquad w^2_{\theta_i}(x) = \left(\mathcal{P}_{\theta_i}\chi_\Omega(x)\right)^{-1} = \frac{1}{2\sqrt{1 - \|x\|^2}}, \quad \forall x \in \theta_i^\perp,$$

cf. section 3.2.

The locally supported basis functions discussed above will serve as the basis elements for our semi-discrete model, i.e., the voxel basis function $\square^d(x)$, cf. definition 6.1 and the Lewitt-Blob basis function, cf. definition 6.3. To compute their forward projection efficiently, we make use of the invariances of the X-ray transform: the forward projection of the basis function $b_j(x) = b(x - x_j)$ is computed by

$$\mathcal{P}_{\theta_i} b_j(x) = \mathcal{P}_{\theta_i} b(x - \mathrm{P}_{\theta_i{}^\perp} x_j),$$

cf. proposition 3.7. For the Pixel and Voxel basis function, $\mathcal{P}_{\theta_i} b$ has to be computed for each θ_i separately whereas the forward projection of the Lewitt-Blob basis is identical for each direction due to its rotational symmetry.

We briefly discuss a possible way to evaluate the projection $\mathcal{P}_{\theta_i} b_j$ for teh two- and three-dimensional case numerically.

(i) Let $d = 2$ and the scanning direction $\theta \in \mathbb{S}^1$ be parameterized by $\beta \in [0, 2\pi)$ as

$$\theta(\beta) = \begin{pmatrix} \cos\beta \\ \sin\beta \end{pmatrix}.$$

Thus, with $\theta^\perp = (-\sin\beta, \cos\beta)^\top$ being the orthogonal direction the X-ray transform of b_k is computed as

$$\mathcal{P}_\theta b_j(x) = \mathcal{P}_\theta b\big(x - \mathrm{P}_{\theta^\perp} x_j\big) = \mathcal{P}_\theta b\big(x - \big(x_j^\top \theta^\perp\big) \cdot \theta^\perp\big).$$

(ii) Let $d = 3$. We describe the direction $\theta \in \mathbb{S}^2$ in spherical coordinates

$$\theta(\beta, \gamma) = \begin{pmatrix} \cos\beta\sin\gamma \\ \sin\beta\sin\gamma \\ \cos\gamma \end{pmatrix},$$

with azimuthal angle $\beta \in [0, 2\pi)$ and polar angle $\gamma \in [0, \pi]$. The direction $\theta(\beta, \gamma)$ is expressed in terms of the unit vector $\mathrm{e}_1 = (1, 0, 0)^\top$ as

$$\theta(\beta, \gamma) = R^z_\beta R^y_{\gamma - \frac{\pi}{2}} \mathrm{e}_1,$$

where R^y and R^z are orthogonal matrices describing a rotation around the y-axis and z-axis, respectively. A positive oriented basis for

$$\theta^\perp = \{x \in \mathbb{R}^3 : x^\top \theta = 0\}$$

is thus given by rotating the unit vectors e_2 and e_3 yielding

$$\theta_1^\perp := R_\beta^z R^y_{\gamma-\frac{\pi}{2}} e_2 = \begin{pmatrix} -\sin\beta \\ \cos\beta \\ 0 \end{pmatrix}$$

and

$$\theta_2^\perp := R_\beta^z R^y_{\gamma-\frac{\pi}{2}} e_3 = \begin{pmatrix} -\cos\beta\cos\gamma \\ -\sin\beta\cos\gamma \\ \sin\gamma \end{pmatrix}.$$

We obtain

$$\mathcal{P}_\theta b_j(x) = \mathcal{P}_\theta b\big(x - \mathrm{P}_{\theta^\perp} x_j\big) = \mathcal{P}_\theta b\big(x - \big(x_j^\top \theta_1^\perp\big)\cdot\theta_1^\perp - \big(x_j^\top \theta_2^\perp\big)\cdot\theta_2^\perp\big).$$

for the three-dimensional X-ray transform of b_j.

Together with the locally supported basis B, we obtain the following semi-discrete model of the X-ray transform:

$$\boldsymbol{P}_k : \big(\mathbb{R}^{|J|}, \langle\cdot,\cdot\rangle_k\big) \to L_2(\theta_k^\perp, w_{\theta_k}), \qquad \boldsymbol{P}_k \boldsymbol{f} := \big(\mathcal{P}_{\theta_k} \mathcal{E}_{B,k}\big)\boldsymbol{f} = \sum_{j\in J} \boldsymbol{f}_j \mathcal{P}_{\theta_k} b_j, \tag{6.4}$$

where we fix the operator partition P of I to $I_P = I$, i.e., $A_k = \mathcal{P}_{\theta_k}$, for convenience. The weight matrices $\{W_k^p\}_k$ are defined as the diagonal matrices introduced in example 4.10,

$$\begin{aligned} \big(W_k^p\big)_{jj} &= \sum_{l\in J} \Big\langle \mathcal{P}_{\theta_k} b_j, \mathcal{P}_{\theta_k} b_l \Big\rangle_{L_2(\theta_k^\perp, w_{\theta_k}^p)} \\ &= \Big\langle \mathcal{P}_{\theta_k} b_j, \sum_{l\in J} \mathcal{P}_{\theta_k} b_l \Big\rangle_{L_2(\theta_k^\perp, w_{\theta_k}^p)} \qquad k \in I_P \end{aligned}$$

for $p = 1, 2$, such that we obtain

$$\|\boldsymbol{P}_k \boldsymbol{f}\|_{Y_k} = \|\boldsymbol{f}\|_k \quad \forall \boldsymbol{f} \in \mathrm{N}(\boldsymbol{P}_k)^\perp \qquad \text{and} \qquad \|\boldsymbol{P}\| = 1.$$

6.2.2 Cone Beam scanning geometry

The Cone Beam scanning geometry is induced by the Cone Beam transforms $\mathcal{D}$ and $\mathcal{X}$, see section 3.3. For the derivation of the semi-discrete model, we will focus on the flat detector Cone Beam transform. The semi-discrete model for the classical Cone Beam transform follows analogously. To compute the Cone Beam transform efficiently for the basis B, we exploit its relation to the X-ray transform.

For the two-dimensional case, we assume that the X-ray source position $a \in \mathbb{R}^2$ is given in polar coordinates as

$$a = r\cdot\theta(\beta), \qquad \theta(\beta) := \begin{pmatrix} \cos\beta \\ \sin\beta \end{pmatrix}$$

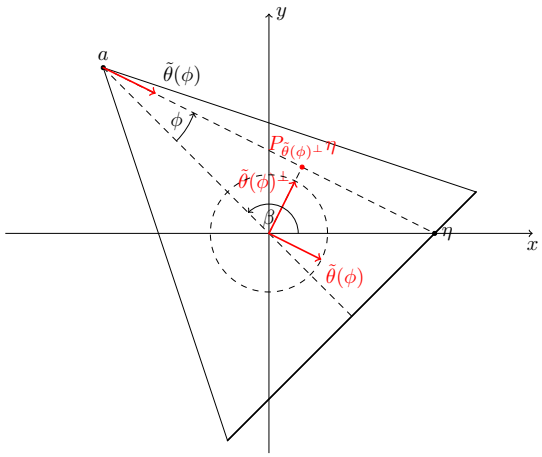

Figure 6.4: Relation between the X-ray transform and the flat detector Cone Beam transform in two dimensions

with $r > 1$ and $\beta \in [0, 2\pi)$. For the three-dimensional case we assume that the X-ray source position $a \in \mathbb{R}^3$ is given in spherical coordinates as

$$a = r \cdot \theta(\beta, \gamma), \qquad \theta(\beta, \gamma) := R_\beta^z R^y_{\gamma - \frac{\pi}{2}} \, e_1 = \begin{pmatrix} \cos\beta \sin\gamma \\ \sin\beta \sin\gamma \\ \cos\gamma \end{pmatrix}$$

for $r > 1$, $\beta \in [0, 2\pi)$ and $\gamma \in [0, \pi]$. We treat both cases separately:

(i) We follow [KS88] to derive a connection between the Cone Beam transform and the X-ray transform. For a given position $\eta \in \theta(\beta)^\perp$ on the detector, let $\phi \in (-\frac{\pi}{2}, \frac{\pi}{2})$ describe the angle between the central ray of the scanning system through the origin and the actually measured X-ray, see figure 6.4. The measured X-rays are thus described by

$$\{a + t\tilde{\theta}(\phi), t \geq 0\}, \qquad \phi \in \left(-\frac{\pi}{2}, \frac{\pi}{2}\right)$$

with $\tilde{\theta}(\phi) := \theta(\beta + \pi + \phi)$ depending on the X-ray source position. The angle ϕ is computed as

$$\phi = -\arctan\left(\frac{\eta^\top \theta(\beta)^\perp}{\|a\| + |\eta^\top \theta(\beta)|}\right)$$

and we obtain

$$\begin{aligned} \mathcal{X}b_j(a, \eta) &= \mathcal{P}b_j\big(\tilde{\theta}(\phi), \mathrm{P}_{\tilde{\theta}(\phi)^\perp} a\big) \\ &= \mathcal{P}b\big(\tilde{\theta}(\phi), \mathrm{P}_{\tilde{\theta}(\phi)^\perp}(a - x_j)\big). \end{aligned} \tag{6.5}$$

(ii) Three-dimensional case ($d = 3$): We compute the angles $\phi, \vartheta \in \left[-\frac{\pi}{2}, \frac{\pi}{2}\right]$ for a given position $\eta \in E_a$. For a given position $\eta \in \theta(\beta)^\perp$ on the detector, let the angles $\phi, \vartheta \in \left[-\frac{\pi}{2}, \frac{\pi}{2}\right]$ denote

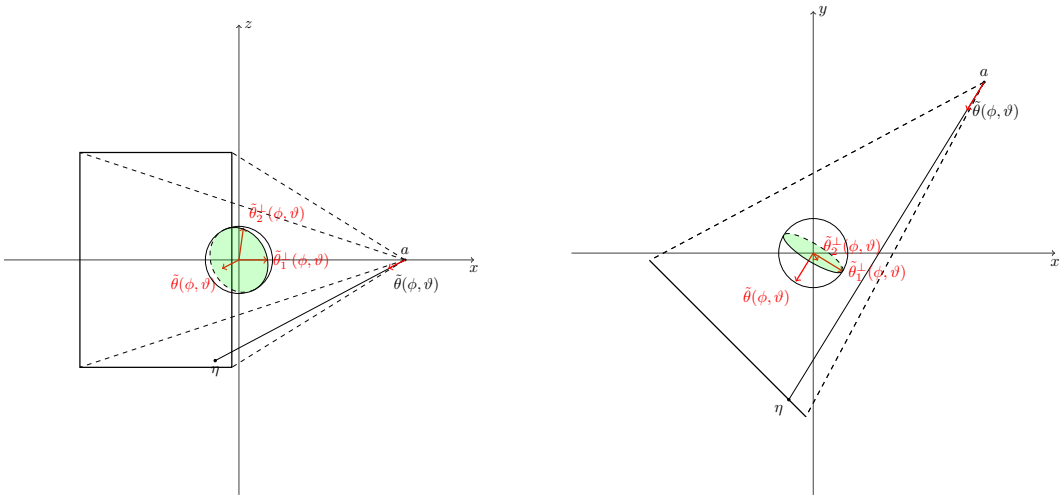

(a) x-z-plane (b) x-y-plane

Figure 6.5: Relation between the X-ray transform and the flat detector Cone Beam transform in two dimensions

the angle in the (tilted) x-y-plane and the angle in the (rotated) x-z-plane, respectively. The X-rays are thus parameterized as

$$a + t\tilde{\theta}(\phi, \vartheta)$$

where

$$\tilde{\theta}(\phi, \vartheta) \coloneqq \theta(\beta + \pi + \phi, \gamma + \pi + \vartheta) = R^z_{\beta+\pi+\phi} R^y_{\gamma+\frac{\pi}{2}+\vartheta} \, \mathrm{e}_1 \, .$$

Analogously to the two-dimensional case, we compute the angles $\phi, \vartheta \in \left[-\frac{\pi}{2}, \frac{\pi}{2}\right]$ describing the direction of the X-ray through the detector position $\eta \in E_a$. With the directions $\theta_1^\perp(\beta, \gamma)$ and $\theta_2^\perp(\beta, \gamma)$ defined as

$$\theta_1^\perp(\beta, \gamma) = R^z_\beta R^y_{\gamma-\frac{\pi}{2}} \, \mathrm{e}_2 = \theta\big(\beta + \frac{\pi}{2}, \frac{\pi}{2}\big)$$

and

$$\theta_2^\perp(\beta, \gamma) = R^z_\beta R^y_{\gamma-\frac{\pi}{2}} \, \mathrm{e}_3 = \theta\big(\beta, \gamma - \frac{\pi}{2}\big),$$

see figure 6.5, we obtain

$$\tan\phi = -\frac{\eta^\top \theta_1^\perp(\beta, \gamma)}{\|a\| + |\eta^\top \theta(\beta)|} \qquad \text{and} \qquad \tan\vartheta = -\frac{\eta^\top \theta_2^\perp(\beta, \gamma)}{\|a\| + |\eta^\top \theta(\beta)|}.$$

Thus,

$$\mathcal{X}b_j\big(a, \eta\big) = \mathcal{P}b\big(\tilde{\theta}(\phi, \vartheta), \mathrm{P}_{\tilde{\theta}^\perp(\phi,\vartheta)}\big(a - x_j\big)\big)$$

with $\phi = -\arctan\Big(\frac{\eta^\top \theta_1^\perp(\beta,\gamma)}{\|a\|+|\eta^\top \theta(\beta)|}\Big)$ and $\vartheta = -\arctan\Big(\frac{\eta^\top \theta_2^\perp(\beta,\gamma)}{\|a\|+|\eta^\top \theta(\beta)|}\Big)$.

The semi-discrete model of the Cone Beam transform follows analogously to the parallel scanning situation. Together with the locally supported basis B, we obtain the following semi-discrete model of the Cone Beam transform:

$$\boldsymbol{X}_k : \Big(\mathbb{R}^{|J|}, \langle\cdot,\cdot\rangle_k\Big) \to L_2(\tilde{E}_{a_k}, w_{a_k}), \qquad \boldsymbol{X}_k \boldsymbol{f} \coloneqq \Big(\mathcal{X}_{a_k} \mathcal{E}_{B,k}\Big)\boldsymbol{f} = \sum_{j\in J} \boldsymbol{f}_j \mathcal{X}_{a_k} b_j. \tag{6.6}$$

Again, the operator partition P of I is fixed to $I_P = I$, i.e., $A_k = \mathcal{X}_{a_k}$, for convenience. The weight matrices $\{W_k^p\}_k$ are defined as the diagonal matrices introduced in example 4.10,

$$\left(W_k^p\right)_{jj} = \sum_{l\in J} \left\langle \mathcal{X}_{a_k} b_j, \mathcal{X}_{a_k} b_l \right\rangle_{L_2(\theta_k^\perp, w_{\theta_k}^p)} = \left\langle \mathcal{X}_{a_k} b_j, \sum_{l\in J} \mathcal{X}_{a_k} b_l \right\rangle_{L_2(\theta_k^\perp, w_{\theta_k}^p)} \qquad p = 1, 2$$

for all $k \in I_P$, such that we obtain

$$\|\boldsymbol{X}_k \boldsymbol{f}\|_{Y_k} = \|\boldsymbol{f}\|_k \quad \forall \boldsymbol{f} \in \mathrm{N}(\boldsymbol{X}_k)^\perp \qquad \text{and} \qquad \|\boldsymbol{X}\| = 1.$$

6.2.3 Incorporation of prior knowledge

Many applications in X-ray tomography suffer from restricted and limited data due to physical limitations of the scanning system or unsuitable dimensions of the inspected objects. This may be the case if high magnification ratios are desired or for large objects or objects with different diameters in longitudinal and transversal direction.

If prior information on the inspected object is available, this information can be included in the reconstruction process. We present two approaches, published in [VS16] and [VS17].

6.2.3.1 Geometrical a *priori* information

We consider that additional geometric information on the outer contour of the object is given. This could be the case if a second imaging modality is used or knowledge of the nominal geometry of the contours, e.g. from a CAD model, is available.

To use this additional information, we assume in the following that the outer contours of the inspected object are known. Let $f \in L_2(\Omega)$ denote the searched-for density function of the inspected object and let the outer support $\Omega_f \subseteq \Omega$ be given as

$$\int_{\Omega\setminus\Omega_f} |f(x)| = 0.$$

We define the subset of indices $J_0 \subseteq J$ as

$$J_0 := \left\{ j : \operatorname{supp} b_j \cap \Omega_f \neq \emptyset \right\} \tag{6.7}$$

and $B_0 := \{b_j\}_{j\in J_0} \subseteq B$. Hence, all basis functions $b_j \in B \setminus B_0$ have no contribution to the basis representation of the best-approximation $\bar{f} = \arg\min_{\varphi\in\mathcal{X}_B} \|\varphi - f\|$ of f. Therefore we restrict the semi-discrete model to the basis B_0 obtaining

$$\boldsymbol{A}_{B_0,k} : \left(\mathbb{R}^{|J_0|}, \langle\cdot,\cdot\rangle_k\right) \to Y_k, \qquad \boldsymbol{A}_{B_0,k}\boldsymbol{f} := \left(A_k \mathcal{E}_{B_0,k}\right)\boldsymbol{f} = \sum_{j\in J_0} \boldsymbol{f}_j A_k b_j.$$

Together with the semi-discrete iteration schemes, we obtain the reconstruction methods adapted to the prior geometrical knowledge.

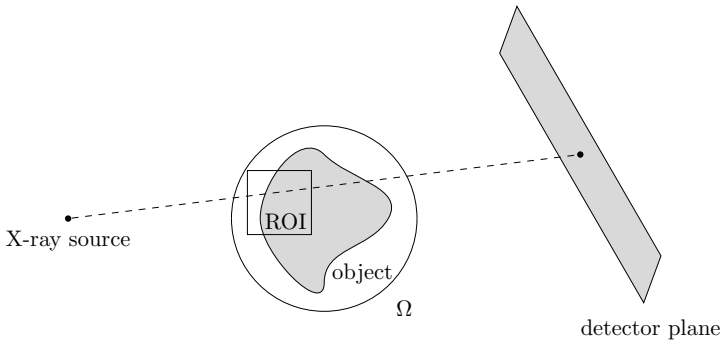

Figure 6.6: Schematic representation of a region-of-interest setup in X-ray tomography.

6.2.3.2 Prior information in region-of-interest reconstruction

The second scenario that we consider is additional knowledge of the involved material properties for region-of-interest (ROI) reconstruction, see figure 6.6. More specifically, we assume that the attenuation inside the object underlies only small changes. This could for example be the case for workpieces made of fiber-reinforced plastic where one is rather interested in the fiber structure or also objects of homogeneous material composition where one is interested in the detection of defects like porosity or cracks. With this assumption, the attenuation inside the inspected object can be modeled to be approximately constant such that the data at any detector position depends only on the way of the X-rays through the object.

Again, let J_0 denote the index set defined in (6.7) and let $J_R \subseteq J_0$ denote the subset of ROI indices. Further, let $\bar{f}$ denote the minimum-norm solution

$$\boldsymbol{A}\bar{f} = \mathrm{P}_{\mathrm{R}(\boldsymbol{A})} g.$$

With the assumption on the data follows

$$\begin{aligned} g &= \mathrm{P}_{\mathrm{R}(\boldsymbol{A})} g + \mathrm{P}_{\mathrm{N}(\boldsymbol{A}^*)} g \\ &= \boldsymbol{A}\bar{f} + \mathrm{P}_{\mathrm{N}(\boldsymbol{A}^*)} g \\ &= \sum_{j \in J_R} \bar{f}_j A b_j + \sum_{j \in J_0 \setminus J_R} \bar{f}_j A b_j + \mathrm{P}_{\mathrm{N}(\boldsymbol{A}^*)} g \end{aligned}$$

and hence

$$\sum_{j \in J_R} \bar{f}_j A b_j = g - \mathrm{P}_{\mathrm{N}(\boldsymbol{A}^*)} g - \sum_{j \in J_0 \setminus J_R} \bar{f}_j A b_j = \mathrm{P}_{\mathrm{R}(\boldsymbol{A})} g - \sum_{j \in J_0 \setminus J_R} \bar{f}_j A b_j.$$

The arising semi-discrete reconstruction problem now reads

$$\boldsymbol{A}^R \boldsymbol{f} = g^R$$

where $\boldsymbol{A}^R$ and g^R are defined as

$$\boldsymbol{A}^R \boldsymbol{f} = \sum_{j \in J_R} f_j A b_j \qquad \text{and} \qquad g^R = \mathrm{P}_{\mathrm{R}(\boldsymbol{A})} g - \sum_{j \in J_0 \setminus J_R} \bar{f}_j A b_j.$$

6.3 Semi-discrete iteration methods in X-ray tomography

In this section, we describe the application of the semi-discrete iteration methods in X-ray tomography, in particular for the parallel scanning geometry and the flat detector Cone Beam geometry treated in the preceding section. The problem at hand is finding a solution of

$$\mathcal{A}f = g \qquad g \in \mathcal{Y}$$

The operator $\mathcal{A}$ is given as

$$\mathcal{A} = \begin{pmatrix} \mathcal{A}_1 \\ \vdots \\ \mathcal{A}_{|I|} \end{pmatrix}$$

where $\mathcal{A}_i$ is either given by the X-ray transform $\mathcal{P}_{\theta_i}$ for a fixed scanning direction θ_i or by the flat detector Cone Beam transform $\mathcal{X}_{a_i}$ for a fixed X-ray source position a_i, respectively.

Let B denote a locally supported basis. We consider the semi-discrete model of the parallel geometry described in equation (6.4),

$$\boldsymbol{P}_k : (\mathbb{R}^{|J|}, \langle\cdot,\cdot\rangle_k) \to L_2(\theta_k^\perp, w_{\theta_k}^p), \qquad \boldsymbol{P}_k \boldsymbol{f} = \sum_{j\in J} \boldsymbol{f}_j \mathcal{P}_{\theta_k} b_j, \qquad k \in I_P$$

and the semi-discrete model of the flat detector Cone Beam scanning geometry described in equation (6.6),

$$\boldsymbol{X}_k : (\mathbb{R}^{|J|}, \langle\cdot,\cdot\rangle_k) \to L_2(\tilde{E}_{a_k}, w_{a_k}), \qquad \boldsymbol{X}_k \boldsymbol{f} \coloneqq (\mathcal{X}_{a_k} \mathcal{E}_{B,k}) \boldsymbol{f} = \sum_{j\in J} \boldsymbol{f}_j \mathcal{X}_{a_k} b_j, \qquad k \in I_P.$$

6.3.1 The semi-discrete Landweber-Kaczmarz method

The semi-discrete Landweber-Kaczmarz method is obtained in terms of the X-Ray transform and the flat detector Cone Beam transform by applying the backward operator $\Psi_k = \lambda_k \boldsymbol{A}_k^\sharp$ to the residual $g_k - \boldsymbol{A}_k \boldsymbol{f}^{m,k}$. The operator $\boldsymbol{A}_k$ denotes the semi-discrete parallel model operator $\boldsymbol{P}_k$ or the semi-discrete flat detector Cone Beam operator $\boldsymbol{X}_k$, respectively. It yields componentwise

$$\begin{aligned} \left(\lambda_k \boldsymbol{A}_k^\sharp (g_k - \boldsymbol{A}_k \boldsymbol{f}^{m,k})\right)_j &= \lambda_k \frac{\left\langle \mathcal{A}_k b_j, g_k - \boldsymbol{A}_k \boldsymbol{f}^{m,k} \right\rangle_{\mathcal{Y}_k}}{\left\langle \mathcal{A}_k b_j, \sum_{l\in J} \mathcal{A}_k b_l \right\rangle_{\mathcal{Y}_k}} \\ &= \frac{\lambda_k}{\left\langle \mathcal{A}_k b_j, \sum_{l\in J} \mathcal{A}_k b_l \right\rangle_{\mathcal{Y}_k}} \left\langle \mathcal{A}_k b_j,\ g_k - \sum_{j\in J} \boldsymbol{f}_j \mathcal{A}_k b_j \right\rangle_{\mathcal{Y}_k} \qquad \text{for } j \in J. \end{aligned}$$

Corollary 6.9. *The iteration steps of the semi-discrete Landweber-Kaczmarz method are given as follows.*

(i) For $g \in \bigoplus_{i\in I} L_2(\theta_i^\perp, w_{\theta_i}^p)$, the iteration step for solving the reconstruction problem

$$\mathcal{P}_{\theta_i} f = g_i \qquad i \in I$$

is given componentwise for all $j \in J$ by

$$f_j^{m,k+1} = f_j^{m,k} + \frac{\lambda_k}{\left\langle \mathcal{P}_{\theta_k} b_j,\ \sum_{l\in J} \mathcal{P}_{\theta_k} b_l \right\rangle_{L_2(\theta_k^\perp, w_{\theta_k}^p)}} \left\langle \mathcal{P}_{\theta_k} b_j,\ g_k - \sum_{j\in J} f_j^{m,k} \mathcal{P}_{\theta_k} b_j \right\rangle_{L_2(\theta_k^\perp, w_{\theta_k}^p)}.$$

(ii) For $g \in \bigoplus_{i\in I} L_2(\tilde{E}_{a_k}, w_{a_k})$, the iteration step for solving the reconstruction problem

$$\mathcal{X}_{a_i} f = g_i \qquad i \in I$$

is given componentwise for all $j \in J$ by

$$f_j^{m,k+1} = f_j^{m,k} + \frac{\lambda_k}{\left\langle \mathcal{X}_{a_k} b_j,\ \sum_{l\in J} \mathcal{X}_{a_k} b_l \right\rangle_{L_2(\tilde{E}_{a_k}, w_{a_k})}} \left\langle \mathcal{X}_{a_k} b_j,\ g_k - \sum_{j\in J} f_j^{m,k} \mathcal{X}_{a_k} b_j \right\rangle_{L_2(\tilde{E}_{a_k}, w_{a_k})}.$$

The convergence of the semi-discrete Landweber-Kaczmarz method was settled in section 5.2 by proposition 5.11 and theorem 5.12. Since the weight matrices $\{W_k^p\}_k$ are definied analogously to example 4.10 it follows $\|A_k\| = 1$. With the notation of proposition 5.11 follows $\beta_k = 1$ and thus

$$\tau_k = \beta_k \|A_k\|_k = 1.$$

Corollary 6.10. *Let $I_P^* \neq \emptyset$ and $C_k \in (0,1]$ such that $\prod_{k\in I_P} \sqrt{\kappa(W_k^p)} \prod_{k\in I_P^*} C_k \leq 1$ and let the relaxation parameters λ_k be defined as*

$$\lambda_k \in (1 - C_k, 1 + C_k) \quad k \in I_P^* \qquad \text{and} \qquad \lambda_k \in (0,2) \quad k \in I_P \setminus I_P^*.$$

The semi-discrete Landweber-Kacmzmarz method converges linearly with $\prod_{k\in I_P} \sqrt{\kappa(W_k^p)} \prod_{k\in I_P^*} C_k \leq 1$ being an upper bound for the convergence rate.

Proof. The result follows immediately with

$$\frac{1 \pm \left((C_k^2 - 1)\tau_k^4 + 1 \right)^{\frac{1}{2}}}{\tau_k^2 \|A_k\|_k^2} = 1 \pm C_k$$

from proposition 5.11 and theorem 5.12. □

The feasible relaxation parameters do still depend on the condition number $\kappa(W_k^p)$ of the weight matrices W_k^p, $p = 1, 2$. For the parallel scanning geometry, we obtain:

(i) $p = 1$, i.e., $w_{\theta_k} = w_{\theta_k}^1 = 1$:

$$\begin{aligned} (W_k^1)_{jj} &= \sum_{l\in J} \left\langle \mathcal{P}_{\theta_k} b_j, \mathcal{P}_{\theta_k} b_l \right\rangle_{L_2(\theta_k^\perp, w_{\theta_k}^1)} \\ &= \int_{\theta_k{}^\perp} \mathcal{P}_{\theta_k} b_j(x) \left(\sum_{l\in J} \mathcal{P}_{\theta_k} b_l(x) \right) dx \end{aligned}$$

$$= \int_{\theta_k^\perp} \mathcal{P}_{\theta_k} b(x - \mathrm{P}_{\theta_k^\perp} x_j) \left(\sum_{l \in J} \mathcal{P}_{\theta_k} b_l(x) \right) dx$$
$$= \left(\mathcal{P}_{\theta_k} b *_{d-1} \sum_{l \in J} \mathcal{P}_{\theta_k} b_l \right) (\mathrm{P}_{\theta_k^\perp}(x_j)). \tag{6.8}$$

The weight matrices depend heavily on the chosen basis B and the scanning direction θ_k. The condition number $\kappa(W_k^1)$ and thus the interval of feasible relaxation parameters differs for every scanning direction θ_k. The representation (6.8) may be used to precompute the weight matrices.

(ii) $p = 2$, i.e., $w_{\theta_k} = w_{2,\theta_k}(x) = \left(\mathcal{P}_{\theta_k} \chi_\Omega(x)\right)^{-1}$. With proposition 3.10,

$$\begin{aligned}(W_k^2)_{jj} &= \sum_{l \in J} \left\langle \mathcal{P}_{\theta_k} b_j, \mathcal{P}_{\theta_k} b_l \right\rangle_{L_2(\theta_k^\perp, w_{\theta_k}^2)} \\ &= \sum_{l \in J} \left\langle b_j, b_l \right\rangle_{L_2(\Omega)}.\end{aligned}$$

The weight matrices W_k^2 can thus be computed by the forward projection $\mathcal{P}_{\theta_k} \chi_\Omega(x)$ and is fully independent of the scanning direction θ_k.

For the Pixel and Voxel basis follows immediately

$$W_k^2 = \mathrm{id} \qquad \forall k \in I_P$$

since the basis generated by the Voxel basis function $\square^d(x)$ is orthonormal. We obtain for the condition number

$$\kappa(W_k^2) = 1$$

using the Voxel basis. For the Blob basis, this holds clearly not true. Although the Strang-Fix conditions 6.7 and thus the partition-of-unity property is only approximately fulfilled, it holds

$$\frac{1}{\mu(b)} \sum_{l \in J} b_l(x) \approx 1$$

where $\mu_\Omega(b) = \int_\Omega b(x)\, dx$ denotes the mean value of b. We obtain

$$\begin{aligned}\sum_{l \in J} \left\langle b_j, b_l \right\rangle_{L_2(\Omega)} &= \int_\Omega b_j(x) \sum_{l \in J} b_l(x)\, dx \\ &\approx \mu_\Omega(b) \int_\Omega b_j(x)\, dx \\ &= \mu_\Omega(b)\, \mu_\Omega(b_j).\end{aligned}$$

Hence, the condition number of W_k^2 for the Blob basis can be approximated by

$$\kappa(W_k^2) \approx \frac{\max_{j \in J} \mu_\Omega(b_j)}{\min_{j \in J} \mu_\Omega(b_j)} = \frac{\mu_\Omega(b)}{\min_{j \in J} \mu_\Omega(b_j)}.$$

6.3.2 The semi-discrete Kaczmarz method

Let $\{e_j\}_{j\in J}$ denote the canonical of $\mathbb{R}^{|J|}$ basis with $\psi_{k,j} \in \mathrm{N}(\boldsymbol{A}_k^\sharp)^\perp$ being its associated reconstruction kernels for all $j \in J$, cf. definition 5.17. Following corollary 5.20, we obtain

$$\begin{aligned}\big(\lambda_k \boldsymbol{A}_k^+ \big(g_k - \boldsymbol{A}_k \boldsymbol{f}^{m,k}\big)\big)_j &= \lambda_k \big\langle \psi_{k,j}, g_k - \boldsymbol{A}_k \boldsymbol{f}^{m,k} \big\rangle_{L_2(\theta_k^\perp, w_{\theta_k}^p)} \\ &= \lambda_k \Big\langle \psi_{k,j},\, g_k - \sum_{j\in J} \boldsymbol{f}_j \mathcal{P}_{\theta_k} b_j \Big\rangle_{L_2(\theta_k^\perp, w_{\theta_k}^p)} \qquad \forall j \in J\end{aligned}$$

for applying the backward operator to the residual.

Corollary 6.11. *The iteration steps of the semi-discrete Kaczmarz method are given as follows.*

(i) For $g \in \bigoplus_{i\in I} L_2(\theta_i^\perp, w_{\theta_i}^p)$, the iteration step for solving the reconstruction problem

$$\mathcal{P}_{\theta_i} f = g_i \qquad i \in I$$

is given componentwise for all $j \in J$ by

$$\boldsymbol{f}_j^{m,k+1} = \boldsymbol{f}_j^{m,k} + \lambda_k \Big\langle \psi_{k,j},\, g_k - \sum_{j\in J} \boldsymbol{f}_j^{m,k} \mathcal{P}_{\theta_k} b_j \Big\rangle_{L_2(\theta_k^\perp, w_{\theta_k}^p)}.$$

(ii) For $g \in \bigoplus_{i\in I} L_2(\tilde{E}_{a_k}, w_{a_k})$, the iteration step for solving the reconstruction problem

$$\mathcal{X}_{a_i} f = g_i \qquad i \in I$$

is given componentwise for all $j \in J$ by

$$\boldsymbol{f}_j^{m,k+1} = \boldsymbol{f}_j^{m,k} + \lambda_k \Big\langle \psi_{k,j},\, g_k - \sum_{j\in J} \boldsymbol{f}_j^{m,k} \mathcal{X}_{a_k} b_j \Big\rangle_{L_2(\tilde{E}_{a_k}, w_{a_k})}.$$

For $I_P^* \neq \emptyset$, the convergence follows of the semi-discrete Kaczmarz method follows immediately from theorem 5.15 for the relaxation parameters $\{\lambda_k\}_{k\in I_P}$ with

$$\prod_{k\in I_P^*} |1-\lambda_k| \prod_{k\in I_P \setminus I_P^*} \max\{1, |1-\lambda_k|\} < 1.$$

To compute suitable reconstruction kernels for the canonical basis $\{e_j\}_{j\in J}$ of $\mathbb{R}^{|J|}$, we solve the normal equation

$$\boldsymbol{A}_k \boldsymbol{A}_k^\sharp \psi_{k,j} = \boldsymbol{A}_k e_j,$$

cf. definition 5.17. This is equivalent to solving

$$\begin{pmatrix} \langle \mathcal{A}_k b_1, \psi_1^k \rangle_{\mathcal{Y}_k} & \cdots & \langle \mathcal{A}_k b_1, \psi_M^k \rangle_{\mathcal{Y}_k} \\ \vdots & & \vdots \\ \langle \mathcal{A}_k b_M, \psi_1^k \rangle_{\mathcal{Y}_k} & \cdots & \langle \mathcal{A}_k b_M, \psi_M^k \rangle_{\mathcal{Y}_k} \end{pmatrix} \begin{pmatrix} \mathcal{A}_k b_1 \\ \vdots \\ \mathcal{A}_k b_M \end{pmatrix} = \begin{pmatrix} \mathcal{A}_k b_1 \\ \vdots \\ \mathcal{A}_k b_M \end{pmatrix} \qquad \forall k \in I_P.$$

The reconstruction kernels solve the normal equation if the matrix on the left-hand side coincides with the identity matrix id,

$$\begin{pmatrix} \langle \mathcal{A}_k b_1, \psi_1^k \rangle_{\mathcal{Y}_k} & \cdots & \langle \mathcal{A}_k b_1, \psi_M^k \rangle_{\mathcal{Y}_k} \\ \vdots & & \vdots \\ \langle \mathcal{A}_k b_M, \psi_1^k \rangle_{\mathcal{Y}_k} & \cdots & \langle \mathcal{A}_k b_M, \psi_M^k \rangle_{\mathcal{Y}_k} \end{pmatrix} = \mathrm{id} \qquad \forall k \in I_P.$$

In other words, the reconstruction kernels have to fulfill

$$\langle \mathcal{A}_k b_j, \psi_l^k \rangle_{\mathcal{Y}_k} = \delta_{jl} \qquad j, l \in J \tag{6.9}$$

where δ_{jl} denotes the Kronecker delta. Without further assumptions on the basis functions, such as orthogonality, or on the reconstruction kernels this system is not solvable.

For the X-Ray transform, we give a heuristic approach. Let the reconstruction kernels $\psi_j^k(x)$ be defined as shifted versions of the standard reconstruction kernel ψ as

$$\psi_j^k(x) := \psi(x - \mathrm{P}_{\theta_k{}^\perp} x_j).$$

We obtain

$$\begin{aligned} \left\langle \mathcal{P}_{\theta_k} b_j, \psi_l^k \right\rangle_{L_2(\theta_k^\perp, w_{\theta_k}^p)} &= \int_{\theta_k{}^\perp} \mathcal{P}_{\theta_k} b_j(x) \psi\big(x - \mathrm{P}_{\theta_k{}^\perp} x_j\big)\, w_{\theta_k}^p(x)\, dx \\ &= \int_{\theta_k{}^\perp} \mathcal{P}_{\theta_k} b(x) \psi\big(x - \mathrm{P}_{\theta_k{}^\perp}(x_j - x_l)\big)\, w_{\theta_k}^p(x)\, dx. \end{aligned}$$

We propose the following choices for the use as reconstruction kernels.

(i) The Dirac delta distribution:

$$\psi_l^k(x) := \delta(x - \mathrm{P}_{\theta_k{}^\perp} x_l) \qquad x \in \theta_k^\perp.$$

We obtain

$$\begin{aligned} \left\langle \mathcal{P}_{\theta_k} b_j, \psi_l^k \right\rangle_{L_2(\theta_k^\perp, w_{\theta_k})} &= \int_{\theta_k{}^\perp} \mathcal{P}_{\theta_k} b_j(x)\, \delta(x - \mathrm{P}_{\theta_k{}^\perp} x_l)\, w_{\theta_k}(x)\, dx \\ &= (w_{\theta_k} \cdot \mathcal{P}_{\theta_k} b_j)(\mathrm{P}_{\theta_k{}^\perp} x_l), \end{aligned}$$

providing a rough approximation to (6.9). The inner product with ψ_l^k then reduces to a point evaluation,

$$\begin{aligned} \left\langle \mathcal{P}_{\theta_k} b_j, \tilde{\psi}_l^k \right\rangle_{L_2(\theta_k^\perp, w_{\theta_k})} &= \int_{\theta_k{}^\perp} \mathcal{P}_{\theta_k} b_j(x)\, \delta(x - \mathrm{P}_{\theta_k{}^\perp} x_l)\, w_{\theta_k}(x)\, dx \\ &= (w_{\theta_k} \cdot \mathcal{P}_{\theta_k} b_j)(\mathrm{P}_{\theta_k{}^\perp} x_l). \end{aligned}$$

(ii) The forward projection of the basis functions,

$$\psi_l^k(x) := \mathcal{P}_{\theta_k} b_l(x) \qquad x \in \theta_k^\perp.$$

Then,

$$\left\langle \mathcal{P}_{\theta_k} b_j, \psi_l^k \right\rangle_{L_2(\theta_k^\perp, w_{\theta_k})} = \left\langle \mathcal{P}_{\theta_k} b_j, \mathcal{P}_{\theta_k} b_l \right\rangle_{L_2(\theta_k^\perp, w_{\theta_k})}$$

$$= \int_{\theta_k^\perp} \mathcal{P}_{\theta_k} b_j(x) \mathcal{P}_{\theta_k} b_l(x)\, w_{\theta_k}(x)\, dx.$$

Using this reconstruction kernel the backward operator coincides with the semi-discrete Landweber-Kaczmarz method for unweighted semi-discrete model operators.

6.3.3 Simultaneous Algebraic Reconstruction Technique (SART)

As a representative of classical iterative algebraic reconstruction methods in X-ray tomography we discuss the widely-used and well-known SART, cf. [AK84]. This method is known to provide suitable reconstruction results for non-regular geometries as for example used in Computed Laminography applications or limited data applications [VS16; VS17; Tra+17]. Although being studied in literature with respect to convergence properties, the SART is usually considered as the fully-discrete iteration scheme

$$\boldsymbol{f}_j^{m,k+1} = \boldsymbol{f}_j^{m,k} + \lambda_k \left(\sum_n a_{nj}^k \right)^{-1} \sum_n \frac{a_{nj}^k \left(g_k(\eta_n) - \sum_{j \in J} \boldsymbol{f}_j^{m,k} a_{nj}^k \right)}{\sum_{j \in J} a_{nj}^k}, \qquad j \in J \tag{6.10}$$

with $a_{nj}^k := \mathcal{A}_k b_j(\eta_n)$ and η_n being the data points on the detector [AK84], [JW03] and [CE02]. For a more detailed discussion on the SART and its relation to the semi-discrete iteration methods, we refer to [VS16; VS17].

In the following, we will derive the SART as a discretization of the semi-discrete Landweber-Kaczmarz method using the trapezoidal rule on the detector for evaluating of the inner products. For the parallel geometry we consider the semi-discrete operator model

$$\boldsymbol{P}_k : (\mathbb{R}^{|J|}, \langle \cdot, \cdot \rangle_k) \to L_2(\theta_k^\perp, w_{\theta_k}), \qquad w_{\theta_k}(x) := \left(\sum_{j \in J} \mathcal{P}_{\theta_k} b_j(x) \right)^{-1},$$

see (6.4). For the iteration step follows

$$\begin{aligned} \boldsymbol{f}_j^{m,k+1} &= \boldsymbol{f}_j^{m,k} + \frac{\lambda_k}{\left\langle \mathcal{P}_{\theta_k} b_j,\, 1 \right\rangle_{L_2(\theta_k^\perp)}} \left\langle \mathcal{P}_{\theta_k} b_j,\, \frac{g_k - \sum_{j \in J} \boldsymbol{f}_j \mathcal{P}_{\theta_k} b_j}{\sum_{j \in J} \mathcal{P}_{\theta_k} b_j} \right\rangle_{L_2(\theta_k^\perp)} \\ &= \boldsymbol{f}_j^{m,k} + \lambda_k \left(\int_{\theta_k^\perp} \mathcal{P}_{\theta_k} b_j(x)\, dx \right)^{-1} \int_{\theta_k^\perp} \mathcal{P}_{\theta_k} b_j(x) \frac{g_k(\eta) - \sum_{j \in J} \boldsymbol{f}_j \mathcal{P}_{\theta_k} b_j(\eta)}{\sum_{j \in J} \mathcal{P}_{\theta_k} b_j(x)}\, dx. \end{aligned}$$

Applying the trapezoidal rule yields

$$\boldsymbol{f}_j^{m,k+1} \approx \boldsymbol{f}_j^{m,k} + \lambda_k \left(\sum_n \rho_n a_{nj}^k \right)^{-1} \sum_n \rho_n \frac{a_{nj}^k (g_k(\eta_n) - \sum_{j \in J} \boldsymbol{f}_j^{m,k} a_{nj}^k)}{\sum_{j \in J} a_{nj}^k} \tag{6.11}$$

with $a_{nj}^k := \mathcal{P}_{\theta_k} b_j(x_n)$ and the weights ρ_n of the trapezoidal rule being $\rho_n = 0.5$ on the detector edges and $\rho_n = 1$ else. For the Cone Beam geometry, the SART follows analogously with the semi-discrete model

$$\boldsymbol{X}_k : (\mathbb{R}^{|J|}, \langle \cdot, \cdot \rangle_k) \to L_2(\tilde{E}_{a_k}, w_{a_k}), \qquad w_{a_k}(\eta) := \left(\sum_{j \in J} \mathcal{X}_{a_k} b_j(\eta) \right)^{-1}$$

see (6.6). Assuming that the projections of the inspected object fit completely on the detector, i.e., the measured data is not truncated, the integration weights are equally 1 and thus neglectable. The discretized iteration step (6.11) matches the SART iteration (6.10). This induces that the convergence of the SART iteration scheme itself as well as the convergence to the solution of the continuous system is settled by the convergence results of the semi-discrete Landweber-Kaczmarz method.

Remark 6.12. *For the classical Cone Beam transform, the following parameterization of the spherically shaped detector is used to apply the trapezoidal rule.*

(i) In two dimensions, $d = 2$, let the ray direction $\theta \in \mathbb{S}^1$ be given as

$$\theta(\phi) = \begin{pmatrix} \cos\phi \\ \sin\phi \end{pmatrix}, \qquad \phi \in [0, 2\pi).$$

Applying the trapezoidal yields

$$\int_{\mathbb{S}^1} \Phi(\theta)\, d\theta = \int_0^{2\pi} \Phi(\theta(\phi))\, d\phi \approx \frac{2\pi}{K} \sum_{k=1}^{K} \rho_k \Phi(\theta_k)$$

for K equally distributed positions $\{\theta_k\}_k$ and the integration weights ρ_k.

(ii) In three dimensions, $d = 3$, the parameterization

$$\theta(t, \phi) = \begin{pmatrix} \sqrt{1-t^2}\cos\phi \\ \sqrt{1-t^2}\sin\phi \\ t \end{pmatrix} \qquad t \in [-1, 1], \phi \in [0, 2\pi)$$

is considered for $\theta \in \mathbb{S}^2$. Then,

$$\int_{\mathbb{S}^2} \Phi(\theta)\, d\theta = \int_{-1}^{1} \int_0^{2\pi} \Phi(\theta(t, \phi))\, d\phi\, dt$$

and the trapezoidal rule yields

$$\int_{-1}^{1} \int_0^{2\pi} \Phi(\theta(t, \phi))\, d\phi\, dt \approx \frac{2}{P} \sum_{p=1}^{P} \frac{2\pi}{Q} \sum_{q=1}^{Q} \rho_{p,q} \Phi\Big(\theta(t_p, \phi_q)\Big) = \frac{4\pi}{K} \sum_{k=1}^{K} \rho_k \Phi(\theta_k)$$

with $K := PQ$, $\theta_k := \theta(t_p, \phi_q)$, $k := (p-1)Q + q$ and integration weights $\rho_{p,q}$.

6.4 Numerics

So far, we considered the given data to be given as $g \in \mathcal{Y}$ and $g_i \in \mathcal{Y}_i$. In the context of X-ray tomography this induces that the data is given continuously on the detector planes with

$$g_i \in L_2(\theta_i^{\perp}, w_{\theta_i}) \qquad \text{and} \qquad g_i \in L_2(\tilde{E}_{a_i}, w_{a_i})$$

the X-ray transform and the flat detector Cone Beam transform, respectively. For measured data, this is clearly not the case. In general, the data is given at discrete positions $\{\eta_n\}_n$ on the detector plane, i.e., the data g_i is given as

$$(g_i)_n := g_i(\eta_n)$$

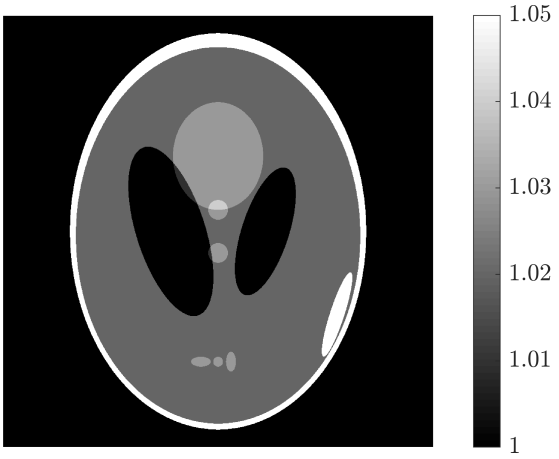

Figure 6.7: The Shepp-Logan head phantom.

for every scanning direction θ_i resp. X-ray source position a_i. To derive the semi-discrete iteration methods for the application in X-ray tomography, we assume in the following that the positions $\{\eta_n\}_n$ are equidistantly distributed on a Cartesian grid on the detector planes. This corresponds to a widely used X-ray tomography setup with flat detector panels for the data acquisition.

For the numerical simulations and validation of the semi-discrete iteration methods, we restrict ourselves to the two-dimensional case. We will consider the following data sets:

(i) The Shepp-Logan head phantom [SL74]. This phantom consists of eleven ellipses with constant values, see figure 6.7. The outer ellipse imitates a skull and has a value of 2. On the inside, the large ellipse has a value of 1.02, the value of the small ellipses varies from 1 to 1.05. Note that we use the original density values of the Shepp-Logan phantom. Since the reconstruction of the small density jumps is very challenging a modified phantom with large density jumps is widely used in literature to verify iterative reconstruction methods. We will create synthetic data for our simulations using the parallel scanning geometry with 500 scanned directions and 1024 detector points.

(ii) As a second data set, measured data from beamline ID15A at the European Synchrotron Radiation Facility (ESRF) in Grenoble, France, is used. This data was measured by Prof. Dr. Ralf Seemann, Department of Physics, Saarland University. From this data fluid flow in porous media is studied. The Synchrotron application generates data in the parallel scanning geometry. To verify the semi-discrete iteration methods, we consider the central slice of a three-dimensional data set containing 500 projections and 512×512 detector pixels each. This data was also used in [HL12] in the context of a fully three-dimensional reconstruction method for the parallel scanning geometry. For the application of the Synchrotron imaging modality, we refer to this publication and the references therein.

(iii) Finally, we verify the semi-discrete Landweber-Kaczmarz method for the Cone Beam scanning geometry using the walnut data set [Häm+15a; Häm+15b]. This data set was originally created for testing sparse-data tomography algorithms. However, the contained high-resolution scans are well-suited for our purpose of evaluating the iteration methods. We downsampled the data to 400 X-ray source positions and 1148 detector points for each position.

The main challenge in applying the iteration steps is the efficient implementation of the semi-discrete forward operators and their corresponding backward operators. With the forward projection being

computed by

$$\boldsymbol{A}_k \boldsymbol{f}^{m,k}(x) = \sum_{l \in J} \boldsymbol{f}_l^{m,k} \mathcal{A}_k b_l(x)$$

the forward projection $\mathcal{A}_k b$ has to be evaluated for all basis function centers $\{x_l\}_{l\in J}$ and every data point $(g_k)_n$ on the detector.

The basis functions discussed in the previous section can be treated as follows: Whereas a closed formula for evaluating the X-Ray transform of the Blob basis function is available, see proposition 6.6, there is no such formula for the Voxel basis existent. Thus, the forward projection of the Voxel $\mathcal{P}_{\theta_k} b(\eta_n - \mathrm{P}_{\theta_k{}^\perp} x_j)$ has to be computed for each detector point $\eta_n \in \theta_k^\perp$ and each Voxel center point x_l, $l \in J$. This can be done for example by using path tracing algorithms specifically designed for the Pixel basis as for example done in [Tra+17], [VS16] and [VS17]. A more general approach is the precomputation of $\mathcal{P}_{\theta_k} b$ at a regular grid and evaluating $\boldsymbol{P}_k \boldsymbol{f}^{m,k}$ by interpolation. For the flat detector Cone Beam transform, we make use of the relation (6.5), i.e.,

$$\mathcal{X} b_j(a, \eta) = \mathcal{P} b\big(\tilde{\theta}(\phi),\, \mathrm{P}_{\tilde{\theta}(\phi)^\perp}(a - x_j)\big) \tag{6.12}$$

with

$$\phi = -\arctan\left(\frac{\eta^\top \theta(\beta)^\perp}{\|a\| + |\eta^\top \theta(\beta)|}\right)$$

where $\tilde{\theta}(\phi) \coloneqq \theta(\beta + \pi + \phi)$.

6.4.1 Parallel scanning geometry

To evaluate the backward operators, we have to compute the inner products

$$\Big\langle \mathcal{A}_k b_j,\, g_k - \sum_{j\in J} \boldsymbol{f}_j^{m,k} \mathcal{A}_k b_j \Big\rangle_{\mathcal{Y}_k} \qquad \text{and} \qquad \Big\langle \psi_{k,j},\, g_k - \sum_{j\in J} \boldsymbol{f}_j^{m,k} \mathcal{A}_k b_j \Big\rangle_{\mathcal{Y}_k}$$

respectively. For the X-Ray transform, we use

$$\begin{aligned}
\big\langle \mathcal{P}_{\theta_k} b_j,\, \varphi \big\rangle_{L_2(\theta_k^\perp, w_{\theta_k}^p)} &= \int_{\theta_k{}^\perp} \mathcal{P}_{\theta_k} b_j(x)\, \varphi(x)\, w_{\theta_k}^p(x)\, dx \\
&= \int_{\theta_k{}^\perp} \mathcal{P}_{\theta_k} b(\mathrm{P}_{\theta_k{}^\perp} x_j - x)\, (w_{\theta_k}^p \cdot \varphi)(x)\, dx \\
&= \big(\mathcal{P}_{\theta_k} b *_{d-1} (w_{\theta_k}^p \cdot \varphi)\big)(\mathrm{P}_{\theta_k{}^\perp} x_j).
\end{aligned}$$

To compute these convolutions efficiently, we proceed analogously to the filtered back-projection algorithm, cf. [Nat01], by replacing the convolution by a discrete convolution at the data grid $\{\eta_n\}_n$,

$$\big(\mathcal{P}_{\theta_k} b *_{d-1} (w_{\theta_k}^p \cdot r_k^m)\big)(\eta_n) \approx \big(\mathcal{P}_{\theta_k} b *_{d-1}^h (w_{\theta_k}^p \cdot r_k^m)\big)_n.$$

Then, the values of the convolution at the positions $\mathrm{P}_{\theta_k{}^\perp} x_j$ are obtained by interpolation. We get the following algorithm for the iteration step of the Landweber-Kaczmarz method. For $k = 1, \ldots, |J|$:

(i) For $\eta_n \in \theta_k^\perp$ compute

$$\sum_{l\in J} \mathcal{P}_{\theta_k} b_l(\eta_n) = \sum_{l\in J} \mathcal{P}_{\theta_k} b\big(\eta_n - \mathrm{P}_{\theta_k{}^\perp} x_l\big) \qquad \text{and} \qquad \boldsymbol{P}_k \boldsymbol{f}^{m,k} = \sum_{l\in J} \boldsymbol{f}_l^{m,k} \mathcal{P}_{\theta_k} b\big(\eta_n - \mathrm{P}_{\theta_k{}^\perp} x_l\big).$$

(ii) Compute the discrete convolution of $\mathcal{P}_{\theta_k} b$ with the residual r_k^m at η_n by

$$\tilde{r}_k^m := \mathcal{P}_{\theta_k} b *_h \left(w_{\theta_k} \cdot r_k^m\right) \qquad \text{and} \qquad \tilde{W}_k := \mathcal{P}_{\theta_k} b *_h \sum_{l \in J} \mathcal{P}_{\theta_k} b_l.$$

(iii) Evaluate

$$f_j^{m,k+1} = f_j^{m,k} + \lambda_k \frac{\tilde{r}_k^m\left(\mathrm{P}_{\theta_k{}^\perp} x_j\right)}{\tilde{W}_k\left(\mathrm{P}_{\theta_k{}^\perp} x_j\right)} \qquad \forall j \in J$$

by interpolation.

Analogously follows for the Kaczmarz iteration,

$$\left\langle \psi_j^k,\, \varphi \right\rangle_{L_2(\theta_k^\perp, w_{\theta_k}^p)} = \left(\psi *_{d-1} (w_{\theta_k}^p \cdot \varphi)\right)\left(\mathrm{P}_{\theta_k{}^\perp} x_j\right),$$

and we obtain the following algorithm. For $k = 1, \ldots, |J|$:

(i) For $\eta_n \in \theta_k^\perp$ compute

$$\sum_{l \in J} \mathcal{P}_{\theta_k} b_l(\eta_n) = \sum_{l \in J} \mathcal{P}_{\theta_k} b\left(\eta_n - \mathrm{P}_{\theta_k{}^\perp} x_l\right) \qquad \text{and} \qquad \boldsymbol{P}_k \boldsymbol{f}^{m,k} = \sum_{l \in J} f_l^{m,k} \mathcal{P}_{\theta_k} b\left(\eta_n - \mathrm{P}_{\theta_k{}^\perp} x_l\right).$$

(ii) Compute the discrete convolution of $\mathcal{P}_{\theta_k} b$ with the residual r_k^m at η_n by

$$\tilde{r}_k^m := \mathcal{P}_{\theta_k} b *_h \left(w_{\theta_k} \cdot r_k^m\right).$$

(iii) Evaluate

$$f_j^{m,k+1} = f_j^{m,k} + \lambda_k \tilde{r}_k^m\left(\mathrm{P}_{\theta_k{}^\perp} x_j\right) \qquad \forall j \in J$$

by interpolation.

6.4.2 Cone Beam scanning geometry

To evaluate the backward operator $\Psi_k = \lambda_k \boldsymbol{X}^\sharp$ the inner product

$$\left\langle \mathcal{X}_{a_k} b_j,\, g_k - \sum_{j \in J} \boldsymbol{f}_j^{m,k} \mathcal{X}_{a_k} b_j \right\rangle_{L_2(\tilde{E}_{a_k}, w_{a_k})}$$

has to be evaluated. With (6.12) follows

$$\begin{aligned} \left\langle \mathcal{X}_{a_k} b_j,\, \varphi \right\rangle_{L_2(\tilde{E}_{a_k}, w_{a_k}^p)} &= \int_{\tilde{E}_{a_k}} \mathcal{X}_{a_k} b_j(\eta) \varphi(\eta)\, w_{\theta_k}^p(\eta)\, d\eta \\ &= \int_{\tilde{E}_{a_k}} \mathcal{P} b\left(\tilde{\theta}(\phi), \mathrm{P}_{\tilde{\theta}(\phi)^\perp}(a - x_j)\right) (w_{\theta_k}^p \cdot \varphi)(\eta)\, d\eta \end{aligned}$$

with

$$\phi = -\arctan\left(\frac{\eta^\top \theta(\beta)^\perp}{\|a\| + |\eta^\top \theta(\beta)|}\right)$$

and $\tilde{\theta}(\phi) := \theta(\beta + \pi + \phi)$. This integral is evaluated using the trapezoidal rule. We obtain the following algorithm to compute the iteration steps. For $k = 1, \ldots, |J|$:

(i) For $\eta_n \in \theta_k^\perp$ compute

$$\sum_{l \in J} \mathcal{X}_{a_k} b_l(\eta_n) = \sum_{l \in J} \mathcal{P}b\big(\tilde{\theta}(\phi), \mathrm{P}_{\tilde{\theta}(\phi)^\perp}(a - x_j)\big)$$

and

$$\boldsymbol{X}_k \boldsymbol{f}^{m,k} = \sum_{l \in J} \boldsymbol{f}_l^{m,k} \mathcal{P}b\big(\tilde{\theta}(\phi), \mathrm{P}_{\tilde{\theta}(\phi)^\perp}(a - x_j)\big).$$

(ii) For $\eta_n \in \theta_k^\perp$ compute

$$\tilde{r}_k^m := \sum_n \mathcal{P}b\big(\tilde{\theta}(\phi), \mathrm{P}_{\tilde{\theta}(\phi)^\perp}(a - x_j)\big)(w_{\theta_k}^p \cdot r_k^m)(\eta_n)$$

and

$$\tilde{W}_k := \sum_n \mathcal{P}b\big(\tilde{\theta}(\phi), \mathrm{P}_{\tilde{\theta}(\phi)^\perp}(a - x_j)\big)\big(w_{\theta_k}^p \cdot \sum_{l \in J} \mathcal{X}_{a_k} b_l\big)(\eta_n).$$

(iii) Evaluate

$$\boldsymbol{f}_j^{m,k+1} = \boldsymbol{f}_j^{m,k} + \lambda_k \frac{\tilde{r}_k^m}{\tilde{W}_k} \qquad \forall j \in J$$

by interpolation.

6.4.3 Results

For all reconstructions, we used a random but fixed order of the scanning directions and a regular grid of 501×501 Lewitt-Blobs with parameters $a = 2$, $m = 2$, and $\alpha = 10.8262$. The value of α was optimized with respect to the criterion (6.3) for $k' = 1$, cf. also [ML96]. The relaxation parameters were chosen heuristically within the range of feasible relaxation parameters λ_k. Figure 6.8 shows the application of the semi-discrete Landweber-Kaczmarz to the data Shepp-Logan head phantom. The reconstruction of the Synchrotron data set is shown in figure 6.9. In figure 6.10, the application of the semi-discrete Landweber-Kaczmarz method to the walnut data set is shown. The application of the semi-discrete Kaczmarz method for the Shepp-Logan head phantom and the Synchrotron data set is shown in figure 6.11 and figure 6.12, respectively.

All reconstruction methods yield suitable reconstructions for the used data. A notable result is that the reconstruction is already close to the desired result after few iterations. For the chosen relaxation parameters λ_k there is almost only 1 iteration needed. Further, the basis coefficients of the Blob basis itself provide already good reconstruction results. Due to the shape of the Blob function, see figure 6.2, the reconstruction after evaluation the basis representation is smoother.

Having a closer look at the results of the semi-discrete Kaczmarz method in figure 6.11 and figure 6.12, the Blob reconstruction kernel yields smoother reconstructions than the Dirac reconstruction kernel.

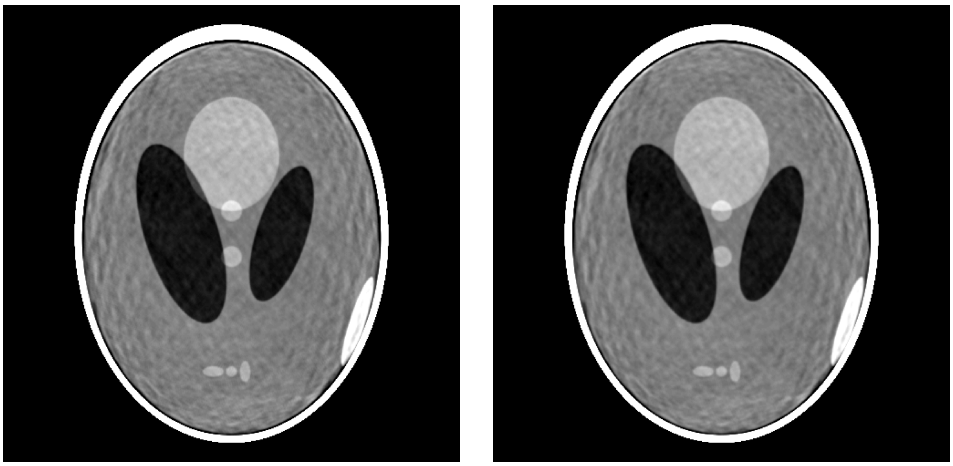

(a) Iteration 1

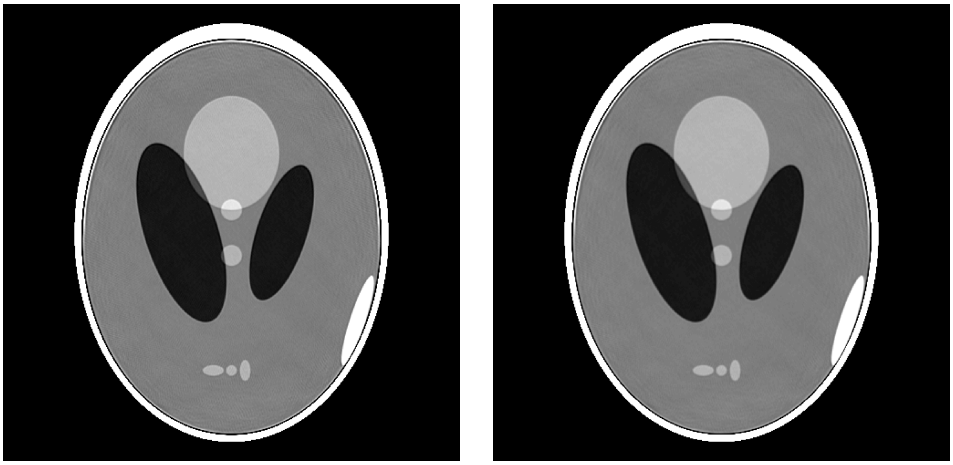

(b) Iteration 3

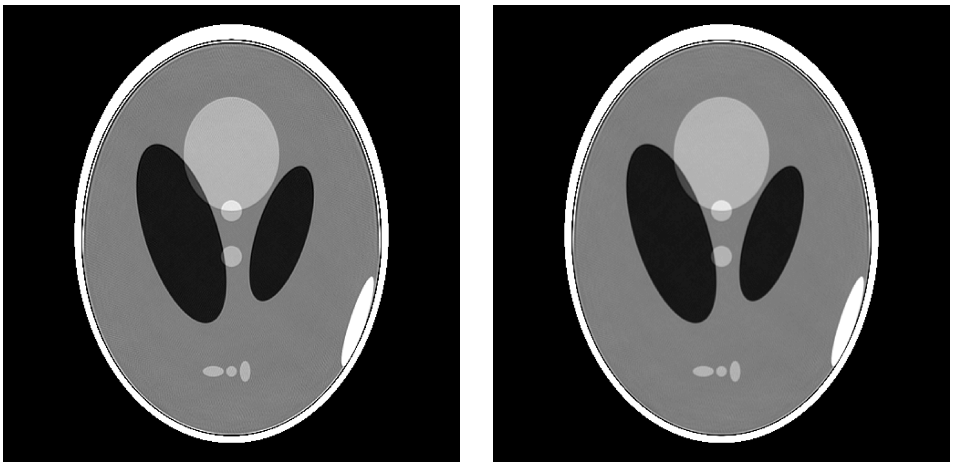

(c) Iteration 5

Figure 6.8: Semi-discrete Landweber-Kaczmarz method applied to Shepp-Logan head phantom data (501×501 Blob basis functions, $\lambda_k \equiv 0.6$): Basis coefficients (left) and evaluated basis coefficients (right).

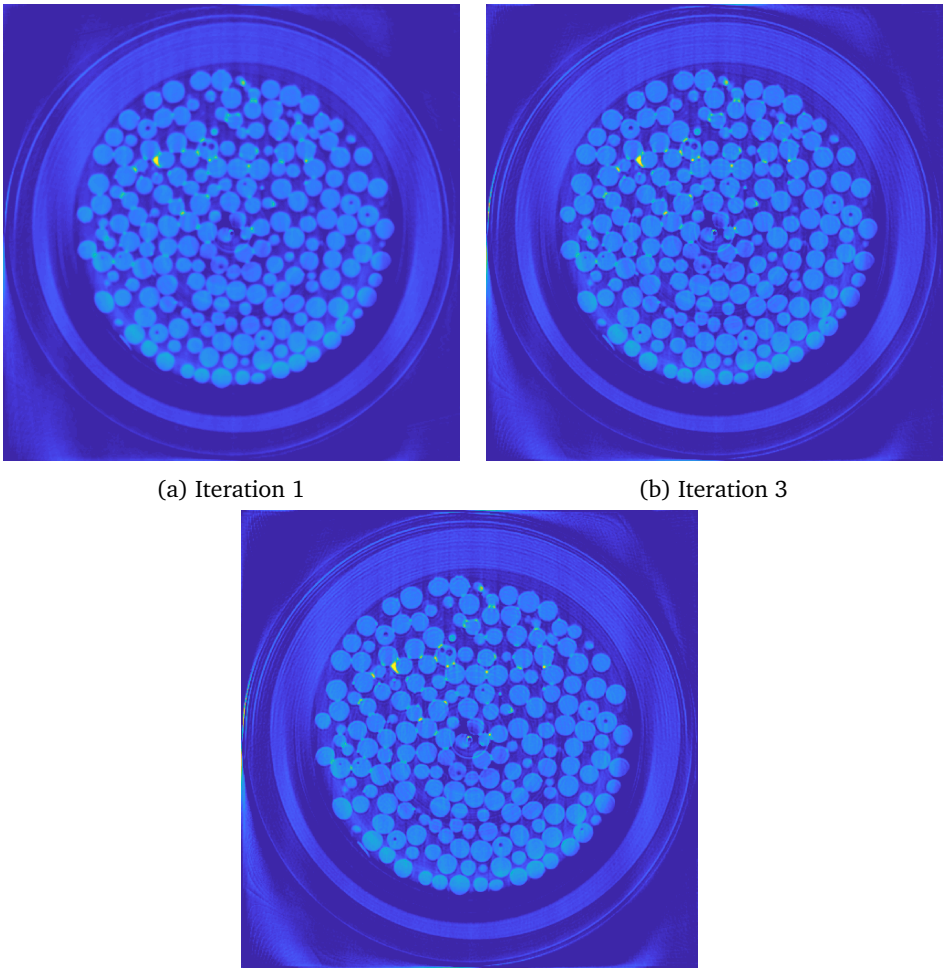

(a) Iteration 1 (b) Iteration 3

(c) Iteration 5

Figure 6.9: Semi-discrete Landweber-Kaczmarz method applied to the Synchrotron data (501×501 Blob basis functions, $\lambda_k \equiv 0.6$): Evaluated basis coefficients.

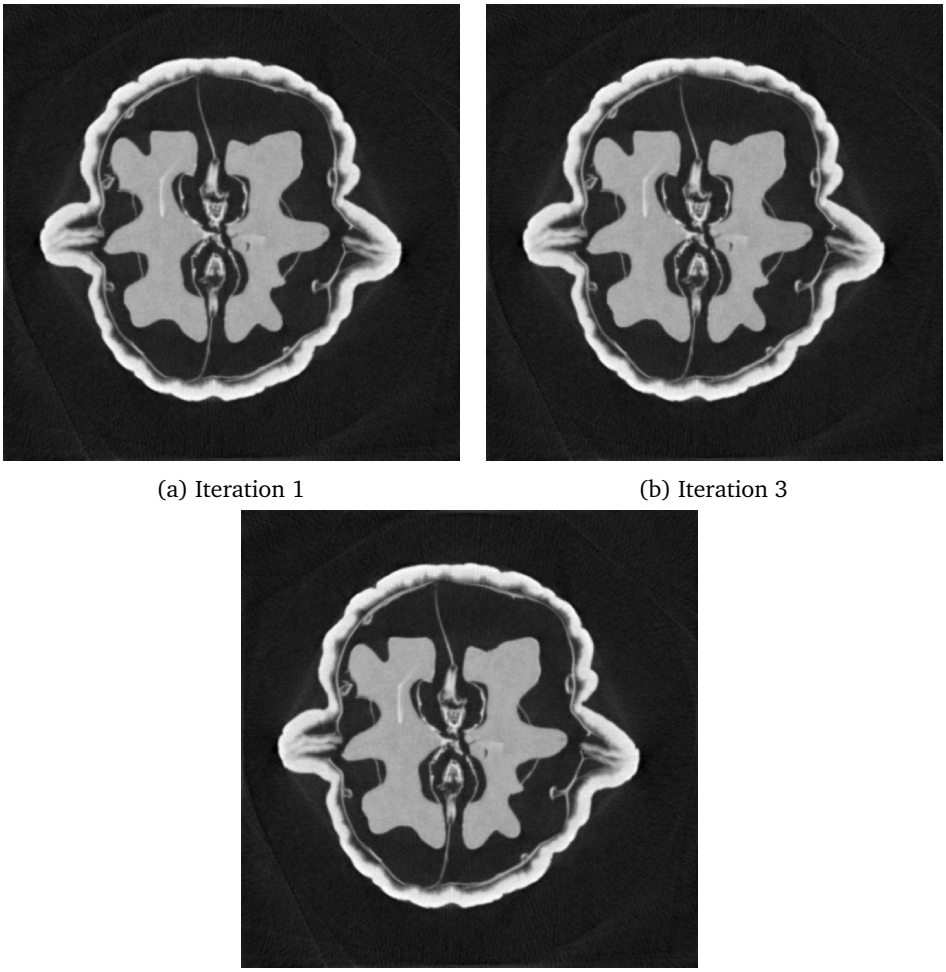

(a) Iteration 1 (b) Iteration 3

(c) Iteration 5

Figure 6.10: Semi-discrete Landweber-Kaczmarz method applied to the walnut data set (501×501 Blob basis functions, $\lambda_k \equiv 0.6$): Evaluated basis coefficients.

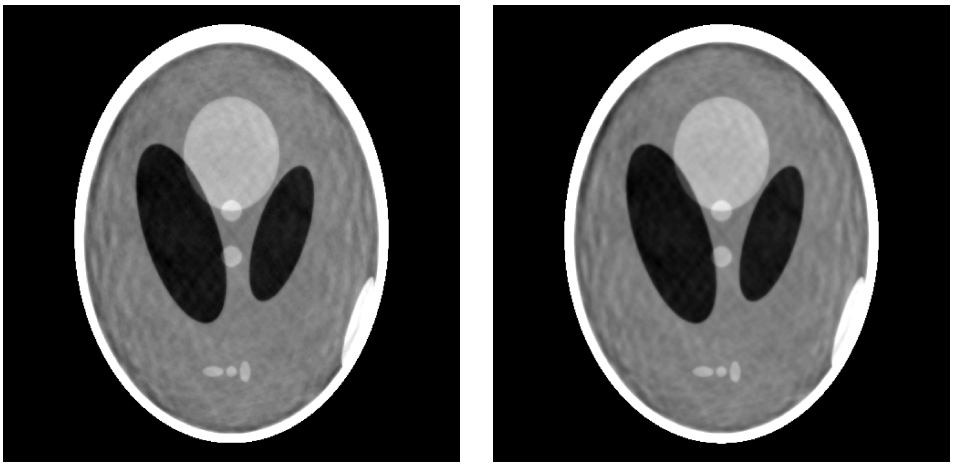

(a) Iteration 1

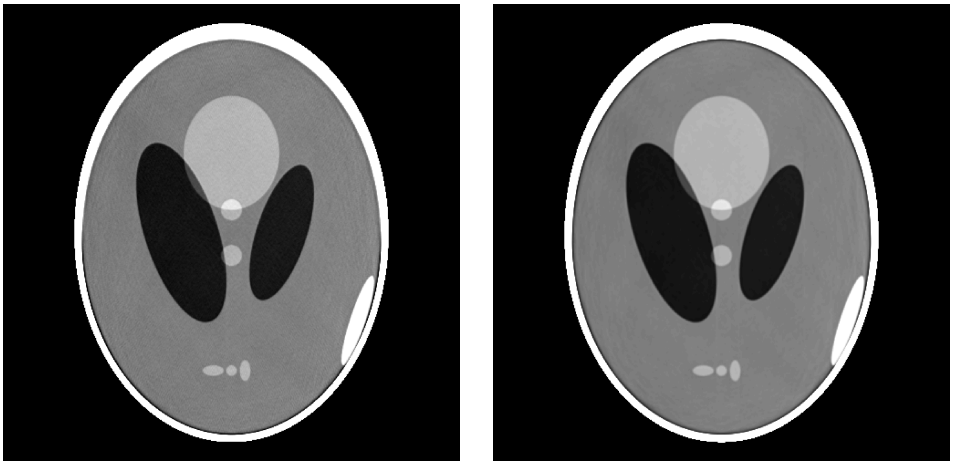

(b) Iteration 3

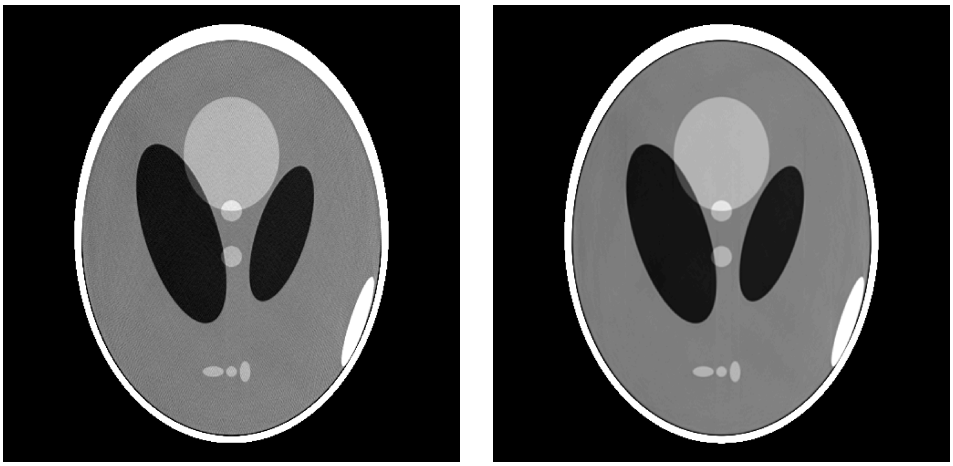

(c) Iteration 5

Figure 6.11: Semi-discrete Kaczmarz method applied to Shepp-Logan head phantom data (501×501 Blob basis functions, $\lambda_k \equiv 0.6$): Evaluated basis coefficients for $\psi_l^k(x) = \delta(x - \mathrm{P}_{\theta_k{}^\perp} x_l)$ (left) and $\psi_l^k(x) = \mathcal{P}_{\theta_k} b_l(x)$ (right).

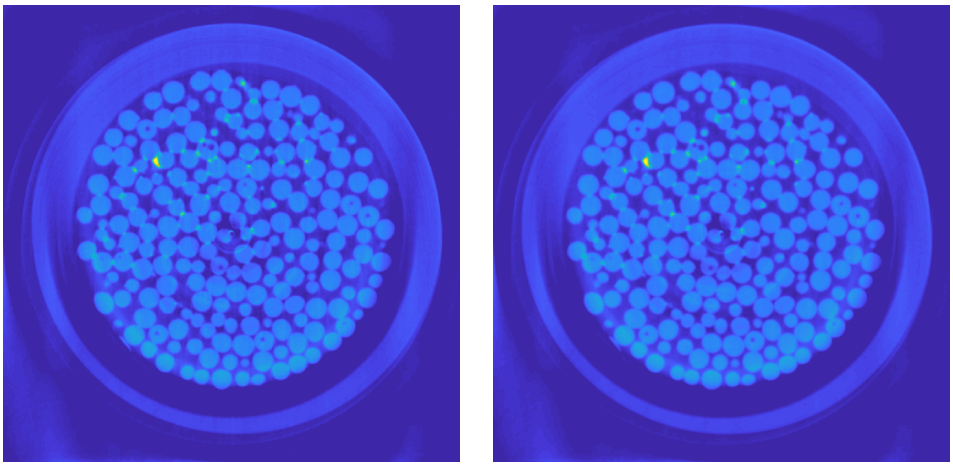

(a) Iteration 1

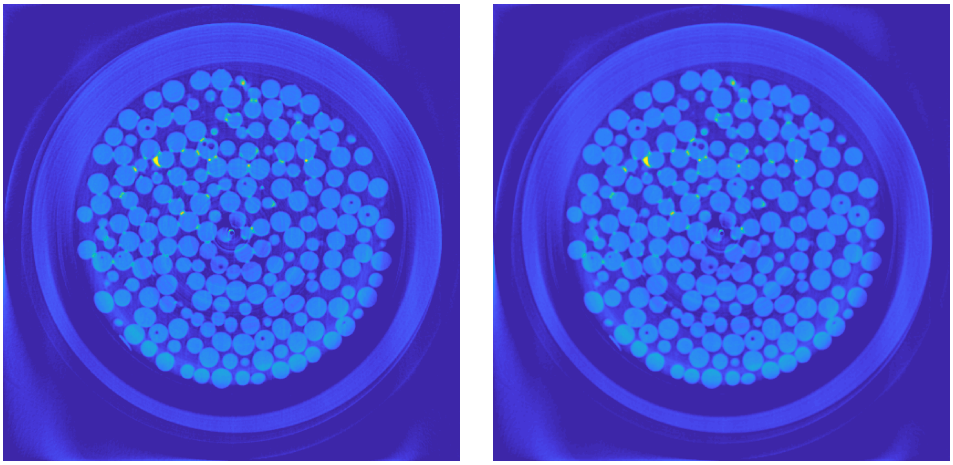

(b) Iteration 3

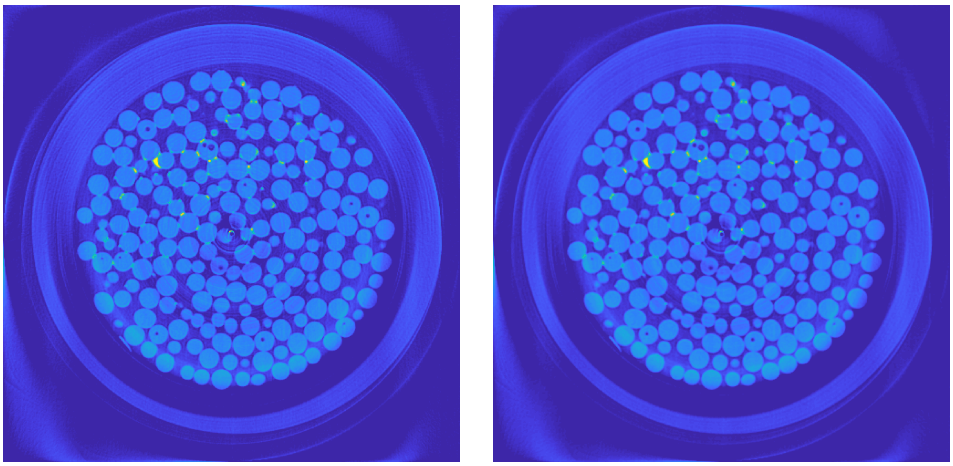

(c) Iteration 5

Figure 6.12: Semi-discrete Kaczmarz method applied to the Synchrotron data set (501×501 Blob basis functions, $\lambda_k \equiv 0.6$): Evaluated basis coefficients for $\psi_l^k(x) = \delta(x - \mathrm{P}_{\theta_k{}^\perp} x_l)$ (left) and $\psi_l^k(x) = \mathcal{P}_{\theta_k} b_l(x)$ (right).

Chapter 7

Conclusion and outlook

We proposed the semi-discrete iteration methods consiting of a semi-discrete operator model and an iteration scheme to solve the semi-discrete model. We showed that the solution of the semi-discrete reconstruction problem converges to the solution of the continuous system for suitable choices of the underlying basis elements, see theorem 4.15. The presented iteration schemes were shown to converge linearly, see theorem 5.6. For the semi-discrete reconstruction problem being a consistent the iteration methods converge to the generalized solution of the reconstruction problem see proposition 5.8. The convergence theory was transferred to the explicit backward operator choices yielding the semi-discrete Landweber-Kaczmarz method in theorem 5.12 and the semi-discrete Kaczmarz method in theorem 5.15, respectively. We further proposed a method to compute the application of the generalized inverse by evaluating inner products, see proposition 5.18.

Further, the semi-discrete iteration methods were applied to applications in X-Ray tomography in chapter 6. The classical Voxel basis function and the Lewitt-Blob basis function were used to derive a semi-discrete model for the parallel and the flat detector Cone Beam geometry. In section 6.2.3 a modified operator model is introduced to incorporate prior information about the inspected object directly into the semi-discrete model. An algorithm for the efficient implementation of the semi-discrete iteration methods were applied in the context of parallel geometries and Cone Beam scanning geometries. In section 6.3.3, the classical algebraic reconstruction method SART was shown to be a discretized version of the semi-discrete Landweber-Kaczmarz method using the trapezoidal rule on the detector. Together with the convergence and approximation properties of the semi-discrete iteration methods this induces convergence and approximation properties of the SART algorithm. The error estimates of theorem 5.6 provide an explanation for the efficiency of algebraic reconstruction methods in CT applications and the impact of the chosen relaxation parameters on the convergence speed.

We also discussed the boundedness of the Radon transform and its related ray transform for fixed X-Ray directions and source positions, respectively, on weighted L_2 spaces. For specific choices of these weights the operator norm is equally 1 and the generalized inverse is identical to the adjoint operator. This induces that the operator norm of the generalized inverse operators is also equally 1, see propositions 3.5, 3.10 and 3.14. This implies also that all these transforms form isometries between the orthogonal complement of their nullspace and the image space. Although these results are known in parts and can be found indirectly for the Radon transform and the X-Ray transform for example in [Nat01] and for the Cone Beam transform for example in [Ham+80], there exists no systematic analysis of this fact for all four transforms to the author's knowledge.

Further studies of semi-discrete iteration methods could involve different choices for the backward operators. Since the presented iteration methods rely on the classical Landweber and Kaczmarz methods other choices of Ψ_k might also be of interest. Although their application was restricted to X-ray tomography using the semi-discrete framework in other applications where systems of linear operator equations are involved seems promising.

Naturally, the study of optimal relaxation parameters might be very useful for further research. A systematic investigation of the choice of relaxation parameters based on the convergence theorems 5.6, 5.12 and 5.15 might yield further insights into the proposed iteration methods. For the fully-discrete case, such results exist together with convergence results for Landweber-type methods, cf. for example [JW03] and [CE02]. For the continuous case there exists also results, see [LA12] and [KL14]. These results might be transferred to the semi-discrete framework. We further saw that the iteration methods converged in the numerical simulations using only a few iteration steps. Thus, the iteration methods could also be treated and analyzed as direct methods. A further topic for future research might be performance investigations and verification of the proposed methods for limited and truncated data.

Clearly, the application of the semi-discrete Kaczmarz method to three-dimensional Cone Beam data is of great interest, in particular, the computation of suitable reconstruction kernels in the sense of definition 5.17. A possible approach might be the exploitation of the relation between the Cone Beam transform and the Radon resp. X-Ray transform, see [Gra91] and [Lou16].

Bibliography

[AS65] M. Abramowitz and I. A. Stegun. *Handbook of Mathematical Functions*. Dover Publications Inc., 1965.

[AK84] A. H. Andersen and A. C. Kak. "Simultaneous Algebraic Reconstruction Technique (SART): A Superior Implementation of the ART Algorithm". *Ultrasonic Imaging* 6: 81–94, 1984.

[AW05] G. B. Arfken and H. J. Weber. *Mathematical Methods for Physicists, 6th Edition*. Academic Press, 2005.

[Aub00] J.-P. Aubin. *Applied Functional Analysis*. John Wiley & Sons, Inc., 2000.

[BJ85] C. de Boor and R.-Q. Jia. "Controlled approximation and a characterization of the local approximation order". *Proceedings of the American Mathematical Society* 95(4): 547–547, 1985.

[CE02] Y. Censor and T. Elfving. "Block-Iterative Algorithms with Diagonally Scaled Oblique Projections for the Linear Feasibility Problem". *SIAM Journal on Matrix Analysis and Applications* 24(1): 40–58, 2002.

[Con94] J. B. Conway. *A Course in Functional Analysis*. Springer New York, 1994.

[EHN96] H. W. Engl, M. Hanke, and A. Neubauer. *Regularization of Inverse Problems*. Springer Netherlands, 1996.

[FDK84] L. A. Feldkamp, L. C. Davis, and J. W. Kress. "Practical cone-beam algorithm". *Journal of the Optical Society of America A* 1(6): 612, 1984.

[GBH70] R. Gordon, R. Bender, and G. T. Herman. "Algebraic Reconstruction Techniques (ART) for three-dimensional electron microscopy and X-ray photography". *Journal of Theoretical Biology* 29(3): 471–481, 1970.

[GR15] I. S. Gradshteyn and I. M. Ryzhik. *Table of Integrals, Series, and Products*. Ed. by A. Jeffrey and D. Zwillinger. Elsevier, 2015.

[Gra91] P. Grangeat. "Mathematical framework of cone beam 3D reconstruction via the first derivative of the radon transform". In: *Mathematical Methods in Tomography*. Springer Berlin Heidelberg, 1991, 66–97.

[HL12] B. N. Hahn and A. K. Louis. "Reconstruction in the three-dimensional parallel scanning geometry with application in synchrotron-based x-ray tomography". *Inverse Problems* 28(4): 045013, 2012.

[Hah+13] B. N. Hahn, A. K. Louis, M. Maisl, and C. Schorr. "Combined reconstruction and edge detection in dimensioning". *Measurement Science and Technology* 24(12): 125601, 2013.

[Ham+80] C. Hamaker, K. T. Smith, D. C. Solmon, and S. L. Wagner. "The divergent beam x-ray transform". *Rocky Mountain Journal of Mathematics* 10(1): 253–284, 1980.

[Häm+15a] K. Hämäläinen, L. Harhanen, A. Kallonen, A. Kujanpää, E. Niemi, and S. Siltanen. "Tomographic X-ray data of a walnut", 2015. arXiv: arxiv.org/abs/1502.04064v1.

[Häm+15b] K. Hämäläinen, L. Harhanen, A. Kallonen, A. Kujanpää, E. Niemi, and S. Siltanen. *Tomographic X-ray data of a walnut*. 2015. URL: https://doi.org/10.5281/zenodo.1254206.

[Hel99] S. Helgason. *The Radon Transform*. Springer US, 1999.

[Hou73] G. N. Hounsfield. "Computerized transverse axial scanning (tomography): Part 1. Description of system". *The British Journal of Radiology* 46(552): 1016–1022, 1973.

[JW03] M. Jiang and G. Wang. "Convergence studies on iterative algorithms for image reconstruction". *IEEE Transactions on Medical Imaging* 22(5): 569–579, 2003.

[Kac37] S. Kaczmarz. "Angenäherte Auflösung von Systemen linearer Gleichungen". *Bull. Internat. Acad. Polon. Sci.* (A35): 355–7, 1937.

[KS88] A. C. Kak and M. Slaney. *Principles of Computerized Tomographic Imaging*. IEEE Press, 1988.

[KL14] S. Kindermann and A. Leitão. "Convergence rates for Kaczmarz-type regularization methods". *Inverse Problems and Imaging* 8(1): 149–172, 2014.

[Kin16] S. Kindermann. "Projection Methods for Ill-Posed Problems Revisited". *Computational Methods in Applied Mathematics* 16(2): 257–276, 2016.

[KS02] R. Kowar and O. Scherzer. "Convergence Analysis Of A Landweber-Kaczmarz Method For Solving Nonlinear Ill-Posed Problems". In: *Ill-Posed and Inverse Problems*. Ed. by V. G. Romanov, S. I. Kabanikhin, Y. E. Anikonov, and A. L. Bukhgeim. De Gruyter, 2002, 253–270.

[Kre78] E. Kreyszig. *Introductory Functional Analysis with Applications*. Wiley India Pvt. Limited, 1978.

[Lan87] S. Lang. *Linear Algebra*. Springer-Verlag New York, 1987.

[LA12] A. Leitão and M. M. Alves. "On Landweber–Kaczmarz methods for regularizing systems of ill-posed equations in Banach spaces". *Inverse Problems* 28(10): 104008, 2012.

[Lew90] R. M. Lewitt. "Multidimensional digital image representations using generalized Kaiser–Bessel window functions". *Journal of the Optical Society of America A, Optics and Image Science* 7(10): 1834–1846, 1990.

[LWT08] A. K. Louis, T. Weber, and D. Theis. "Computing Reconstruction Kernels for Circular 3-D Cone Beam Tomography". *IEEE Transactions on Medical Imaging* 27(7): 880–886, 2008.

[Lou03] A. K. Louis. "Filter design in three-dimensional cone beam tomography: circular scanning geometry". *Inverse Problems* 19(6): 31–40, 2003.

[Lou84] A. K. Louis. "Nonuniqueness in inverse radon problems: The frequency distribution of the ghosts". *Mathematische Zeitschrift* 185(3): 429–440, 1984.

[Lou16] A. K. Louis. "Exact cone beam reconstruction formulae for functions and their gradients for spherical and flat detectors". *Inverse Problems* 32(11): 115005, 2016.

[Lou89] A. K. Louis. *Inverse und schlecht gestellte Probleme*. Vieweg+Teubner Verlag, 1989.

[LM90] A. K. Louis and P. Maass. "A mollifier method for linear operator equations of the first kind". *Inverse Problems* 6(3): 427–440, 1990.

[ML95] S. Matej and R. M. Lewitt. "Efficient 3D grids for image reconstruction using spherically-symmetric volume elements". *IEEE Transactions on Nuclear Science* 42(4): 1361–1370, 1995.

[ML96] S. Matej and R. M. Lewitt. “Practical considerations for 3-D image reconstruction using spherically symmetric volume elements”. *IEEE Transactions on Medical Imaging* 15(1): 68–78, 1996.

[Mül66] C. Müller. *Spherical Harmonics*. Springer Berlin Heidelberg, 1966.

[Nat77] F. Natterer. “Regularisierung schlecht gestellter Probleme durch Projektionsverfahren”. *Numerische Mathematik* 28(3): 329–341, 1977.

[Nat01] F. Natterer. *The mathematics of computerized tomography*. Society for Industrial and Applied Mathematics, 2001.

[NW01] F. Natterer and F. Wübbeling. *Mathematical Methods in Image Reconstruction*. Society for Industrial and Applied Mathematics, 2001.

[Nil+15] M. Nilchian, J. P. Ward, C. Vonesch, and M. Unser. “Optimized Kaiser–Bessel Window Functions for Computed Tomography”. *IEEE Transactions on Image Processing* 24(11): 3826–3833, 2015.

[Rad17] J. Radon. “Über die Bestimmung von Funktionen durch ihre Integralwerte längs gewisser Mannigfaltigkeiten”. *Berichte Sachsische Akademie der Wissenchaften, Leipzig, Mathematische-Physikalische Klasse* 69: 262–267, 1917.

[Rie03] A. Rieder. *Keine Probleme mit Inversen Problemen*. Vieweg+Teubner Verlag, 2003.

[Rud91] W. Rudin. *Functional Analysis*. New York: McGraw-Hill, 1991.

[Rud76] W. Rudin. *Principles of Mathematical Analysis*. New York: McGraw-Hill, 1976.

[SM13] C. Schorr and M. Maisl. “Exploitation of geometric a priori knowledge for limited data reconstruction in nondestructive testing”. In: *Proceedings of Fully3D Conference*. 2013.

[SK11] H. R. Schwarz and N. Köckler. *Numerische Mathematik*. Vieweg+Teubner Verlag, 2011.

[SL74] L. A. Shepp and B. F. Logan. “The Fourier reconstruction of a head section”. *IEEE Transactions on Nuclear Science* 21(3): 21–43, 1974.

[Sle65] D. Slepian. “Analytic Solution of Two Apodization Problems”. *Journal of the Optical Society of America* 55(9): 1110–1115, 1965.

[Sne95] I. N. Sneddon. *Fourier Transforms*. Reprint of the 1951 original. Dover Publications, Inc., New York, 1995.

[SF73] G. Strang and G. Fix. “A Fourier Analysis of the Finite Element Variational Method”. In: *Constructive Aspects of Functional Analysis*. Springer Berlin Heidelberg, 1973, 793–840.

[Tra+17] P. Trampert, J. Vogelgesang, C. Schorr, M. Maisl, S. Bogachev, N. Marniok, A. Louis, T. Dahmen, and P. Slusallek. “Spherically symmetric volume elements as basis functions for image reconstructions in computed laminography”. *Journal of X-Ray Science and Technology* 25(4): 533–546, 2017.

[Tuy83] H. K. Tuy. “An Inversion Formula for Cone-Beam Reconstruction”. *SIAM Journal on Applied Mathematics* 43(3): 546–552, 1983.

[Vog19] J. Vogelgesang. “A semi-discrete iteration method in X-ray tomography”. *Oberwolfach Reports.*, 2019.

[VS16] J. Vogelgesang and C. Schorr. “A Semi-Discrete Landweber-Kaczmarz Method for Cone Beam Tomography and Laminography Exploiting Geometric Prior Information”. *Sensing and Imaging* 17(1), 2016.

[VS17] J. Vogelgesang and C. Schorr. “Iterative Region-of-Interest Reconstruction from Limited Data Using Prior Information”. *Sensing and Imaging* 18(1), 2017.

[Wat95] G. N. Watson. *A Treatise on the Theory of Bessel Functions*. Reprint of the second (1944) edition. Cambridge University Press, Cambridge, 1995.

[Wer18] D. Werner. *Funktionalanalysis*. Springer Berlin Heidelberg, 2018.

[Yos95] K. Yosida. *Functional Analysis*. Springer Berlin Heidelberg, 1995.